Chapter 5   Results and discussion of the resistive switching properties in the LaAlO-based memory devices

5.1 Introduction

Transparent electronics has emerged as an important new class of devices for a wide range of application since the announcement of transparent thin film transistors [1] and other first-generation transparent electronics [2] in 2003. They are typically fabricated from transparent conductive oxides (TCO), which are both electrically conductive and visually transparent. Such materials have enable a host of transparent passive and active devices, including liquid crystal display (LCDs) [3], organic light emitting diodes (OLED) [4], solar cells [5], and optical sensors [6]. In particular, transparent resistive random access memory (T-RRAM) [7] has found widespread application in consumer devices such as cell phones, computers, TV monitors, and watches.

The basic T-RRAM concept involves a transition metal oxide (TMO) film sandwiched between two transparent electrodes, such as ZnO:B, fluorine-doped tin oxide (FTO) or indium-doped tin oxide (ITO). The deposition of this stack on a transparent substrate produces a transparent capacitor device. The first transparent nonvolatile memory - ITO/ZnO/ITO sandwiched structures – were successfully fabricated by Seo et al. in 2008 [7]. Large-band-gap TMO materials are highly transparent in the visible portion of the electromagnetic spectrum. Following from this concept, other transparent devices exhibiting bipolar resistance switching properties have been reported. Such devices are made by sandwiching ZnO:Mg films between ITO and FTO electrodes on a glass substrate [8]. Although a variety of materials have been used for RRAM device fabrication – including TMOs such as NiO [9], TiO_2 [10], ZrO_2 [11], perovskite oxide such as doped-$SrZrO_3$ (SZO) [12], and doped manganites

[13] - T-RRAM devices have only been realized in ZnO-based materials. Since the materials used in RRAM devices are all highly transparent, they might also be suitable for dependence on insulator materials; it is essential to investigate the switching properties on other oxide materials.

The ternary oxide $LaAlO_3$ (LAO) is one of the materials that has been identified by the semiconductor industry as a potential replacement for SiO_2 in gate dielectric layers. It has a high dielectric constant of 24 [14] and has large band offsets (over 2 eV) with silicon [15]. Furthermore, the thin film of LAO is amorphous until 800 °C [16], the band gap is predicted to be 6.2 eV [17], and is theoretically thermally stable in contact to silicon up to 1000 °C [18], as well as high dielectric breakdown field (6.3 MV/cm). The LAO thin film used on RRAM application here was the first time, therefore, the fundamental factor - oxygen partial pressure is needed to be discussed. Furthermore, it should be noted that for the polycrystalline structure, grain boundaries can enable the development of filaments. As the MIM materials integrated with 22 nm technology projected for 2016, its cell size will become comparable to the grain diameter thus causing detrimental variations in switching characteristics. The amorphous high-k gate dielectrics have already been applied on the semiconductor technology. Especially for the lanthanum based high-k dielectrics, it has been considered as one of the candidates beyond the hafnium-based technology. Once the lanthanum based materials can exhibit reliable RS properties, it can be a good choice for 1T1R integration application. Furthermore, the dielectric layer with amorphous phase is less being discussed compared to the polycrystalline structure on the RRAM field. Its forming process, conducting mechanism, electrical properties, as well as the switching characteristics, may differ with the polycrystalline one. For a thoroughly understanding on the switching properties, it's needed to have a detailed investigation on the correlation between thin film quality and electrical characteristics.

In this chapter, we report on the structural and electrical properties of LAO based capacitor device under various oxygen partial pressure ranging from 7×10^{-3} torr to 2.8×10^{-2} by pulsed laser deposition (PLD). Correlation between the fabrication process and thin film properties of a LaAlO based capacitor device is discussed. Applying the background gas pressure during deposition, both gas-phase and surface reactions will be important for the oxidation process, and may dominate the LAO thin film quality, surface morphology, electrical properties, and resistive switching characteristics. The change in thin film properties and switching behavior are discussed in terms of oxygen vacancies contents inside LAO film, which was formed during forming process. A possible model based on the correlated barrier hopping is proposed to elucidate the switching mechanism of the ITO/LaAlO/ITO T-RRAM device.

5.2 Experimental details

The commercial ITO (Corning 1737) glass substrates deposited with 300-nm-thick transparent conducting indium tin oxide (ITO) thin films prepared as the bottom electrode. Then, PLD was used to deposit the LaAlO using LaAlO target as the resistive layer of T-RRAM device. A KrF excimer laser (λ=248 nm) was used as the light source of PLD with a pulse duration of 25 ns, a repetition rate of 3Hz, and a laser energy of 500 mJ. The distance from the target to the substrate was 10 cm and the target rotation rate was 5 rpm. The ambient oxygen pressure, which is the most important process parameter of PLD, was varied with 7×10^{-3}, 1.4×10^{-2}, and 2.8×10^{-2} Torr. At last, we use ITO as a top electrode, a 100 nm-thick ITO thin film is deposited by dc sputter system using a shadow mask with a diameter of 1200 μm. Electrical characteristics were performed on Agilent 4156C semiconductor parameter analyzer (SPA) at room temperature. Current flow from the top to the bottom electrode was defined as positive sweep.

5.3 Thin film properties and its characteristics of ITO/LaAlO/ITO capacitor devices

This section is aimed at an understanding of how the different oxygen pressure influences the microstructure and surface morphology, such as film growth mode, in the PLD of multi-component ceramics. We have clearly explained the substrate temperature effect on the Gd_2O_3 film growth in last chapter and investigated its corresponding resistive switching characteristics. In this section, we are going to introduce another fundamental parameter that significantly dominate the thin film quality and electrical properties - background oxygen pressure. In general, deposited oxide ceramics in vacuum usually tend to deficient to oxygen content, therefore, the background gas is sometimes admitted in situ during PLD, to compensate the loss of a constituent element such as oxygen or nitrogen in ceramics. Once the background gas is admitted into the chamber during PLD process, the growth condition is quite different compared to the vacuum chamber, and greatly depends on the chamber circumstance. The effect of inert ambient gas pressure on the nature is more likely to the increased collisions between the ejected species and the ambient gas inside the chamber, resulting in a more complex reaction during deposition. Therefore, it is essential to make a clear understanding on the correlation between the thin film properties and the electrical characteristics, as well as the resistive switching behaviors. First, we will discuss the fabrication process effect on the thin film morphology, surface roughness, crystallinity, and material composition by varying oxygen pressure during PLD process of LAO film in section 5.3.1. The electrical characteristics of the three samples, such as leakage current, breakdown voltage, temperature effect to conducting current, and conducting behavior will be discussed in section 5.3.2. Finally, how a forming process deteriorates the oxide thin films will be

discussed at last.

5.3.1 Thin film properties of the ITO/LaAlO/ITO capacitors

After the LAO thin film deposition by PLD process, we measured the surface roughness of LAO thin film where the LAO films were deposited at various oxygen partial pressure of 7×10^{-3} (L-7), 1.4×10^{-2} (L-14), and 2.8×10^{-2} (L-28) torr by atomic force microscope (AFM). The surface roughness of L-7, L-14, and L-28 samples in room mean square (RMS) is about 3.66, 4.00, and 4.38 nm, respectively. The results indicate that the surface roughness increases with the increase of the oxygen pressures, which may be related to the oxygen contents during the LaAlO thin film deposition. Let's back to discuss the mechanism of PLD fabrication process. The evaporants vaporized from the target surface are highly forward-directed plume along the target normal, therefore, the substrate generally displaced opposite to the target. Under the vacuum circumstance, the kinetics energies of the vaporized evaporants may directly be related to the laser energy and pulsed duration time because there are no or less collisions during the transferring between the target and substrate. However, when the ambient gas pressure increases, the vaporized species will undergo enough collisions that these vaporized species to form larger clusters will occur by nucleation growth before they arrive at the substrate surface. The ambient oxygen gas inside the chamber will be ionized to atomic oxygen via electron or photon impact ionization. The atomic oxygen is quite reactive and tends to easily interact with the vaporized evaporants. The higher the oxygen pressure, the more atomic oxygen will be generated, and then the reaction and collision between the vaporized species and the oxygen gas will increase. For example, at a pressure of the order of 1 mtorr, the mean free path is approximately 5 cm, while the mean free path of ejected species becomes 0.05 cm at a higher pressure of 100 mtorr. The specific effect of the target-to-substrate distance and

ambient pressure are interrelated by Dyer et al. [19]. They proposed that due to the increased collisions between the vaporized plume and the ambient gas, the plume dimension decreases as the ambient gas pressure increases. The plume length L and the oxygen pressure P_o will follow the equation: $L \; \alpha \; (E/P_o)^{1/3\gamma}$, where E is the laser-pulse energy, and γ is the ratio of specific heats of the elements in the plume. Schematic diagrams shown for PLD process under low and high oxygen partial pressure is depicted in Fig. 5-4 and Fig. 5-5, respectively. When the target-to-substrate distance is much smaller than L, no obvious difference in the cluster size and density will be observed. As the target-to-substrate distance increases larger than L, the concentration of the smaller ones decreases and the larger clusters appear indicating that during a longer time of transferring, the clusters will merge via reaction. For the higher oxygen pressure, the corresponding plume length L is shorter, which enlarge the distance between plume and substrate thus causing deterioration of the thin film morphology. Since the adhesion of the ejected matter may also be poor, a rougher surface may be expected [20]. From the basic PLD process theory, it can well explain why the surface roughness increases with increasing the oxygen pressure during thin film deposition. The top view of the L-7, L-14 and L-28 samples were investigated by scanning electron microscopy (SEM) as shown in Fig. 5-6 ~ Fig. 5-8, respectively. The L-28 samples in Fig. 5-8 exhibit rougher surface than that of L-7 ones, which is consistent with the observed AFM data shown in Fig. 5-5. The L-28 samples undergone more collisions and reaction with the atomic oxygen during LAO thin film deposition also reflects on the stoichiometry of the LAO composition. Fig. 5-9(a) and 5-9(b) show the XPS spectra of the La 3d and Al 2p core level electrons. In Fig. 5-9(a), the peak binding energy of the La 3d core level electron shifts to higher binding energy with the oxygen pressure increasing from 7 to 28 mtorr, which may be attributed to highly oxidized of the LAO film and fewer structural defects are

introduced. Xiang et al. [21] claimed that LAO film deposited under a high oxygen pressure of 10^{-1} Pa, the kinetic energy and internal energy of the flying particles are easily lost by frequent collisions between the evaporated particles and the oxygen gas. When oxygen pressure was higher than 2×10^{-3} Pa, the stoichiometry ratio of La, Al, and O in the deposited LAO films can be maintained and approached 1:1:3, or the oxygen content will decrease with decreasing oxygen pressure. Fig. 5-9(b) shows the Al 2p core level electron shifts from 72 to 74 eV with the increasing of oxygen pressure, which corresponds to the peak binding energy shifts from metal Al^{0+} to the oxidized Al^{3+} spectra. From XPS data analysis as shown in Fig. 5-9(a) and 5-9(b), we further confirm that when increasing oxygen pressure, the amount of atomic oxygen can compensate the oxygen deficient of vaporized species by collision or reaction, resulting in the stronger binding energy of the oxidized peak and accompanying less defects existence inside LAO thin film. From the investigation by K. Xiong et al. [22], the energy levels of three main defect types inside LAO film, including oxygen vacancy (V_o), oxygen interstitial defects (I_o), and the Al antisite (Al_{La}), were calculated by using the screened exchange (sX) and weighted density approximation (WDA) methods. They believe that the V_o will be the key defect in LAO with 0.7 eV energy level lied below the upper oxide band gap, but not the Al_{La} antisite because the formation energy of the neutral antisite is large, 6.8 eV. Therefore, it is rationally to make the relationship between the oxygen pressure and the oxygen vacancies contents. With increasing the oxygen pressure during PLD process, excess collision and interaction with the atomic oxygen will occur, which corresponds to stronger binding energy of the oxidized peak and less oxygen vacancy defects existence inside LAO thin film. The oxygen vacancies contents inside LAO thin film can greatly dominate thin film's properties, which correspond to its leakage current, breakdown voltage, and conducting behavior, as well as the resistive switching characteristics. In the

following section, we will have a systematic investigation on the electrical characteristics.

The cross sectional structures of the stacked ITO/LAO/ITO devices were characterized by high resolution transmission electron microscopy (HR-TEM) image shown in Fig. 5-10 ~ 5-12, respectively. It can be seen clearly that there exists a very clear interfacial layer (IL) with a more rough surface between the ITO substrate and the LAO film deposited in 2.8×10^{-2} torr oxygen. But nearly no evidence of IL was observed between the ITO substrate and the LAO film deposited in 7×10^{-3} torr oxygen. This indicates that the interfacial reaction between LAO films and ITO is also greatly affected by the oxygen pressure and higher oxygen pressure would be favorable for the formation of IL. The phenomenon can be generally observed at the LAO/Si interface at high oxygen pressure, but was less investigated at the LAO/ITO interface. Once the larger the oxygen ambient gas was purged into the reaction chamber, the more atomic oxygen content will be generated. More collision and reaction is expected to occur at higher oxygen pressure, and more the atomic oxygen may be kicked or impinged onto the substrate surface. This behavior may cause the growth of the interfacial layer during thin film deposition. Formation of the IL during PLD process at low temperature (RT) may lead to lattice distortion or strain near the interface, which causes a rough substrate surface for LAO thin film deposition. From the HRTEM images, three samples show the amorphous phase. The LAO thin films have been reported that the crystallization temperature is about 900-1000 °C, which is anticipated that deposited films may remain amorphous even in the presence of a relatively high-temperature processing. Fig. 5-13 compares the transmittance of ITO/LAO/ITO devices where the LAO films were deposited at various oxygen pressure of 7×10^{-3}, 1.4×10^{-2}, and 2.8×10^{-2} torr. The logo under the transparent device can be seen clearly owing to the transparent ITO, LAO, and glass substrate.

Distinction on the transmittance of the three samples was attributed to the distinction on the structural composition.

5.3.2 The electrical characteristics of forming procedure in ITO/LaAlO/ITO capacitor

LAO thin film properties of the three samples before forming process were investigated here. Fig. 5-14(a) shows the leakage current density of the LAO MIM samples from zero bias to 1 MV/cm. As show in Fig. 5-14(a), with increasing the oxygen pressure, the leakage current density of LAO thin films decreases steeply. In this study, LAO films deposited at low oxygen pressure are believed to have more oxygen vacancies than that of LAO films deposited at higher oxygen pressure, based on the XPS analysis and PLD film growth mechanism as shown above. Under higher oxygen pressure ambient during PLD process, the evaporated species will have excess collision and interaction with the atomic oxygen, thus, stronger binding energy of the oxidized peak and less oxygen vacancy defects existence inside LAO thin film will occur. In has been also evidenced by other groups that oxygen vacancies often exists for oxide film deposited by PLD or Laser MBE. According to Choopun et al. [23], larger leakage current is expected for films with larger density of oxygen vacancy. These results are also coincident with the literature reported by Lu et al. [24] and Xiang et al. [21] The conducting electrons mediate inside LAO film has been regarded via hopping through oxygen vacancies inside the insulator film. Xiang et al. further claimed that the LAO deposited at a higher oxygen pressure promoted the fabrication of highly oxidized films, and consequently reduced the concentration of the oxygen vacancies inside the insulator films. Therefore, the LAO films grown at higher oxygen pressure has lower leakage current owing to lower oxygen vacancies contents. Another reason may be that the absence of oxygen will lead to the

generation of dislocations in the films. Dislocation is also a leakage path, which leads to the increase of leakage current of LAO films. Fig. 5-14(b) compares the breakdown (BD) voltage of the three samples. The L-7 sample exhibits the lowest BD voltages (spread from -17.5 to -18.5 V) while the L-28 samples show the highest one (spread from -26 to -28 V) among the three samples. The evolution of the electroforming is expected to degrade the oxide film and result in the oxygen vacancies generation inside the LAO films. Fig. 5-15(a) shows the leakage current density at positive bias operation. A similar trend to the negative bias operation was observed when oxygen pressure increases form zero to 1 MV/cm, which the current reducing with the oxygen pressure increasing. The breakdown voltage measured at positive bias was shown in Fig. 5-15(b) that a similar tread of increasing the breakdown voltage with the oxygen pressure increases. The need for larger voltage value to degrade the LAO device further confirms that the films in higher oxygen pressure during PLD can lead to higher densification of the film structure. More dense and less relaxation space inside the L-28 samples result in the increased difficulty for oxygen vacancies formation and migration, thus larger applied voltage is further needed. The breakdown information not only demonstrates the integrity and reliability of oxide film but also dominates the following resistive switching properties, which will be discussed in the next section.

The breakdown property of the LAO devices is also investigated by measuring the electrical I-V characteristics at various temperatures from 25 °C to 125 °C. Fig. 5-16(a) ~ 5-16(c) shows the relationship of the BD voltage values versus the temperature. The BD process involves the oxygen vacancies migration and formation under the applied bias. As we can see in the three figures, all the BD voltages decrease with the increasing measured temperature, which indicates that the external thermal heat can facilitate the migration and formation of the oxygen vacancies. In oxide ion conductors, if the number in the unit volume of oxygen vacancies is denoted by n_v, we

may write, for the ionic conductivity, σ_i, the expression:

$$\sigma_i = n_v q \mu_v \tag{5-1}$$

The motion of the oxygen vacancy can be expressed as follows:

$$\mu_v = \mu_v^0 \exp\left(\frac{-E_a}{kT}\right) \tag{5-2}$$

$$\mu_v^0 = \left(\frac{\upsilon a_0^2 q}{kT}\right) \exp\left(\frac{\Delta S}{k}\right) \tag{5-3}$$

Where μ_v is the vacancy mobility, E_a is the activation energy for motion of V_o, μ_v^0 is the pre-exponential factor, T is the absolute temperature, k is Boltzman's constant, is the lattice vibration frequency factor, a_0 is the jump distance and ΔS is a sum of the activation entropy ΔS_a, and the configuration entropy ΔS_f, respectively.

As clearly been seen from the above equation, we can understand why the breakdown voltage decreases with the measurement temperature increasing. High temperature circumstance can provide enough energy for the oxygen ions to jump out from its original lattice site resulting in formation of an oxygen vacancy, and the motion ability of oxygen vacancy directly proportional to the temperature. Because the energy needed for formation and migration of the oxygen vacancy are both provided from the external environment, the voltage value needed to successfully breakdown the oxide film can be gradually reduced as the measured temperature gradually increasing.

To explore the conducting behavior of the LAO devices, the plot of ln (J) vs ln (V) of device was shown in Fig. 5-17(a). The purpose of this discussion is to demonstrate the conducting mechanism during the evolution of the electroforming process by sweeping voltage. In the low voltage region (V < 0.7 V), the curve presents slope of 1 for the L-7 sample. For L-14 and L-28 samples, it also exhibits the slope of 1 in the low voltage region of V < 0.5 V and V < 0.4 V, as shown in Fig.

5-17(b) and 5-17(c), respectively. The observed results in the low voltage region indicate that there might be some preexisted tiny defects such as oxygen vacancies inside the pristine LAO thin films for all the samples, thus contributes the leakage current via electron hopping in the low voltage region. We further investigate on the dependence between conducting current and the temperature as a function of *ln(|I|) vs. $T^{1/4}$* shown in Fig. 5-18. The results confirm that the conducting behavior follow the hopping conduction, which jumps between the discrete defects inside the LAO films. The L-7 sample exhibits longer hopping region than the others, indicating more oxygen vacancies may be expected to preexist inside the LAO films for L-7 samples. One advantage of LAO film is that it has much lower atomic diffusion rates than other binary oxides, such as TiO_2 or HfO_2, which hinders the oxygen vacancy from random migration. Therefore, in the hopping region, neither the Vo migration nor the Vo formation occurs because there may not be enough applied energy for the LAO films to change its microstructure. This case is different from the polycrystalline Gd_2O_3 films that the V_o tends to segregate to the grain boundaries inside the oxide film even under low voltage because the segregation energy of V_o near grain boundaries is quite small, which means that the variation on the LAO films' microstructure may happen at low voltage bias.

In the middle voltage region (about 1 V < V < 6 V), the re-plotted I-V curve can be well fitted to the Schottky emission. It is natural to suggest that the ITO/LAO/ITO structure has a Schottky barrier in the interface because the LAO has a quite low electron affinity. The I-V relation can be expressed as follows:

$$\ln\left(\frac{J}{T^2}\right) = \frac{-q\Phi_b + q\sqrt{\left(qE \middle/ 4\pi\varepsilon_o\varepsilon_r\right)}}{kT} + \ln A^* \tag{5-4}$$

where J is the current density, e is the electronic charge, ε_o is the permittivity of free space, ε_i is the optical dielectric constant, V is the applied voltage, d is the thickness of

a film, k is the Boltzmann's constant, and T is temperature. If the Schottky conduction is obeyed, a linear relationship between $ln\ (J/T^2)$ vs $E^{1/2}$ should be obtained and the slope should give the refractive index n ($n=\varepsilon i^{1/2}$). Fig. 5-19(a) shows the curves of ln (J/T^2) vs $E^{1/2}$ for L-7 sample in the middle voltage region, where linear behaviors are observed. The refractive index calculated from the slope is about 1.874 (with the temperature T of 298 K and thickness d of 30 nm), which is very close to the value of 1.82 for LAO. Hence, it appears that the I-V characteristics of the LAO film are governed by the Schottky conduction mechanism in the voltage region of 0.7 V < V < 6.5 V. Fig. 5-19(b) and 5-19(c) shows the curves of $ln\ (J/T^2)$ vs $E^{1/2}$ for L-14 and L-28 sample in the middle voltage region, where linear behaviors and the refractive index calculated from the slope is about 1.86 and 1.84 are observed. These values are quite reasonable because the lanthanum aluminum oxide contains Al_2O_3 ($n = 1.64$) and La_2O_3 ($n = 2$). Lim et al. [25] observed that the $La_{0.5}Al_{1.5}O_3$ had a refractive index of 1.73 and increased to 1.8 for the $La_{0.9}Al_{1.1}O_3$ films, owing to larger refractive index value of La_2O_3 films. The Schottky emission behavior is further confirmed by the plots shown in Fig. 5-20(a) and Fig 5-21(a) where $ln\ (J/T^2)$ vs $1000/T$ for L-7 and L-28 samples. The activation energies at each voltage $[-q\Phi_b+q\sqrt{(qV/4\pi d\varepsilon_o\varepsilon_i)}]$ are obtained from the slopes in Fig. 5-20(a) and Fig 5-21(a) and are re-plotted in Fig. 5-20(b) and Fig. 5-21(b). The activation energy decreases linearly with V which is in agreement with the Schottky-type thermionic emission theory. The interfacial potential barriers (Φ_b) at the top electrode interfaces were obtained by extrapolating the plots to V=0. The Φ_b at top electrode interface is about 0.73 and 1.46 eV for L-7 and L-28 samples, respectively. Seo et al. [26] have reported that higher oxygen content inside TMO films may result in higher electron affinity of the insulator film, thus leads to a higher interfacial potential barriers between top electrode interface. Jha et al. [27] observed that the work function of the Ru in the Ru/HfO_2 system was found

to be strongly influenced by the oxygen concentration at the metal oxide interface. Interface with deficiency in oxygen atoms result in the lowering of work function for Ru, while interfaces with excess oxygen concentration lead to the increase of work function of Ru. Therefore, a more well-defined Schottky contact will be formed at the interface of oxygen-rich LAO films. Our results are quite consistent with the previous reports. The higher the oxygen pressure during PLD process, the lower oxygen vacancy concentration and an oxygen-rich LAO films interface will be formed. Thus, a shorter hopping behavior at V < 0.4 V follows a longer Schottky conduction at voltage range of 0.4 V < V < 6 V is obeyed, with a larger potential barrier of 1.46 eV at the ITO/LAO interface. The interfacial potential barriers (Φ_b) is increased from 0.73 eV for L-7 to 1.46 eV for L-28, which further confirm that interfacial Schottky barrier might be one of the main reasons why the leakage current is decreased.

When the voltage is near the breakdown voltage, LAO film is expected to have shallow oxygen vacancies generation, and the Frenkel-Poole (FP) conduction mechanism usually fits well with defect-rich LAO thin films. During FP conduction, trapped charge carriers hop between potential wells that define the trap states, and an applied electric field enhances the hopping state because of the barrier-lowering effect. The current density and the electric filed (J-E) characteristics follow the relationship:

$$\ln\left(\frac{J}{E}\right) = \frac{-q\Phi_t + q\sqrt{\left(\frac{qE}{\pi\varepsilon_o\varepsilon_r}\right)}}{kT} + \ln A^* \tag{5-5}$$

where E is the electric field, e is the electronic charge, ε_o is the dielectric constant of free space, ε_i is the high-frequency dielectric constant, k is the Boltzmann's constant, and T is temperature, and ϕ_t is the trap energy level with respect to the conduction band. The *ln (J/E)* was plotted as a function of the inverse temperature in Fig. 5-22(a) and 5-22(b) for L-7 sample. According to this equation, the experimental data results in a straight line with an electric field dependent slope at 6 V < V < V_{BD}. The

activation energies E_a of L-7 samples are obtained from the slopes in the Arrhenius plot, which decrease from 0.41 eV at low voltage to 0.32 eV at higher voltage for top electrode injection, as shown in Fig. 5-22(b). Fig. 5-22(c) shows the plotting of the extracted activation energy values E_a as function of the applied electric field. The trap energy level ϕ_t is estimated from the ordinate intercept point at E = 0 and a value of 0.8 eV is derived. The electrical curves of L-28 sample were also fitted to the FP conduction as shown in Fig. 5-23(a) ~ 5-23(c). The experimental data shows a linear straight slope in the voltage range of 6 V < V < V_{BD}, as shown in Fig. 5-23(a), confirmed the L-28 sample also follow the FP conduction during the voltage range. The activation energies E_a about 1.01 eV of L-28 samples are also extracted out based on the above technique, obtaining the slope decreases from 0.61 eV to 0.52 eV as the voltage increases from 6 V to 9 V. The trap energy level can be interpreted as an electron trap level below the conduction band. The extracted values are close to the energy levels of the oxygen vacancies in LAO calculated in the literature. From K. Xiong et al.'s [22] reports, they have calculated the vacancy state level of LAO films by using the screened exchange (sX) and weighted density approximation (WDA) methods, and claimed that V_o will be the key defect in LAO films. The V_o level inside LAO films lie in the upper oxide bandgap, about 0.7 eV deep for V_o and 0.5 or 0.6 for V_o^{2+}. From the F-P conduction curve fitting, the V_o level in our L-7 and L-28 samples are estimated to be 0.8 and 1.01 eV, respectively, which is quite consistent with the reported data. The trap depth of ϕ_t is increased from 0.8 eV for L-7 to 1.01 eV for L-28, which further indicates that some of the trap states are contributed from the O interstitial because its defect state is much lower than that of V_o defect state. From the fabrication process point of view, the L-28 samples deposited at higher oxygen partial circumstance may suffer highly collision and reaction during films deposition, which will reasonably incorporate some O interstitials inside thin films. Both interfacial

Schottky barrier height and the trap depth of ϕ_t for L-28 samples is deeper than that of L-7 one, which might be the main reasons why the leakage current is decreased.

All the samples in LAO films during the electroforming process follow the three conduction mechanism: Hopping conduction $\rightarrow$ Schottky emission $\rightarrow$ Frenkel-Poole emission, as the applied voltage increases to breakdown voltage (V_{BD}). In the low voltage region, the applied voltage is not high enough for the V_o formation or migration, thus, only trapped electrons hop via the tiny preexisted defects for this conduction. As the applied voltage increases, the dominant conduction current becomes Schottky emission, which reveals that most of the injected electrons gain enough energy to jump across the interfacial barrier. As the voltage value evolves, the V_o might be gradually generated in this Schottky emission region. Until the oxygen vacancy concentration values is high enough, the injected electrons can directly tunnel into the V_o defect states in LAO film instead of jumping across the Schottky barrier height. Since the V_o defect states are about 0.8 ~ 1.0 eV below the conduction band, which is lower than that of interface Schottky barrier height 1.42, therefore, once the defect states form, the current will further increase by conducting through the generated defects.

From the experimental results it was identified that the electroforming in LAO are influenced by the thin film composition and ambient temperature. Some groups observed the evolution of oxygen bubble gas at the anode and identified by using TOF-SIMS [28]. In our LAO films, we also observed the film structural deformation at the anodic side. The evolution of oxygen gas at the anode of ITO/LAO/ITO might be attributed to the formation of oxygen vacancies in LAO. The electrochemical reaction of oxygen vacancy and gas formation at the anode can be expressed in the Kröger-Vink notation as

$$O_o^X \rightarrow V_o^{2+} + 2e^- + \frac{1}{2}O_2 \qquad (5\text{-}6)$$
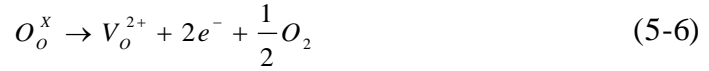
During electroforming LAO molecules are decomposed into free oxygen ions and oxygen vacancies at the anode. Each free oxygen ion donates two electrons to the conduction band (La 4d and Al 2p band). The La and Al ions in the oxygen deficient (oxygen-vacancy-enriched) regions might be reduced to fulfill the local charge neutrality, according to $La^{3+} + ne^- \rightarrow La^{(4-n)+}$ and $Al^{3+} + ne^- \rightarrow Al^{(4-n)+}$, by capturing electrons from the cathode. Therefore, the captured electrons fill the La 4d and Al 2p band. The reduced La and Al ions and the oxygen vacancies can form conduction paths in the insulating LAO matrix. According to the above equation, oxygen vacancies are created in the vicinity of the anode during electroforming, including the decrease in resistance of LAO. The nonhomogeneous growth of the conduction paths is most probably due to the nonuniform distribution of the electric field over the switching cell, which dominates the following resistive switching characteristics.

5.4 Resistive switching characteristics of ITO/LaAlO/ITO T-RRAM devices

In this section, we investigate the influence of oxygen pressure during PLD process of LAO films on the unipolar and bipolar resistive switching characteristics. The surface morphology, atomic composition ratio, crystallinity, grain size, reaction with underlying layer, etc. are greatly influenced by the oxygen partial pressure during deposition. Several groups have reported that the oxygen partial pressure during thin film deposition is a key factor on the switching properties. Park et al. [29] reported on NiO film that whether the stable RS exists or not greatly depending on the oxygen contents during sputtering deposition. As oxygen content increased from 5%

to 10% during NiO film deposition, the resistance value of the NiO film drastically increased, and a resistive switching behavior was observed. However, as the oxygen content increased to 20%, the resistive switching behavior disappeared. According to RBS and XRD data, both metallic nickel defects and nickel vacancies coexist in a NiO film and as they increase oxygen content in the gas mixture, metallic nickel defects decrease and nickel vacancies increase. Because the HRS and LRS current of NiO film is mainly mediated with these metallic nickel defects and nickel vacancy proposed by Seo et al., thus the different metallic nickel defects or nickel vacancies contents will lead to different RS properties. Chang et al. [30] observed that oxygen content in the sputtering gas can determine the peak intensity of anatase or rutile phase. With increasing the oxygen content in the sputtering gas mixture, the peak intensity of anatase phase and HRS resistance values significantly increases. It may be related to the increase of anatase content in TiO_2 matrix as the anatase phase has a wider bandgap and higher resistivity than rutile phase at room temperature. From the above reports, we know that the oxygen pressure influence the atomic composition ratio, crystallinity orientation, oxygen vacancy concentration and distribution inside a TMO layer, thus it will determine the thin film properties as well as the RS characteristics.

We have investigated the thin film properties including surface morphology, crystallinity, structural composition in the last parameter. In this section, we will discuss these parameters in relation to RS characteristics including switching properties, operation voltage dispersion, endurance, retention, readout test, conduction behaviors, and switching mechanism of PLD-deposited LAO films by modulating the oxygen pressure during PLD process.

5.4.1 Bipolar resistive switching characteristics in ITO/LaAlO/ITO T-RRAM

devices

(a) Comparison on different growth oxygen pressure of LAO thin films

To perform the RS characteristics, the electroforming process is necessary to activate the RS characteristics for all the LAO devices. The detail electroforming procedure has been discussed detail in Section 5.3.2. The current compliance of 10 mA was chosen for an appropriate current value level for reducing the operation power, even if larger current compliance can also perform the RS properties. After the electroforming process, the devices were tested under different switching polarity. As can be seen in Fig. 5-24, three devices all exhibit a bipolar RS behavior, and the RS from the low resistance state (LRS) to high resistance state (HRS) can all be realized under positive voltages (clockwise loop). To evaluate the memory performance of the ITO/LAO/ITO devices, the endurance characteristics were measured. Fig. 5-25(a) ~ 5-25(c) compares the endurance characteristics of the three LAO devices. The devices were measured in the voltage list sweep mode by performing a series of consecutive set/read/reset/read cycles. Among the consecutive switching cycles, several times of switching-failure cycles are observed on the L-7 devices, while the resistance values in both states become distinguishable on the L-28 devices. The average values of the resistance ratio measured at the bias voltage of 0.1 V is about 4.7, 9.7, and 26.7 for the L-7, L-14, and L-28 samples, respectively. As a NVM device application, the RRAM devices usually require a large resistance ratio between HRS and LRS for obtaining a high signal-to-noise ratio. Furthermore, a long endurance characteristic under repetitive switching test still maintaining a distinguishable high to low resistance ratio is the key issue for us to seek. Thus, a detailed research on the relationship between the RS characteristics and the microcrystalline structure is necessary to elucidate the detailed switching mechanism. Then, we further collected the operation voltage for the discussion on the switching stability. Fig. 5-26(a) ~ 5-26(c) shows the SET and

RESET voltage distribution of the three LAO thin films grown at 7×10^{-3}, 1.4×10^{-2}, and 2.8×10^{-2} torr, respectively. As we can clearly see from these three figures, the SET and RESET voltage distribution decreases with the growth oxygen pressure increases. We suggest that the difference on the RS characteristics may come from the intrinsic material difference between the samples grown at different oxygen pressure.

(b) Electroforming procedure

To explain why samples grown under different oxygen pressure during LAO films deposition will cause different electrical characteristics, voltage/resistance dispersion and its physical mechanism, the forming process is the key factor to be discussed. For the amorphous LAO films, it requires much higher energy for the oxygen ions and vacancies migration inside the amorphous film, and no preferred orientation or grain boundaries exist inside LAO films. Though we have introduced the electroforming process of the Gd_2O_3 films in the last chapter, however, the electroforming procedure was quite different compared to the LAO films. The main distinction between the two samples is attributed to their crystallinity: the Gd_2O_3 film is polycrystalline and the LAO film is amorphous. The electrochemical reaction of oxygen vacancy at the anode can be expressed in the Kröger-Vink notation as we shown above. When using negative voltage application to the TE, a large number of oxygen vacancies are introduced at the LAO/BE interface according to the electrochemical reaction, leading to the reduction of the SBH at the interface. Therefore, the LAO/BE interface serves as a source of oxygen vacancies. Several groups have reported that the oxygen vacancies will migrate away from the anode and accumulate at the insulator/cathode interface on a variety of materials [31,32]. However, the LAO films in our study are all amorphous, and these oxygen vacancies inside LAO films are hard to migrate. In addition, the oxygen vacancy diffusion

coefficient inside the amorphous LAO film is quite low. This results in a much larger forming voltage of the LAO films during the electroforming process. C. Tang et al. [33] have calculated the diffusion of O vacancies near Si:HfO$_2$ interface by using the VASP code with the Vanderbilt ultrasoft pesudopotentials. A detailed first principles calculations on several types of Si:HfO$_2$ interface both to assess their relative stability and to understand the tendency for the atomic level diffusion of O vacancies. They concluded that the strong thermodynamic and kinetic driving forces exist for the segregation of O vacancies to the interface. K. McKenna et al. [34] used empirical pair potentials and the METADISE code to generate a number of prospective low energy boundary configurations. He calculated segregation energies of an oxygen vacancy in the vicinity position away from the GB, and observed that the segregation energy of a vacancy from a bulklike three-coordianted position to a site at the GB (barrier : 0.42 eV) is much smaller than that away from the GB (barrier : 1.14 eV). And the diffusion of a vacancy parallel to the boundary is in barrier of about 0.57 eV. He further observed that for a wide range of concentrations, vacancies are significantly closer together at the GB than in the bulk. About 86% of the defects segregate to the GB, which the GB can act as sinks for oxygen vacancies then percolation paths may be preferentially generated along these GB. The existence of the GB inside ITO film near LAO/ITO (BE) interface may act as a catalyst for oxygen vacancies migration along the GB. Based on the reported literature, the energy needed for oxygen vacancy to migrate (E$_{migr}$) is much lower than to form (E$_{form}$), especially lower in the interface than that in the bulk. For the L-7 samples, the LAO films directly contacts with the ITO electrode due to no additional IL formation at the LAO/ITO interface. The conductivity of ITO is n-type as a result of oxygen vacancies and the presence of tin dopant which has a higher valence than indium. These oxygen vacancies provide electrons by acting as singly or doubly charged donors, and films

239

are generally sufficiently oxygen deficient that the electron gas in the conduction band is degenerate. For L-7 samples, during electroforming process under negative bias, oxygen vacancies are generated at the bottom of LAO films first near GB since it has the lowest segregation energy, as discussed above and shown in Fig. 5-27(a) ~ 5-27 (c). Oxygen vacancies are preferentially formed at the LAO/ITO (BE) interface than that in the bulk, and then the process toward to the ITO (TE)/LAO side with the forming voltage increasing. The oxygen vacancies are generated in a broad range at the LAO/ITO (BE) while the other side is only a small measurement probe tip. The probe contact size difference causes a gradual distribution on the oxygen vacancy concentration, as shown in Fig. 5-27(c). As we compared the L-7 and L-28 samples, a more dense (with trap depth of 1.01 eV), well-defined Schottky barrier (with barrier height of 1.46 eV), and an additional IL was formed on the L-28 sample. For L-28 samples, this additional layer blocks the LAO film from the ITO (BE) electrode. Furthermore, under the high oxygen pressure circumstance, the oxygen adatoms will deposit on ITO (BE) film surface, diffuse into the ITO film, and reoxidize with In or Sn atoms at the grain boundary. This will increase the grain size of the ITO (BE) films. Wu et al. [35] reported the presence of oxygen enhances the crystallization of the film. Film grain size increases as more oxygen is added. It was also confirmed from the transmittance of the ITO films. In previous work, it was argued that the oxygen deficiency in the ITO film would contribute to blackening of the ITO film. Therefore, once the additional oxygen gas is added on the ITO films, the blackening of the transmittance of the ITO films will be improved, as shown in Fig. 5-13. This additional amorphous thin layer will contribute on the uniform generation of the oxygen vacancies inside the LAO films, as shown in Fig. 5-28(c). It will change from the gradual generation (trapezoid shape, from bottom ITO film toward top ITO film) to uniform generation (rectangle shape) of oxygen vacancies, since there was no

preferentially preexistence of the defects, dislocation, and grain boundaries. The schematic diagrams of the forming procedure were shown in Fig. 5-28(a) ~ 5-28(c). The higher oxygen pressure during PLD process can effectively compensate the oxygen vacancies concentration near the interface, thus causing a blocking oxide at the LAO/ITO (BE) interface. This GB inside ITO films was not only reduced but also terminated by the additional thin layer. We argued that this structural difference under different oxygen pressure will also cause a distinction on the switching characteristics, reliability and stability. Many residual tiny defects may be generated at the LAO/ITO (BE) interface of L-7 samples owing to lower segregation energy during eletroforming process. These tiny defects may contribute on higher concentration of oxygen vacancies at the bottom interface. Because of the amorphous phase of our LAO films, these oxygen vacancies are difficult to migrate or diffuse, acts as like fixed states near the interface. When negative bias was applied to the device, injected electrons can hop via the various tiny defects to the bottom ITO electrode, thus causing the state to LRS. During the RESET process, positive bias was needed to rupture the conducting paths. The positive bias can attract the oxygen ions back to reoxidize with the oxygen vacancy and rupture the conducting paths. However, because of many residual tiny defects exists at the interface and high conducting mobility of the oxygen ions inside ITO film, the oxygen ions supply for this reduction process may be insufficient. This will sometimes cause a RESET-failure phenomenon during switching and fail on the reliability of the resistance state, as shown in Fig. 5-27(d) and (e). For L-28 samples, the oxygen vacancy and grain boundary at the ITO (BE) surface will be much reduced under the oxygen gas circumstance of PLD process. The will avoid preferentially formation of the oxygen vacancy at the interface. Furthermore, a blocking layer growth between LAO and ITO (BE) electrode terminate the extended defects formation. This leads to a uniform distribution on the

oxygen vacancy concentration from top to bottom insulator film, and the oxygen vacancy will not segregate at the bottom interface. Therefore, once a sheet layer of the LAO films near the bottom interface was reoxidized under positive bias, the state can be switched back to HRS accurately, as shown in Fig. 5-28(d).

(c) Switching parameters test

To further understand the effect of applied voltage on the RS characteristics, the detailed switching parameters are operated and tested here. First, we sweep the I-V curve by fixing the V_{reset} of 2 V and varying the V_{set} from -0.5 to -10 V on L-7 samples, as shown in Fig. 5-29(a). In this test, we observed on the effect of different V_{set} values to the high to low resistance ratio, while the V_{reset} is fixed. The resistance value versus set voltage is plotted and shown in Fig. 5-29(b). The LRS resistance value shows highly dependent on the V_{set} (the LRS resistance values decreases with increasing the V_{set}), while HRS is nearly independent. The resistance ratio increases with V_{set} from 1.3 to 8. The set process is corresponding to the formation of oxygen vacancies inside the LAO films under the external negative bias. Therefore, larger V_{set} values means that a stronger or more conductive leaky paths are formed inside the insulator matrix, as a result of lower LRS resistance values. The independent correlation between HRS and V_{set} may be owing to the fixed V_{set} values of 2 V for all the operation. We also performed the same V_{set} test measurement on L-14 and L-28 samples, as shown in Fig. 5-30(a) and 5-31(a), respectively. The L-14 and L-28 devices show the similar tendency on the applied set voltage like the L-7 sample, which the resistance ratio increases with the applied V_{set} values, as shown in Fig. 5-30(b) and 5-31(b), respectively. The resistance ratio increases with V_{set} increasing from 1 to 7.3 and from 1 to 8.63 for the L-14 and L-28 samples, respectively. A rapid decrease on the LRS resistance values when V_{set} is operated under $0 < V_{set} < |-2|$ V,

while saturated to a nearly constant value at larger |-2| V in all samples. It means that the |-2| V is already enough for a LAO-based memory device to perform the RS characteristics. Then, we sweep the I-V curve by fixing the V_{set} of -3 V and varying the V_{reset} from 0.5 to 10 V on L-7, L-14, and L-28 samples, as shown in Fig. 5-32(a), 5-33(a), and 5-34(a), respectively. In this test, we observed on the effect of different V_{reset} values to the high to low resistance ratio, while the V_{set} is fixed. The resistance value versus set voltage is plotted and shown in Fig. 5-32(b), 5-33(b), and 5-34(b), respectively. As we can see from the three figures, we obtain an opposite correlation compared to the previous test that the HRS resistance value shows highly dependent on the V_{reset} (the HRS resistance values increases with increasing V_{set} value), while LRS is nearly independent. The reset process is corresponding to the rupture of the conducting filaments by reoxidation inside the LAO films under the external positive bias. Therefore, larger V_{reset} values means that the more conductive filaments are broken or ruptured inside the insulator matrix, as a result of higher HRS resistance values. We obtain the similar tendency on the three samples that the HRS resistance values increases with the V_{reset} voltage. The high to low resistance ratio varied from 2 to 21, from 1 to 17, and from 3 to 34 for the L-7, L-14, and L-28 samples, respectively. We also observed that a rapid increase on the HRS values when voltage is near 2 V, while saturated when reset voltage is larger than 2 V. When an appropriate set/reset voltage was chosen to perform the RS cycle, we can obtain more endurable RS characteristics with a resistance ratio margin large enough. We further compare the relationship of V_{set} and V_{reset} to resistance ratio among the three samples. The V_{set} value variation shows stronger dependence on the resistance ratio at low voltage region V < |-2| V than that of V_{reset} one. The results reveal that the rate of formation and rupture of the conducting filaments is asymmetry under certain same voltage values but opposite polarity, and formation of conducting filaments are much easier

than that of rupture them though the detailed switching mechanism of LAO-based memory still not discussed. Therefore, we conclude that the switching mechanism based on merely trapping/detrapping of injected electron carriers and migration of the oxygen ions or vacancies can be excluded because of highly asymmetry on the response to the applied voltage values. The higher resistance variation response to the applied voltage values indicates that the lower time it takes to achieve the same resistance value. The rupture of conducting defects takes more time than that of formation, which means that there might be reaction involved during the RS. We also observed that the dependence of HRS resistance values as a function of V_{set} reduces with the oxygen pressure increases. The variation sensitivity for V_{set} on L-7 samples is about 3200 ohm/V, while reduces to 2200 and 1200 ohm/V for L-14 and L-28 samples. However, the variation sensitivity for V_{reset} is about 480, 600, and 820 ohm/V for L-7, L-14, and L-28, which means that the variation sensitivity increases with the growth oxygen pressure. Our proposed model in last paragraph can also well explain this phenomenon. Since the LAO film of L-7 sample directly contacts with the ITO (BE) electrode without IL, higher oxygen vacancies concentration may be formed and many tiny oxygen defects may exist at the interface. In addition, the high oxygen ions migration mobility inside ITO films can easily diffuse away through the GB, therefore, the much higher variation sensitivity for V_{set} on L-7 sample is observed. An addition IL existence between the LAO and ITO (BE) electrode on the L-28 samples blocks the easy formation of the oxygen vacancy at the interface and limits easy migration along the GB. Oppositely, the variation sensitivity for V_{reset} of L-7 samples exhibits a reverse result. Many tiny residual defects at the LAO/ITO (BE) interface are hard to be ruptured, which results in larger applied voltage value is needed to back to HRS on L-7 samples.

(d) Where to rupture

To further confirm our switching model, we have also investigated on where to rupture the conducting paths inside a LAO film. In the case of conventional I-V measurement, the bias was applied from top-to-bottom electrode with grounded bottom electrode. In contrast, we applied bias from top-to-top electrodes (horizontally) when one pad is applied bias and the other one is bottom grounded. First, we electroform two RRAM devices separately, which one is by negative bias (pad A) and the other is by positive bias (pad B). This was equivalent to achieve a series of negative bias to switching on the device, as shown in Fig. 5-35(a) and 5-35(b). After electroforming process, then the RRAN with a series of two pads can be switched to LRS and HRS under the applied bias. The resistance values of pristine, HRS and LRS in the A-G, B-G, and A-B films were measured in Fig. 5-36. Operation 1 shows the resistance values of the pristine samples in the order of several hundreds MΩ. The resistance values variation with the HRS and LRS are also shown in the inset of Fig 5-36. As we clearly observed in this figure, only the B-G resistance values change during the continuous switching, while the A-G operation remains the same. It means that only the dielectric films near bottom electrode was altered during the RESET process, i.e. the B-G side. This measurement results further confirm that the change of the resistances values occurs in the vicinity of the cathode electrode. Therefore, the microstructure and components difference at the LAO/ITO (BE) interface may greatly dominate the RS characteristics, and the switching model can well explain why different RS properties are observed under different thin film fabrication process.

5.4.2 Polarity issue of the bipolar resistive switching characteristics in ITO/LaAlO/ITO T-RRAM devices

The bipolar RS characteristics of LAO films operated under negative bias for

SET and positive bias for RESET process (clockwise loop) have been thoroughly investigated in last paragraph. And the different polarity issue on the RS behaviors will be discussed in this parameter. The opposite polarity of the bipolar RS characteristics can both be performed on our LAO films, i.e. it can be operated by the clockwise sweeping loop or by the counter-clockwise sweeping loop. However, the RS properties under the two kinds of operation are quite different. Fig. 5-37(a) ~ 5-37(c) show the RS I-V curves of the three samples. Three LAO films can all be operated by the counter-clockwise sweeping loop. We can further observe that the LAO films deposited at higher oxygen pressure have the longest endurance performance, as shown in Fig. 5-25(a) ~ 5-25(c). It was quite different to samples under the clockwise sweeping operations, the high-to-low resistance ratio is improved with increasing the oxygen pressure from 7 to 28 mtorr. Though our ITO/LAO/ITO capacitor structures look like symmetry, we prove from the XPS and TEM analysis above that our LAO structures were asymmetry. The critical factor to cause the structure asymmetry is the PLD process during LAO films deposition. The difference of the asymmetric structure of ITO/LAO/ITO films may contribute to distinct electrical characteristics. We have discussed detailed in last section that the structural difference will cause a different oxygen vacancy distribution inside the LAO films, thus determine the final switching properties. In this section, we will discuss on the LAO films under positive bias electroforming procedure and compare how different voltage polarity causes the distinction on the defects distribution inside the LAO films.

We applied electroforming process on LAO films by positive bias on ITO (TE) when the counter-clockwise sweeping loop was performed. Under positive voltage, oxygen vacancies are formed at the ITO (TE)/LAO interface, and lead to the reduction of the SBH at the ITO (TE)/LAO interface. In this case, the three cases are

246

quite the same (no additional interfacial layer), and only a little oxygen contents difference for the LAO films. Oxygen vacancies in a gradual distribution within the LAO films will be obtained after electroforming process. The switching cycles increase with increasing the oxygen pressure indicates the oxygen vacancies inside the LAO films should be well controlled. However, the RS was quite poor compared to the clockwise loop, since the absence of additional IL at the interface. The IL can serve as an oxygen reservoir or a good diffusion barrier to terminate the oxygen ions random migration along the extended GB at the interface. When the devices were operated at the counter-clockwise sweeping loop, the oxygen ions can easily diffuse in and out via the GB inside ITO electrode to the atmosphere. Chemical oxidation may also take place by virtue of external oxygen to cause the conduction path reoxidation. Thus, the RS properties will much poor than that of clockwise loops.

5.4.3 Switching mechanism of the ITO/LaAlO/ITO T-RRAM devices – Random resistor network model

For an amorphous LAO thin film, the conducting current is based on the density of oxygen vacancy inside the insulator film, which was determined from the chamber condition during PLD deposition. The cluster defects, such as dislocation or grain boundary, are expected to be absent in an amorphous film, as shown in Fig. 5-9(a). Based on Miller and Abrahams's model [36], the conduction for an electron transition from one defect site to another in amorphous thin films can be regarded as an equivalent network of random resistors. The schematic diagram of the random resistor network is shown in Fig. 5-38(a). They assumed that a random network is effectively equivalent to a set of independent chains of resistances, each chain passing through the entire sample from one electrode to the other. The resistances of a single chain are in series, and hence the chain resistance is given by the sum of individual resistances

R_{ij}. A simple interpretation of their calculation for relatively high temperature is of the order of unity and $R_{ij} = R_{ij}^0 \exp(\xi_{ij})$, where $\xi_{ij} = \dfrac{2r_{ij}}{a}$ and $R_{ij}^0 = \dfrac{kT}{e^2 \gamma_{ij}^0}$. ξ_{ij} is isotropic impurity wave functions, R_{ij} is the distance between site i and j, and a is the Bohr radius. When a critical number of sites is occupied by these traps, a percolation path is formed between the two electrodes and the *I-V* characteristics of the whole system can behave like a power law, $V = \rho_{eff} I^{\alpha}$, where ρ_{eff} is the effective resistivity of the system, and α exponent is obtained from the slope of the *V-I* curves [37,38]. Shklovskii and Efros [39] proposed a method of calculating the random network conductivity, based on the mathematical theory of percolation. Random sites are chaotically distributed points in insulator film, and a percolation path formed under the applied bias contributed to the resistivity in the form of $\rho_{eff} = \rho_0 \exp\left[\alpha /(N^{1/3} a)\right]$, where N is the concentration of vertices of the Miller-Abrahams network, which coincides with the concentration of the major dopant. We suggest that the resistivity of the network system decreases with increasing the applied voltage is related to the generation of a critical number of electron traps in the oxide film. The main defects inside the LAO thin film are reported to be oxygen vacancy by Xiong et al. [22], therefore, we may rationally suggest the concentration of the dopants N are the oxygen vacancies inside LAO film.

Then, we can propose the switching mechanism of amorphous LAO thin film as follows. The conduction transition between IRS, HRS and LRS is consequently attributed to the electron transport controlled by the feature of oxygen vacancies. In the beginning, the separation between oxygen vacancy is in a large distance (larger than the critical percolation radius r_c), thus, only tiny leakage current can be obtained. Electroforming triggers the percolation process occurrence by inducing more oxygen vacancy N in the insulator film, as shown in Fig. 5-38(b). The percolation radius r_c

depends solely on the site concentration N ($r \propto N^{-1/3}$), while N can be determined from compliance current during electroforming. Therefore, whether the RS exists or not will as a function of the compliance current, as shown in Fig. 5-39. After electroforming, it turns out the exponent in the electrical conductivity is entirely determined by jumping over the distance of the percolation radius. At LRS in Fig. 5-38(b), oxygen vacancies are considered to be separated by a smaller distance r, leading to the smaller resistivity of LAO thin film. When an opposite electric field is applied onto the MIM structure, some oxygen vacancies are annihilated or recovered, causing the r to be larger and the state switches to HRS. The dotted circle shown in Fig. 5-38(c) represents the enlarged percolation radius. The oxygen vacancies are not necessarily aligned in filamentary configurations throughout the capacitor to the LRS. These defects will be arranged in a feature of percolation network as long as the portion of the defect density exceeds certain threshold to form the LRS. One can use the percolation network model to estimate the expected resistance values and/or determine the desired compliance current for a reliable switching operation for a certain material of insulator film free from overshooting.

5.4.4 Conduction mechanism in ITO/LaAlO/ITO T-RRAM devices

(a) Conducting mechanism

In order to obtain an extended understanding about the switching characteristics of RRAM devices, the conduction mechanisms of the HRS and LRS were examined. The plots of the ln (J) - ln (V) in the L-7 and L-28 devices are shown in Figs. 5-40 ~ 5-41. The conduction behavior in the LRS (the curve 2 and 3) under both positive and negative bias undergoes Ohmic transport, because the curve of the ln (J) - ln (V) is a linear line with a slope of about 1 for all the samples. The conduction behavior in the HRS is also governed by Ohm's law at a low voltage region due to the straight slope

(~1). Taking into account the fact that forming process is necessary to develop resistance switching, the filament conduction is suggested in the low voltage region for both the stable LRS and HRS. However, it seems that an entirely different conducting mechanism is dominated in the high voltage region. This linear relation changes from 1 to 2 at larger voltage indicates that the conducting behavior is dominated by the space-charge-limited conduction (SCLC), for all the samples. In the sweeping curve 1 as shown in Fig. 5-40 (a) and Fig. 5-41 (a), the residual electrons inside the LAO films contribute to the Ohmic conduction behavior in the HRS. As the applied voltage continuously increases, the amounts of injected electrons will be larger than the residual electrons, and hop through the oxygen vacancies which were generated during the electroforming process, thus contribute on the SCLC behavior. From the Kröger-Vink notation as we shown above, an oxygen vacancy and two electrons will be generated once an oxygen atom was removed. These oxygen vacancies can provide defect states for injected electrons occupancy, therefore, the conductivity of the LAO films may be increased. Since we have discussed above that the main defects inside the LAO films are oxygen vacancies, the numbers of the trapped electrons will dominate the conducting current. Once all the traps are filled by the injected electrons, the state was switched to LRS. The state then can be switched back to HRS by applied positive values to drive the oxygen ions back into LAO films. When the oxygen vacancies are recovered by reoxidation with the oxygen ions, the current gradually reduced and the state was switched to HRS, as shown in curve 4 in the Fig. 5-40 (b) and Fig. 5-41 (b). To obtain a reliable resistance value of the respective state, the same voltage values have to be added. Otherwise, an intermediate state with a different resistance value will be obtained. It implies that the multi-level states are possible to be achieved.

We observed that the conducting behavior of the LAO films changes in the

following procedure of Hopping conduction → Schottky emission → Frenkel emission during the electroforming process. After electroforming, the conducting mechanism changes to the SCLC. The conduction behavior changes from contact limited (Schottky emission) to the bulk limited (SCLC) indicating that the well-defined Schottky barrier was destructed during the forming procedure. We suggest that the total destruction of the Schottky barrier was occurred at the voltage value when the conduction behavior changes from Schottky emission to Frenkel emission. Owing to low oxygen vacancy mobility inside the amorphous LAO films, a larger electroforming voltage is needed to break the Schottky barrier. At the same time, oxygen vacancies were also generated inside bulk LAO films during the forming process.

(b) Reliability

As a NVM device, reliable and stable data retention for a long time is required to maintain the information accuracy. And the switching between HRS and LRS must have a large resistance ratio to keep a high signal-to-noise ratio during the repeated switching. So, the reliability issues of the LAO-based T-RRAM devices were tested here. The retention data of the three samples measured at a positive voltage of 0.1 V at RT were shown in Fig. 5-42(a) ~ 5-42(c). The resistance values of high and low resistance states were almost constant for more than 10000 s without any fluctuation or degradation. We perform the acceleration test by elevating the measured temperature. Fig. 5-43 shows the resistance values of OFF state and ON state of L-28 samples as a function of reciprocal temperatures. It is found that the current of the HRS exhibits positive dependence on temperature like the pristine samples, implying the semiconductor-like behavior. The relationship between the resistance of OFF state and temperature can be well fitted to $R = R_o \exp(Ea/kT)$, where R_o is a constant

251

independent of temperature, k the Boltzmann's constant, T the temperature, and Ea is the activation energy for charge carriers. The Ea for the HRS is about 0.46 eV. Different from the HRS, the resistance values of the LRS increases with increasing temperature, which indicates the conduction mechanism is metallic like.

5.5 Conclusion

We have successfully fabricated the LAO based T-RRAM capacitor devices and investigated its RS characteristics. The high-k dielectric LAO thin film deposited by pulsed laser deposition grown at different oxygen partial pressure is investigated in this study. Based on the pulsed laser deposition growth mechanism, we clearly explain how different oxygen partial pressure influences the surface roughness, the formation of the interfacial layer, the leakage current density, the breakdown voltage, and the resistive switching characteristics of the LAO thin films. The micro-structure and oxygen concentration difference inside LAO thin films may be the main reason for the distinction of the resistive switching characteristics. Conduction behavior of the electroforming procedure was investigated under the electrical fitting curve. It changes from Ohmic conduction, to Schottky emission in the middle voltage value, and to Frenkel emission in the vicinity of breakdown voltage. The residual electrons inside LAO contribute to the space-charge-limit conduction during the RS operation. LAO films grown at higher oxygen partial pressure is beneficial for a more reliable resistive switching performance, because the formation of the interfacial layer and lower oxygen vacancy concentration exist in the LAO thin film. The interfacial layer can serve as a good oxygen reservoir residence and the more oxygen ions involve can ensure the switching reliability. Migration of the oxygen ions between the interfacial layer and the LAO films under applied bias may be the possible switching mechanism. We also construct the electroforming model to explain why the switching properties

will differ after forming process. A blocking layer growth between LAO and ITO (BE) terminate the extended defects, which leads to a uniform distribution on the oxygen vacancy concentration from top to bottom insulator film. The high to low resistance ratio as a function of compliance current reveals the correlation between the resistive switching properties and the percolation theory of nonlinear conductor networks. The ITO/LAO/ITO device may be a strong candidate for future nonvolatile memry application.
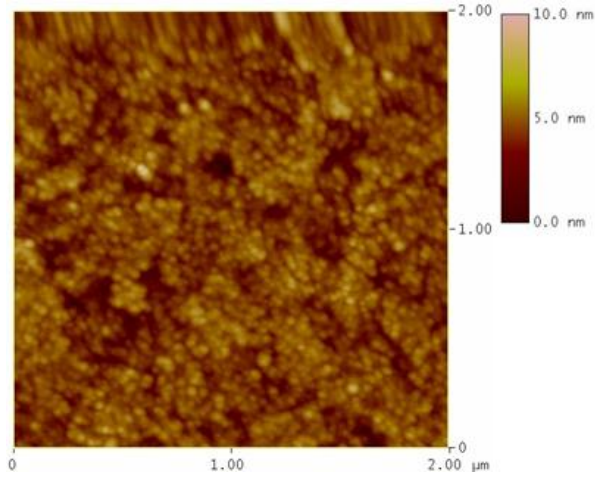
Fig. 5-1   AFM image of the LaAlO films grown at oxygen partial pressure of 7×10^{-3} torr.
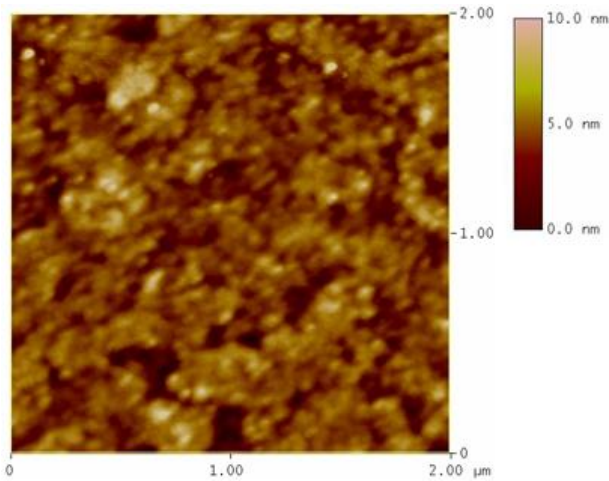
Fig. 5-2   AFM image of the LaAlO films grown at oxygen partial pressure of 1.4×10^{-2} torr.
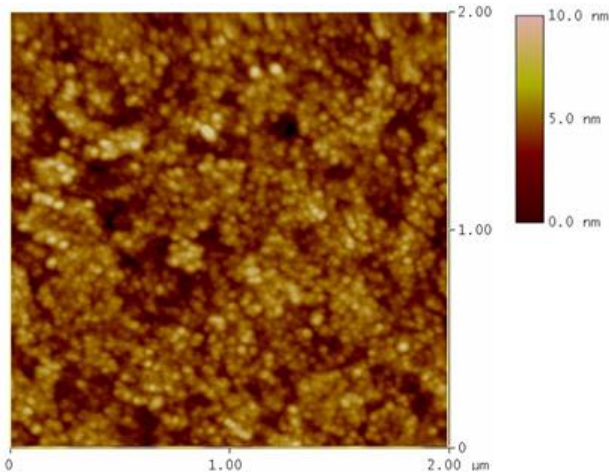
Fig. 5-3   AFM image of the LaAlO films grown at oxygen partial pressure of 2.8×10^{-2} torr.
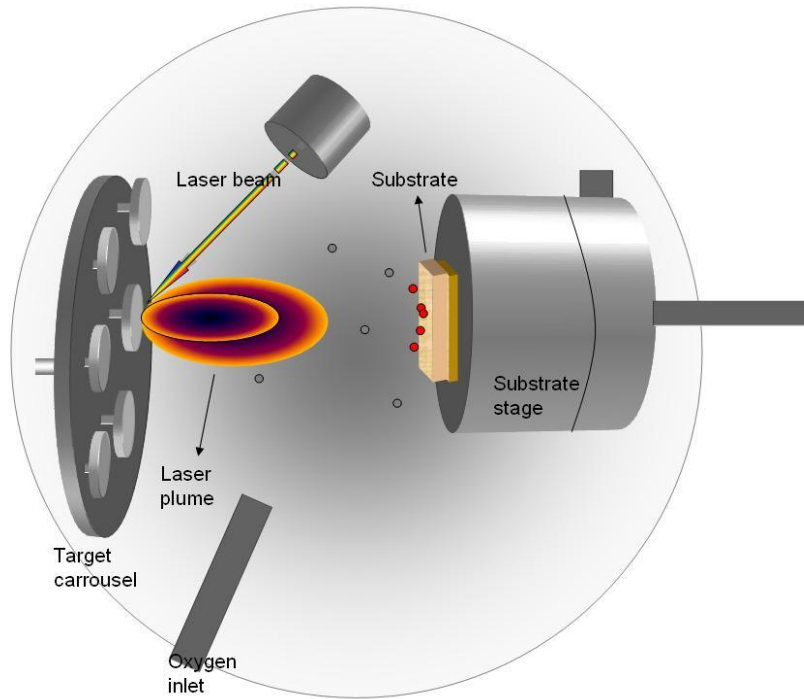
Fig. 5-4 Schematic diagram depicts the pulsed laser deposition fabrication process in low oxygen partial pressure.
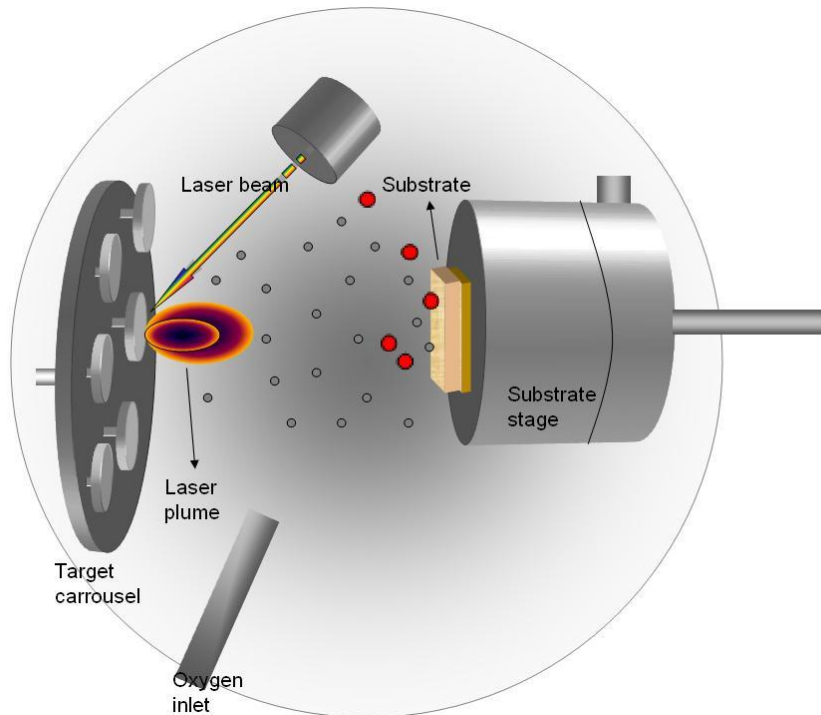
Fig. 5-5 Schematic diagram depicts the pulsed laser deposition fabrication process in high oxygen partial pressure.
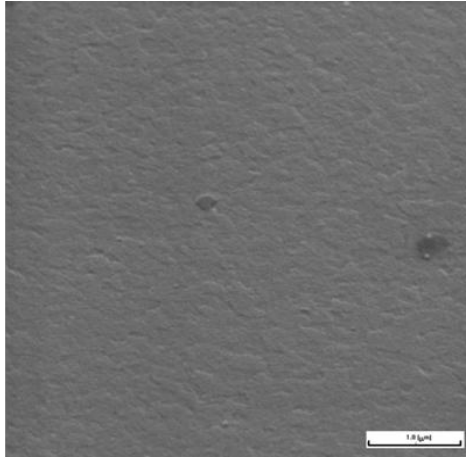
Fig. 5-6   Surface morphology image of the LaAlO films grown at oxygen partial pressure of 7×10^{-3} torr.
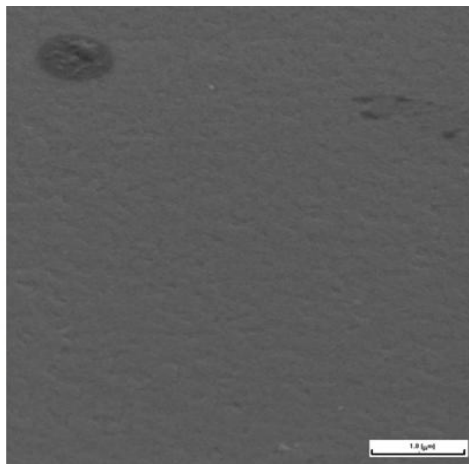
Fig. 5-7   Surface morphology image of the LaAlO films grown at oxygen partial pressure of 1.4×10^{-2} torr.
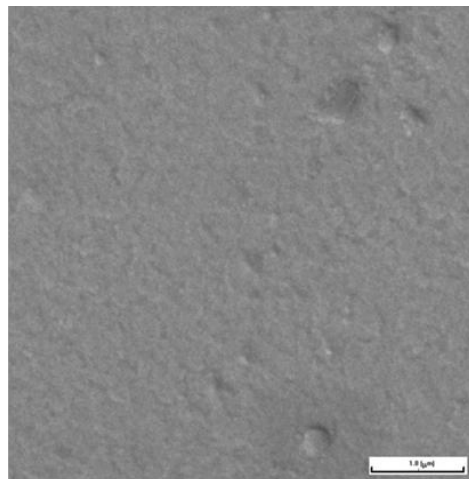
Fig. 5-8   Surface morphology image of the LaAlO films grown at oxygen partial pressure of 2.8×10^{-2} torr.
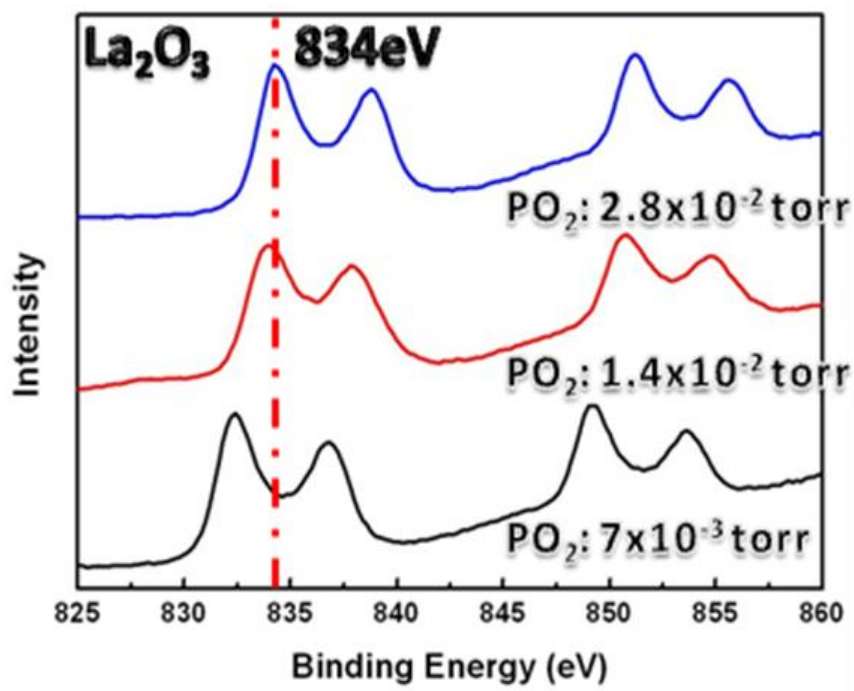
Fig. 5-9 (a)   The La 4d spectrum of LAO deposited at various oxygen pressure.
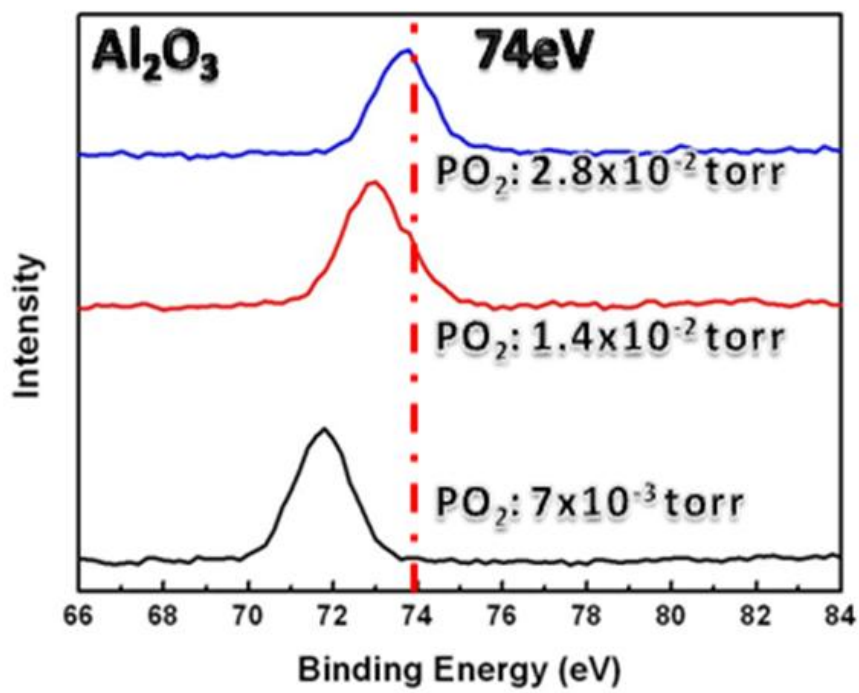
Fig. 5-9 (b)   The Al 2p spectrum of LAO deposited at various oxygen pressure.
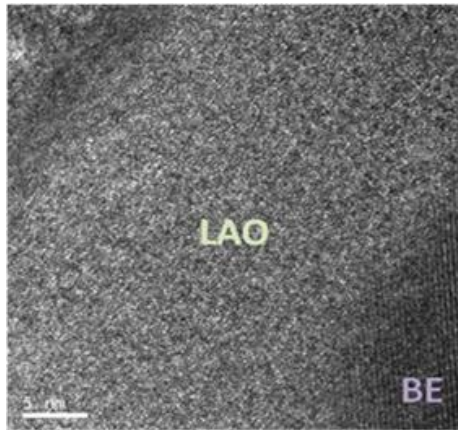
Fig. 5-10　High resolution cross-sectional TEM image of the LaAlO films grown at oxygen partial pressure of 7×10^{-3} torr.
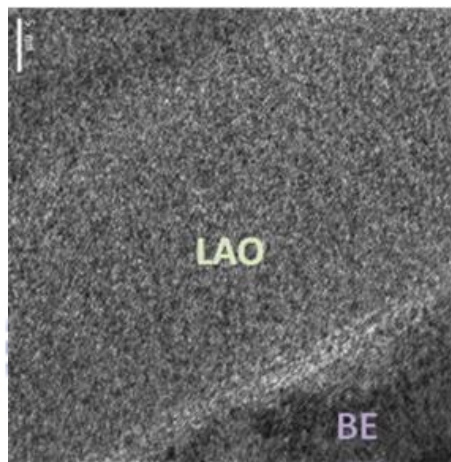
Fig. 5-11　High resolution cross-sectional TEM image of the LaAlO films grown at oxygen partial pressure of 1.4×10^{-2} torr.
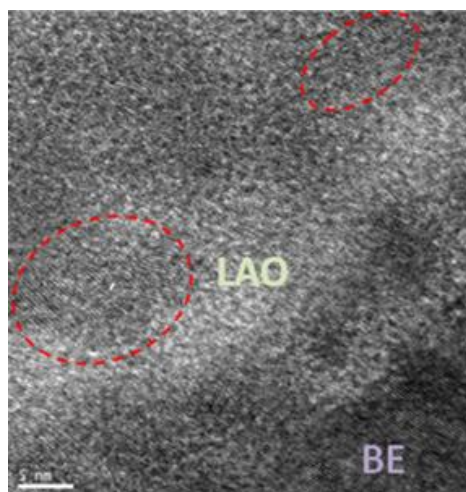
Fig. 5-12　High resolution cross-sectional TEM image of the LaAlO films grown at oxygen partial pressure of 2.8×10^{-2} torr.
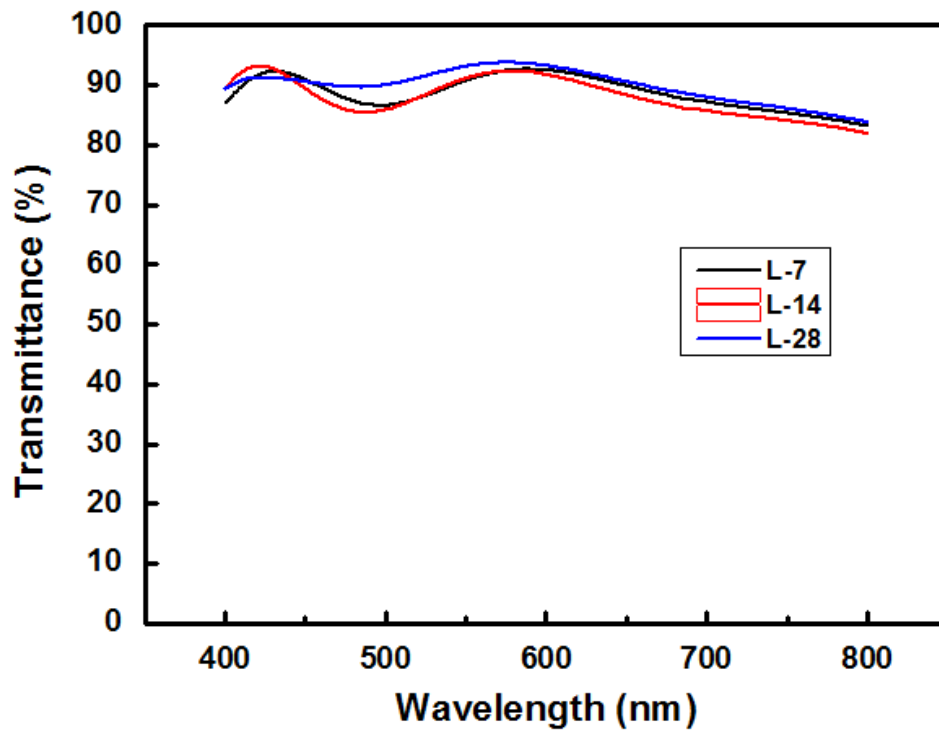
Fig. 5-13   Transmittance of the ITO/LAO/ITO structure grown at various oxygen pressure of 7×10^{-3} (L-7), 1.4×10^{-2} (L-14), and 2.8×10^{-2} (L-28) torr under wavelength of visible light in the range of 400-800 nm.
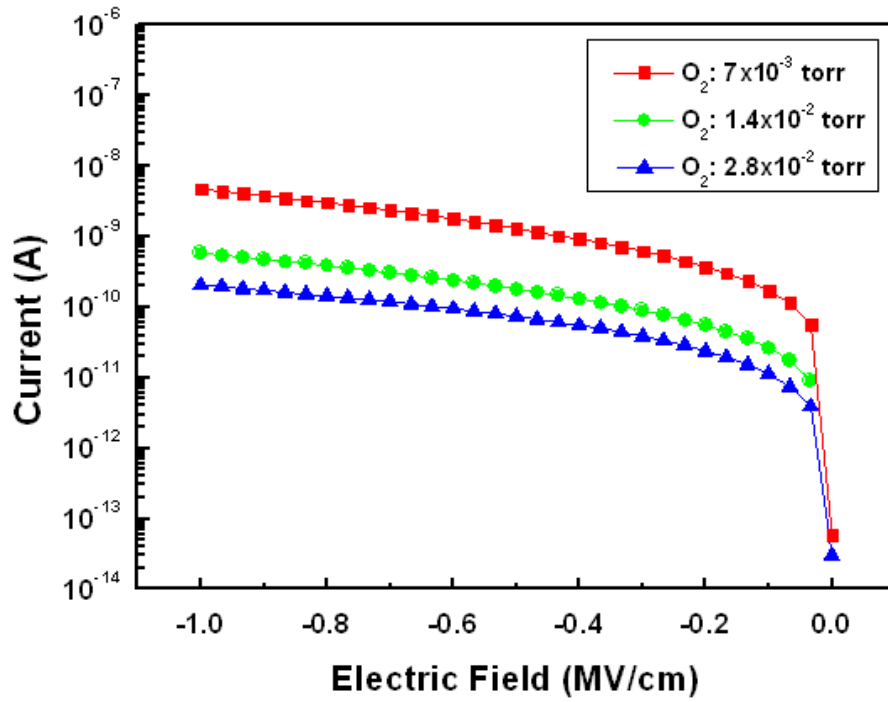
Fig. 5-14(a) Leakage current I versus electric field of LAO films deposited at various oxygen pressures.
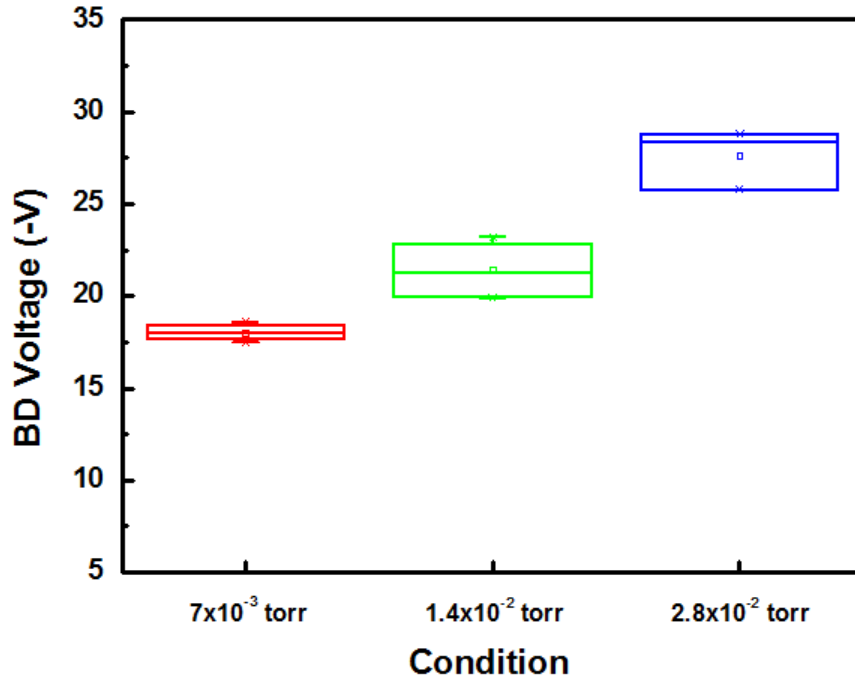
Fig. 5-14(b) Comparison on the breakdown (BD) voltages of LAO films deposited at various oxygen pressures.
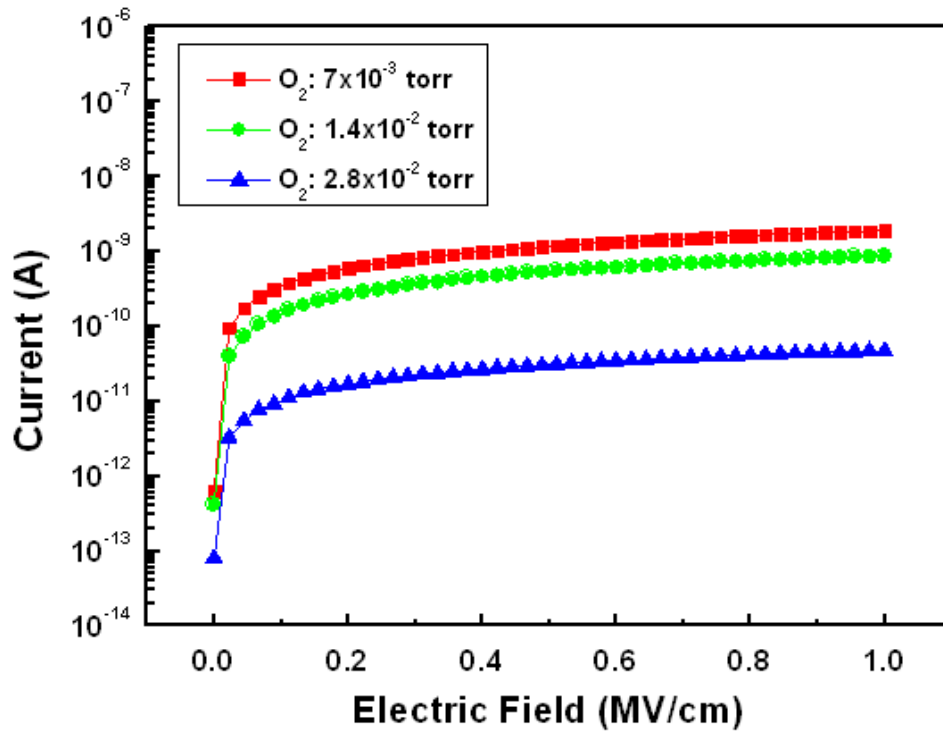
Fig. 5-15(a) Leakage current I versus electric field of LAO films deposited at various oxygen pressures.
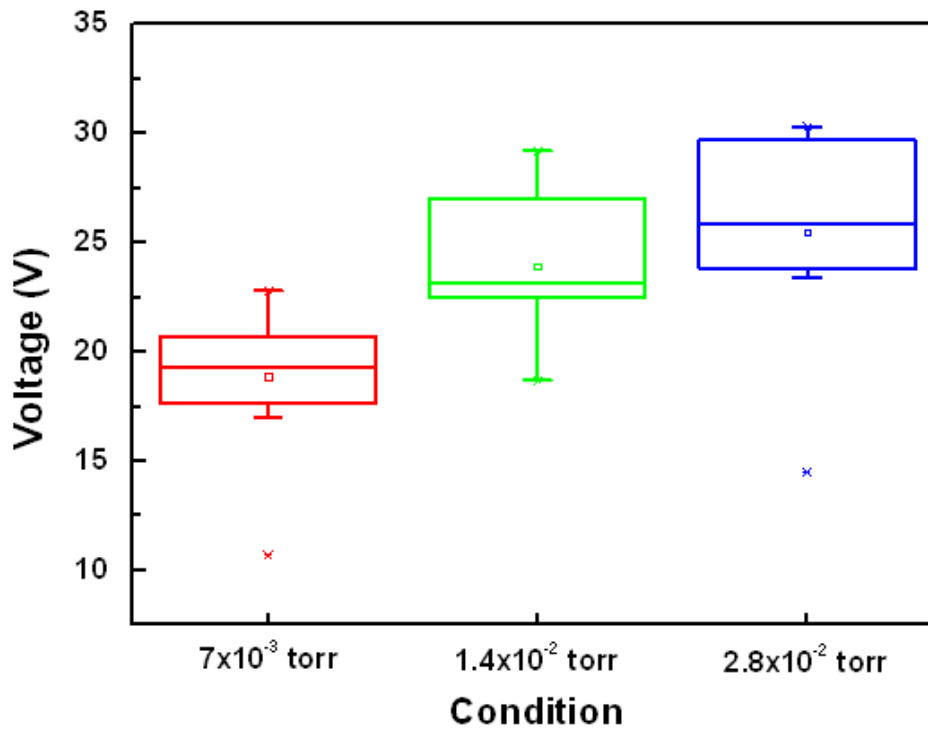
Fig. 5-15(b) Comparison on the breakdown (BD) voltages of LAO films deposited at various oxygen pressures.
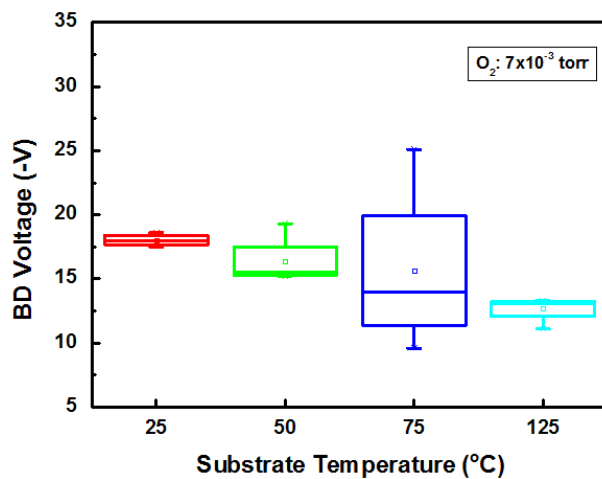
Fig. 5-16(a)   Forming voltages for the LAO films grown at oxygen pressure of 7×10^{-3} torr at various measured temperature.
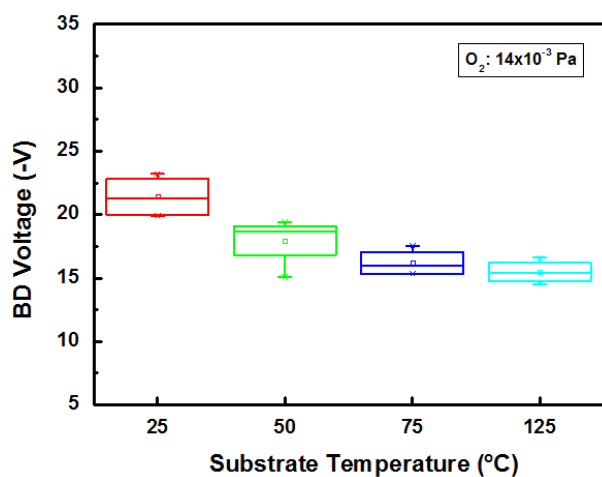
Fig. 5-16(b)   Forming voltages for the LAO films grown at oxygen pressure of 1.4×10^{-2} torr at various measured temperature.
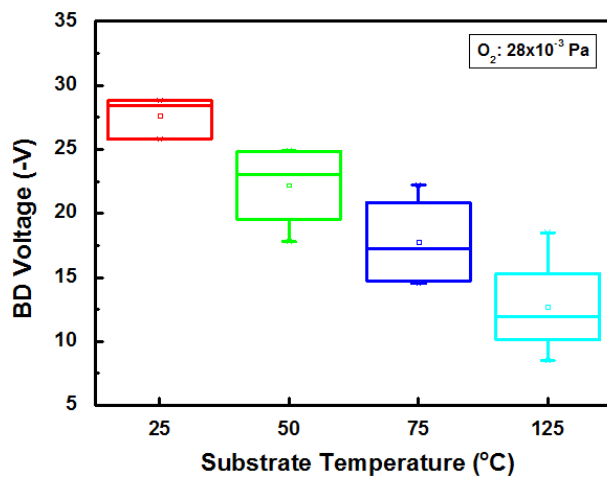
Fig. 5-16(c)   Forming voltages for the LAO films grown at oxygen pressure of 2.8×10^{-2} torr at various measured temperature.
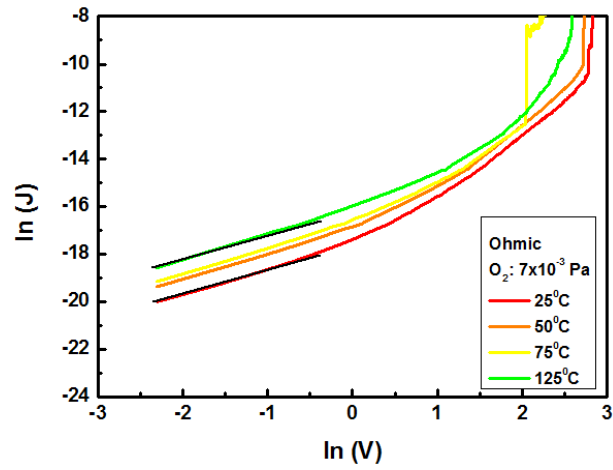
Fig. 5-17(a)   Plots of ln J vs ln V curve for the LAO films grown at oxygen pressure of 7×10^{-3} torr.
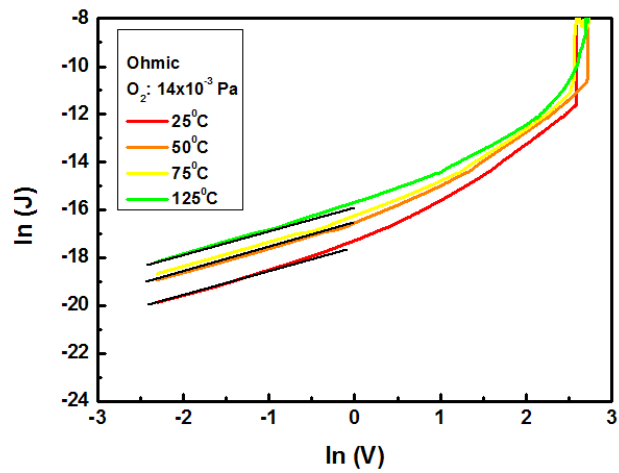
Fig. 5-17(b)   Plots of ln J vs ln V curve for the LAO films grown at oxygen pressure of 1.4×10^{-2} torr.
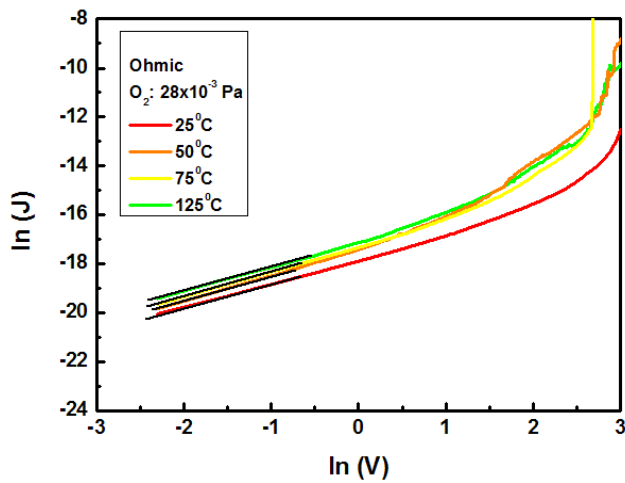
Fig. 5-17(c)   Plots of ln J vs ln V curve for the LAO films grown at oxygen pressure of 2.8×10^{-2} torr.
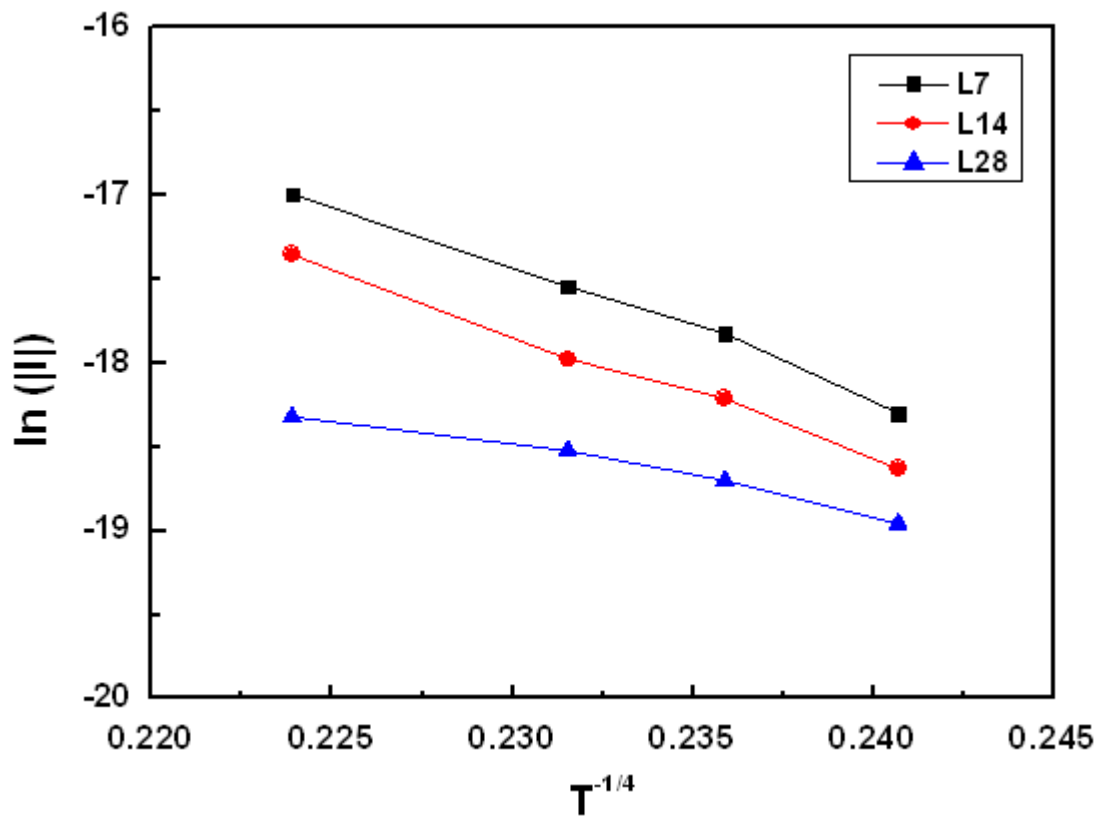
Fig. 5-18　The ln (|I|) values versus $T^{-1/4}$ for the LAO films grown at different oxygen pressure.
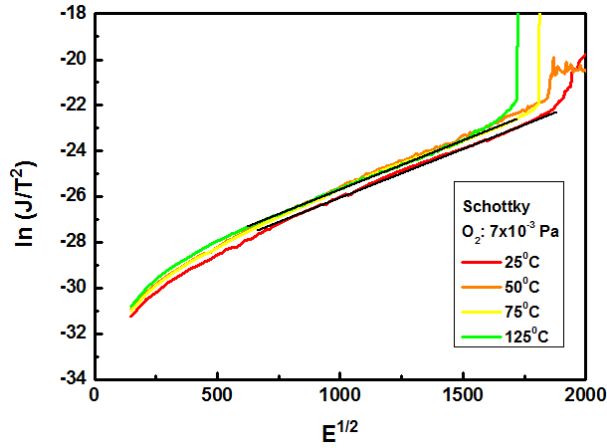
Fig. 5-19(a) Plots of ln (J/T^2) vs E$^{1/2}$ curve for the LAO films grown at oxygen pressure of 7×10^{-3} torr.
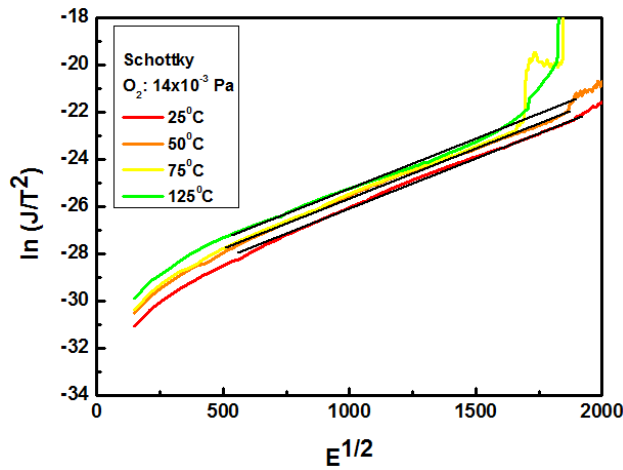
Fig. 5-19(b) Plots of ln (J/T^2) vs E$^{1/2}$ curve for the LAO films grown at oxygen pressure of 1.4×10^{-2} torr.
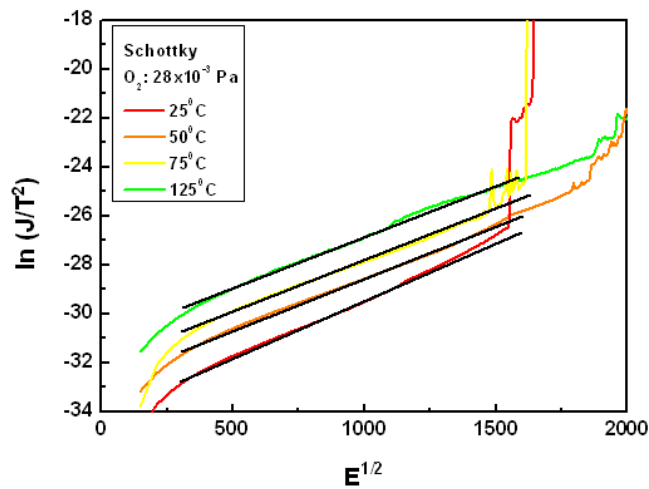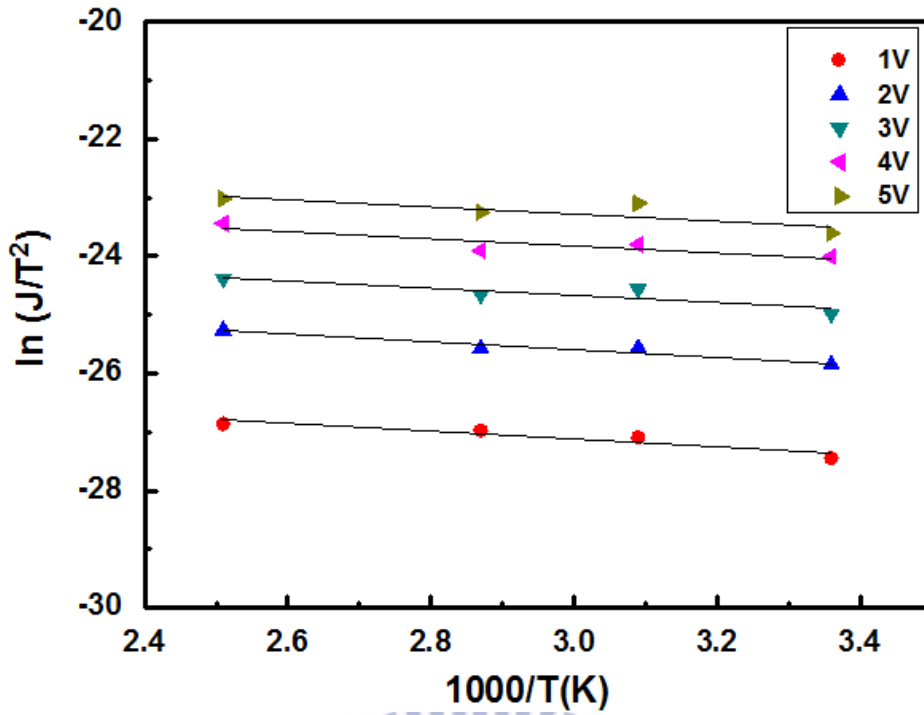

Fig. 5-19(c) Plots of ln (J/T^2) vs E$^{1/2}$ curve for the LAO films grown at oxygen pressure of 2.8×10^{-2} torr.

Fig. 5-20(a)　Variations of ln (J/T^2) with 1/T of the ITO/LAO(L-7)/ITO capacitor, where the J represents the measured value at voltages over the range of 1 to 5 V.
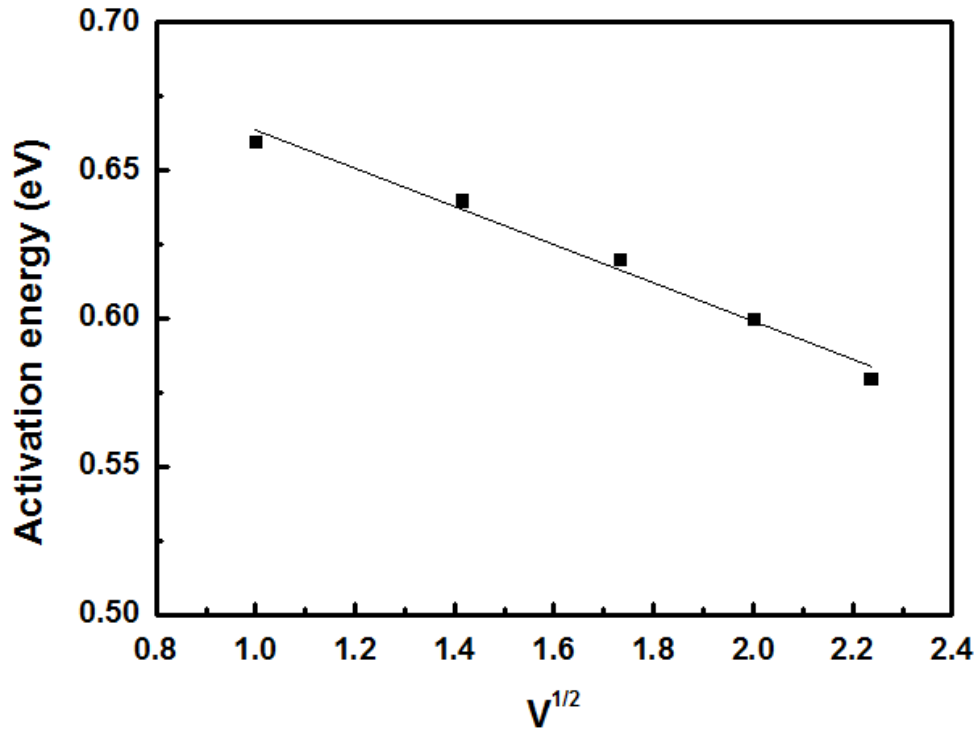
Fig. 5-20(b)　Variation in activation energies of the ITO/LAO(L-7)/ITO capacitor as a function of V$^{1/2}$.
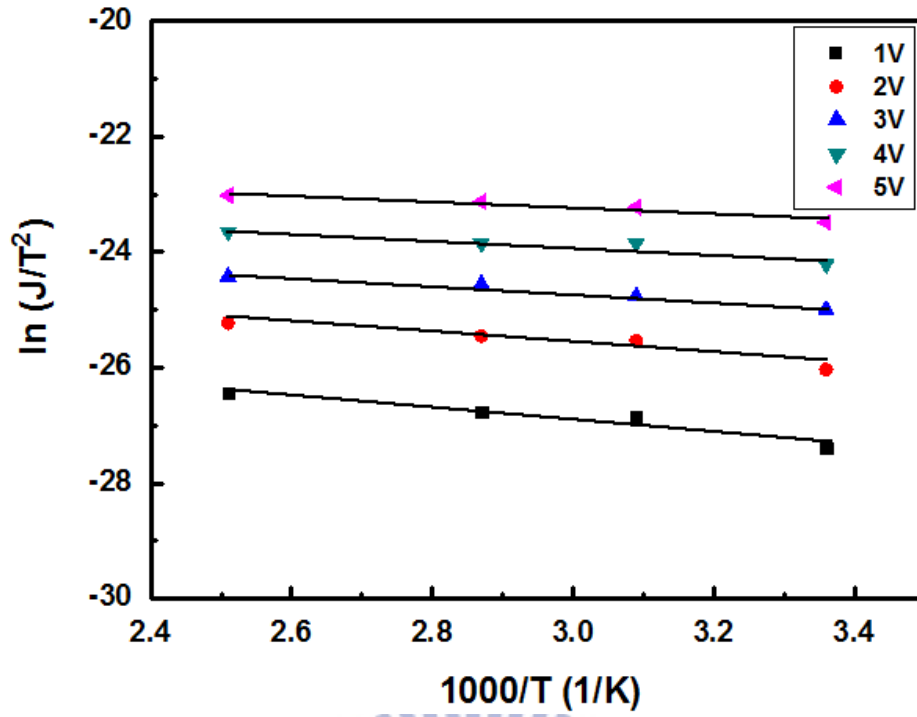
Fig. 5-21(a) Variations of ln (J/T^2) with 1/T of the ITO/LAO(L-28)/ITO capacitor, where the J represents the measured value at voltages over the range of 1 to 5 V.
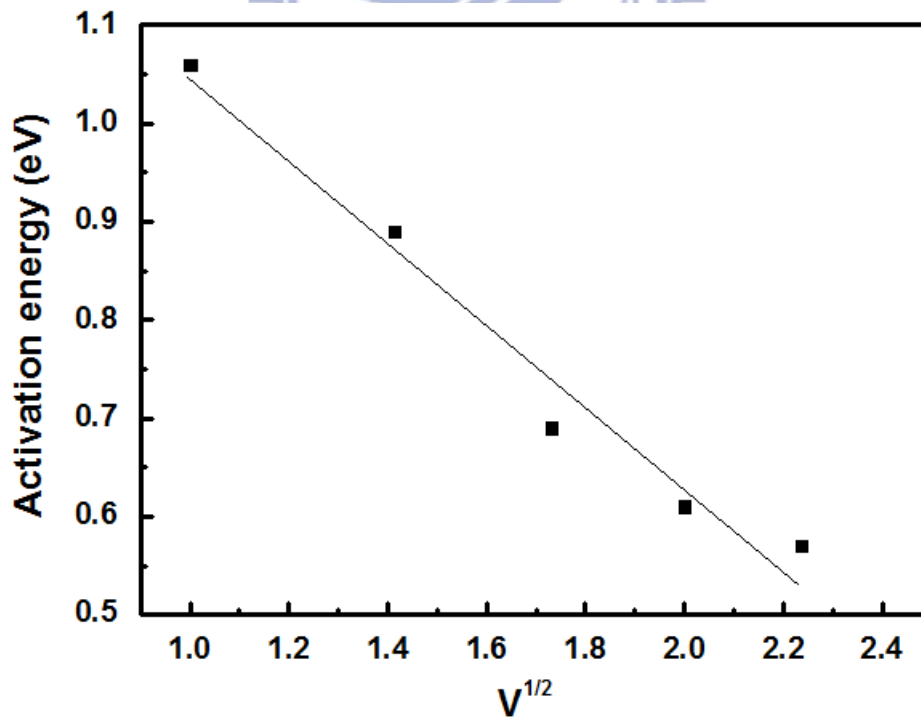

Fig. 5-21(b) Variation in activation energies of the ITO/LAO(L-28)/ITO capacitor as a function of $V^{1/2}$.
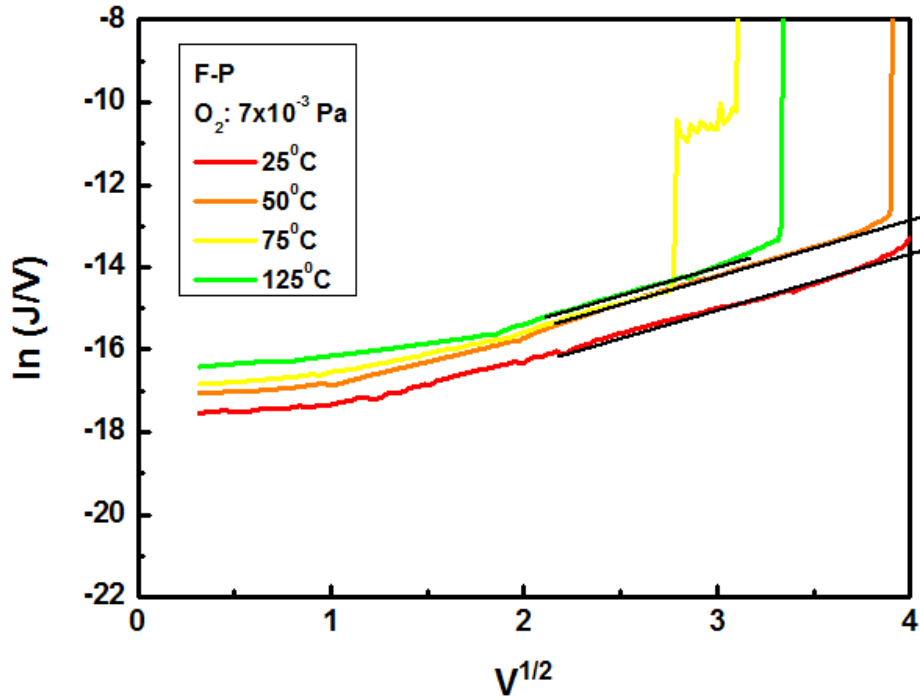
Fig. 5-22(a) Plots of ln (J/V) vs $V^{1/2}$ curve for the LAO films grown at oxygen pressure of 7×10^{-3} torr.
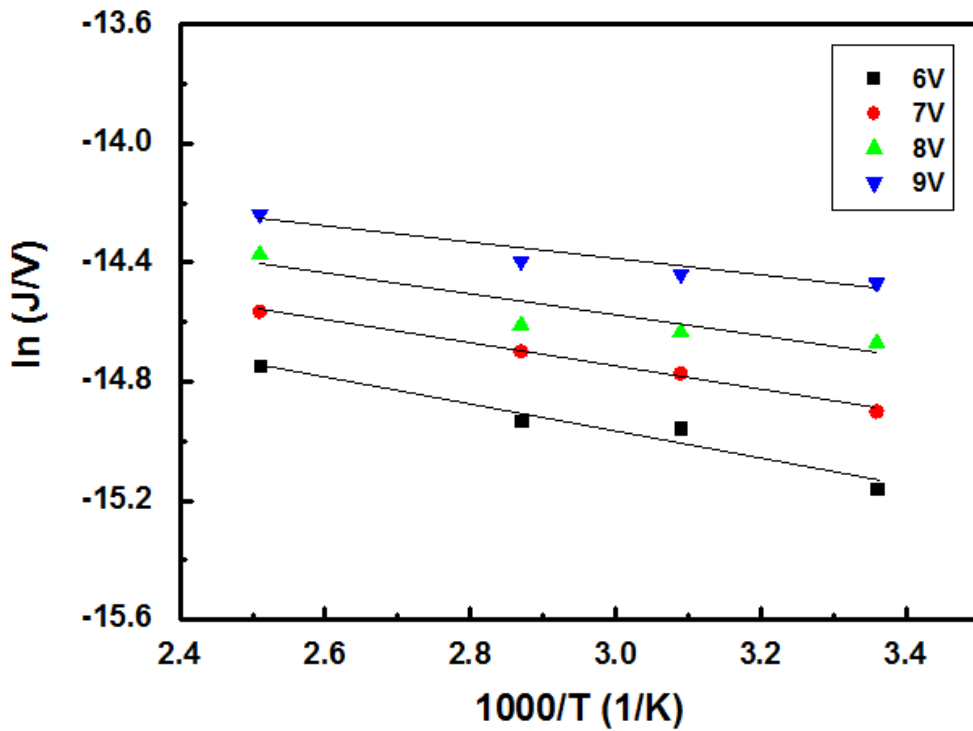

Fig. 5-22(b) Variations of ln (J/V) with 1/T of the ITO/LAO/ITO capacitor, where the J represents the measured value at voltages over the range of 6 to 9 V.
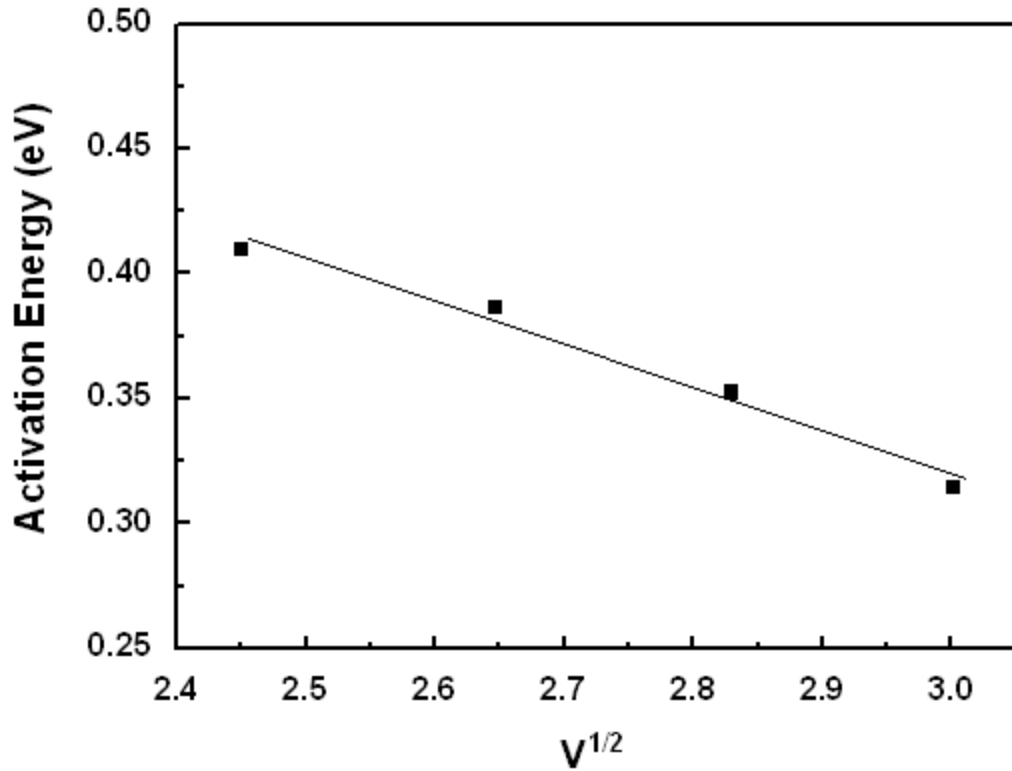
Fig. 5-22(c) Variation in activation energies of the ITO/LAO/ITO capacitor as a function of $V^{1/2}$.

Fig. 5-23(a) Plots of ln (J/V) vs $V^{1/2}$ curve for the LAO films grown at oxygen pressure of 2.8×10^{-2} torr.

Fig. 5-23(b)　Variations of ln (J/V) with 1/T of the ITO/LAO/ITO capacitor, where the J represents the measured value at voltages over the range of 6 to 9 V.

Fig. 5-23(c)　Variation in activation energies of the ITO/LAO/ITO capacitor as a function of $V^{1/2}$.
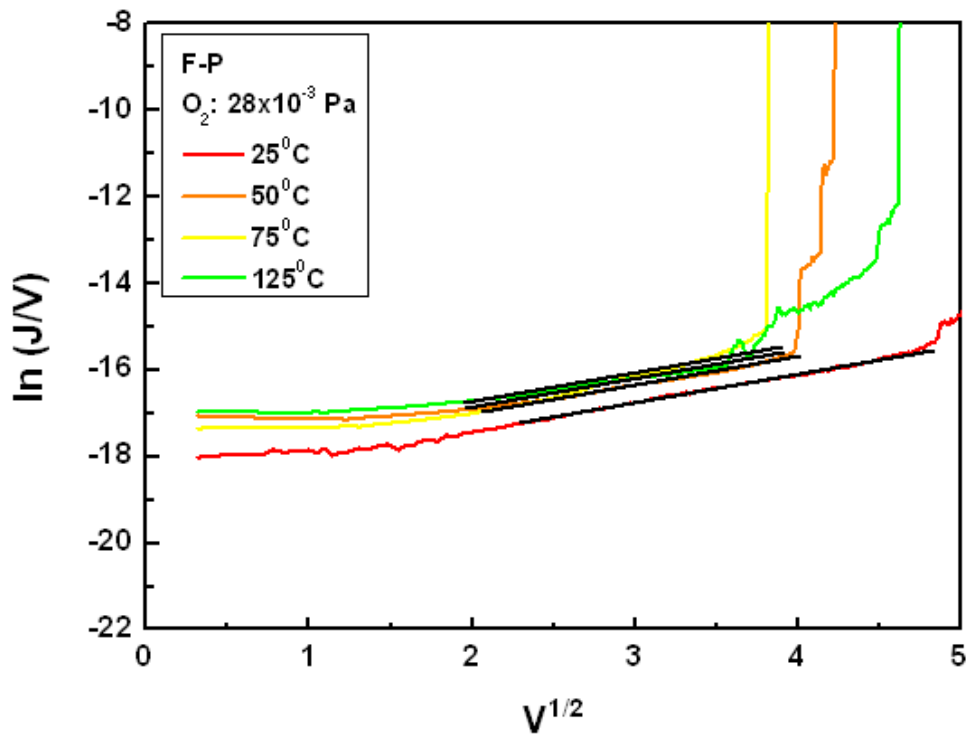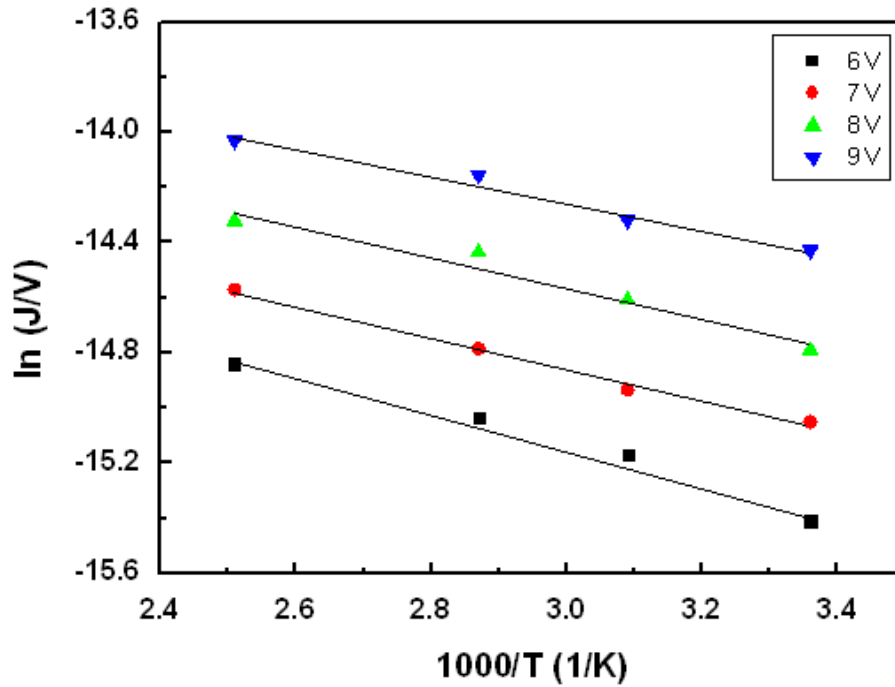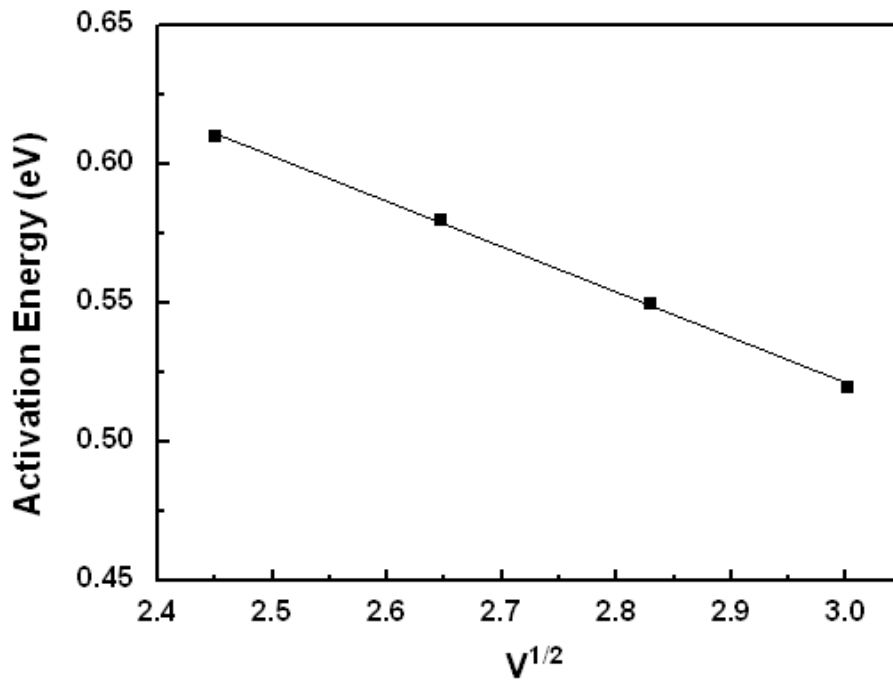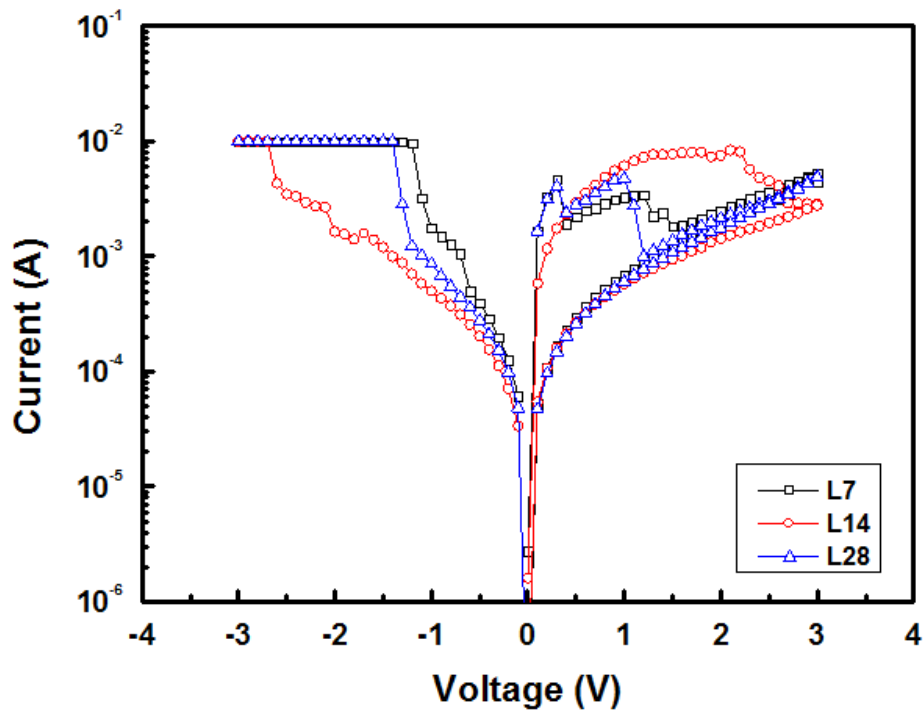
Fig. 5-24   I-V curves of LAO-based memory device grown at various oxygen pressures.
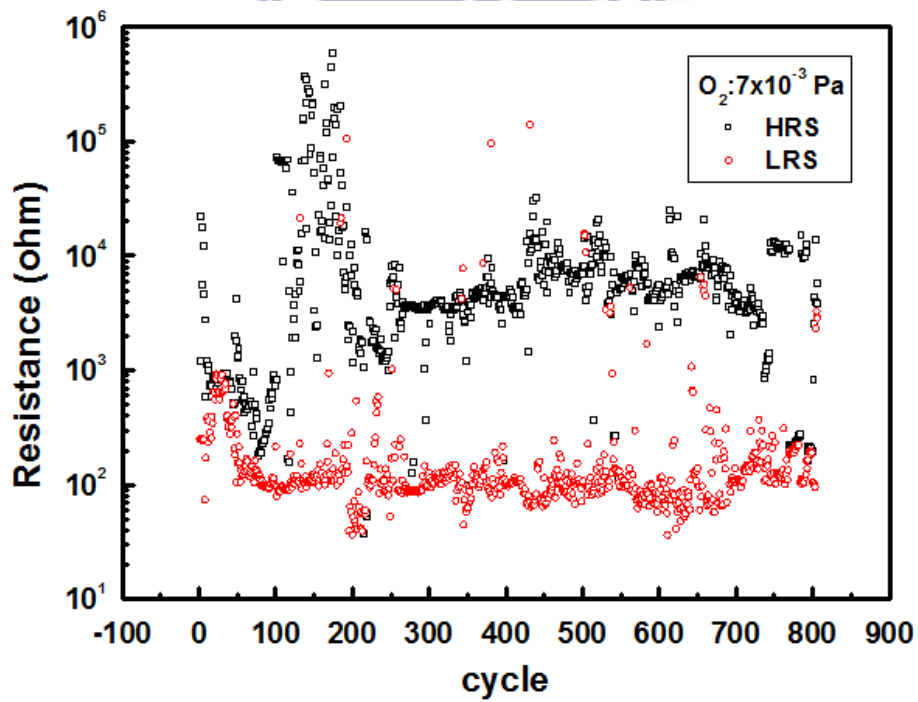
Fig. 5-25(a)   The resistance values of both ON-state and OFF-state at 0.1 V of LAO-based memory device grown at 7×10^{-3} torr.
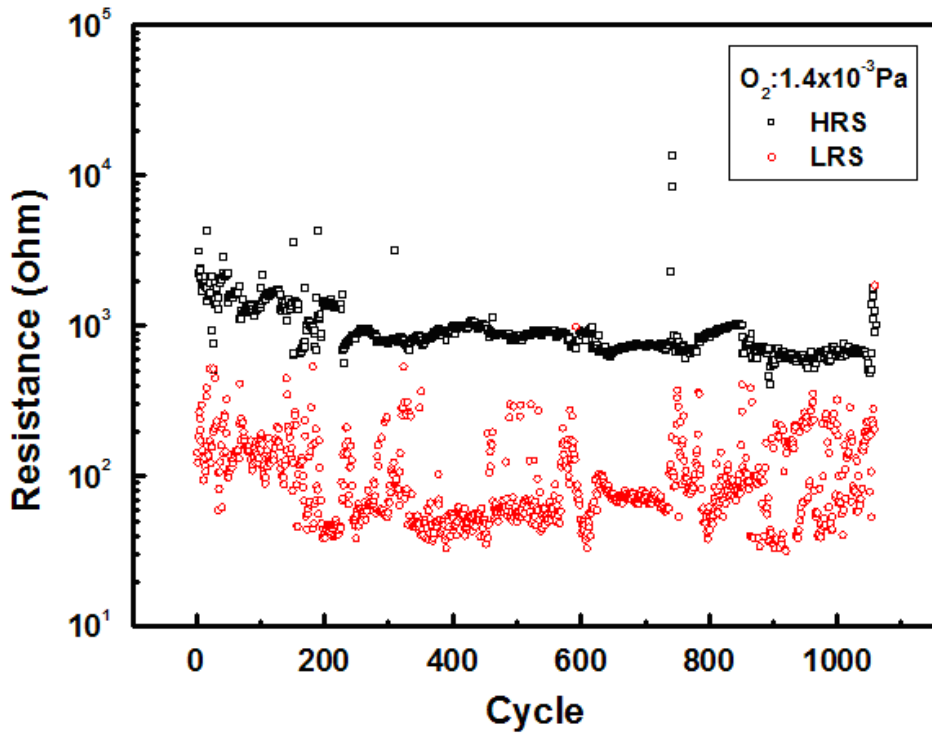
Fig. 5-25(b)　The resistance values of both ON-state and OFF-state at 0.1 V of LAO-based memory device grown at 1.4×10^{-2} torr.
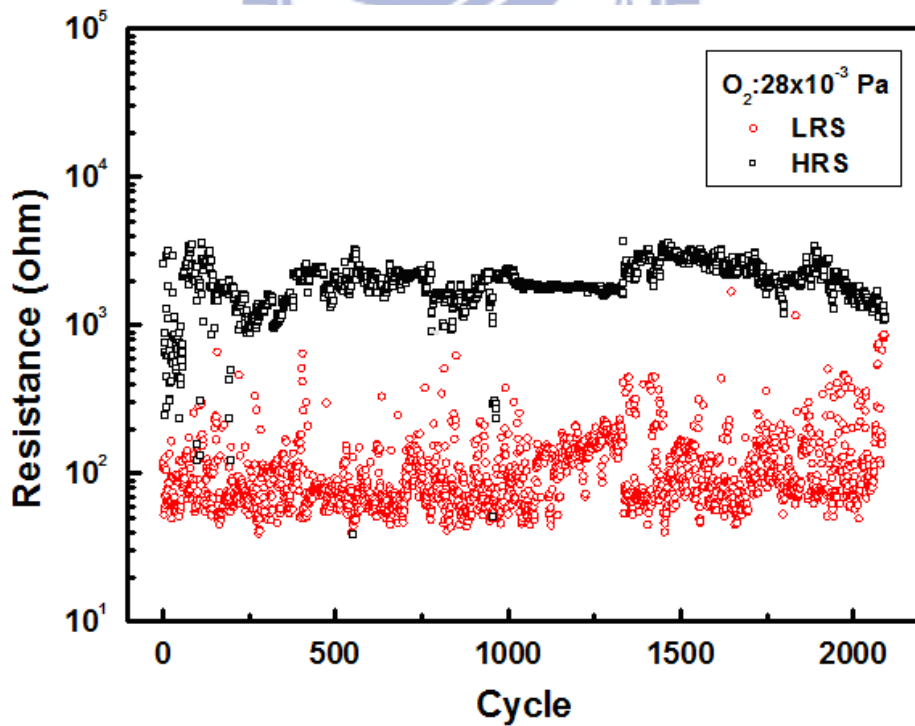
Fig. 5-25(c)　The resistance values of both ON-state and OFF-state at 0.1 V of LAO-based memory device grown at 2.8×10^{-2} torr.
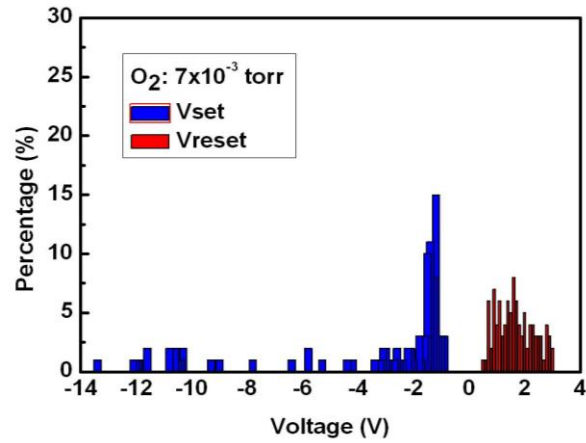
Fig. 5-26(a)　Vset and Vreset distribution among 500 switching cycles of LAO-based memory device grown at 7×10^{-3} torr.
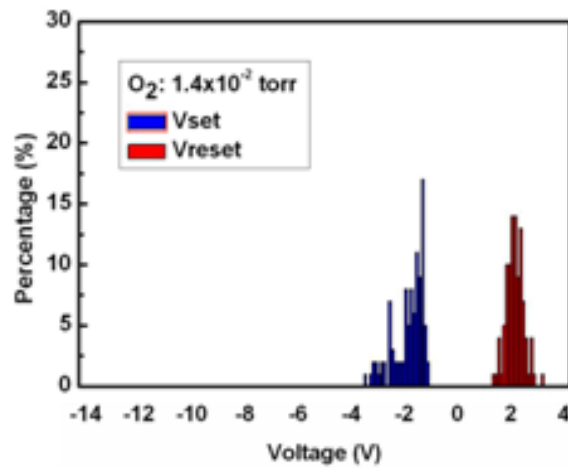
Fig. 5-26(b)　Vset and Vreset distribution among 500 switching cycles of LAO-based memory device grown at 1.4×10^{-2} torr.
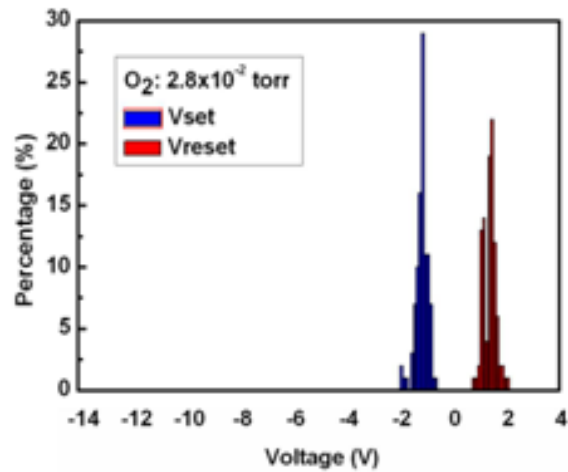
Fig. 5-26(c)　Vset and Vreset distribution among 500 switching cycles of LAO-based memory device grown at 2.8×10^{-2} torr.
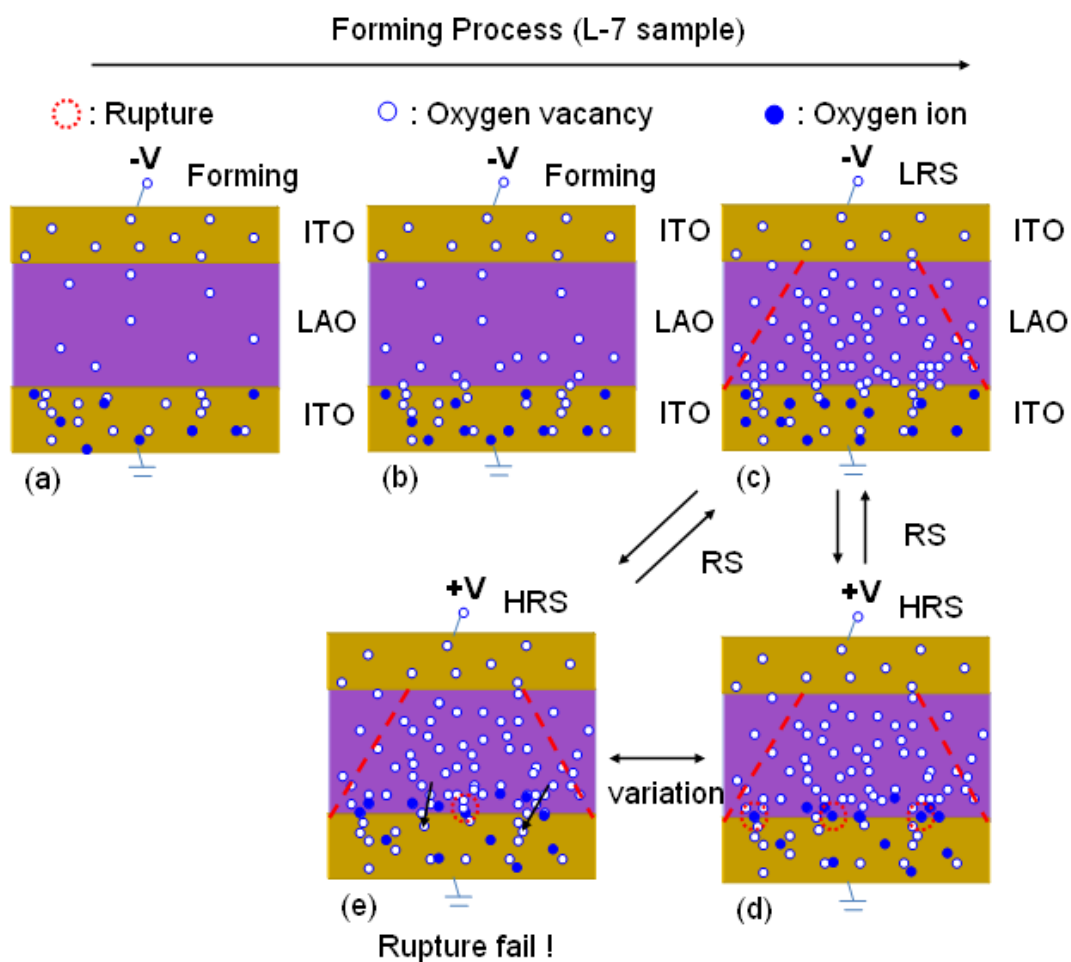
Fig. 5-27　Schematic diagrams for resistive switching mechanism in ITO/LAO/ITO structure on forming process (a) at low voltage bias (initial), (b) at middle voltage bias (|-0.7| V < V < |-8| V), (c) at large voltage bias (V > |-8 V|) to LRS. Under the positive bias, the oxygen ions can migrate back to reoxidize in the insulator film. (d) and (e) represent different HRS picture of the insulative matrix.
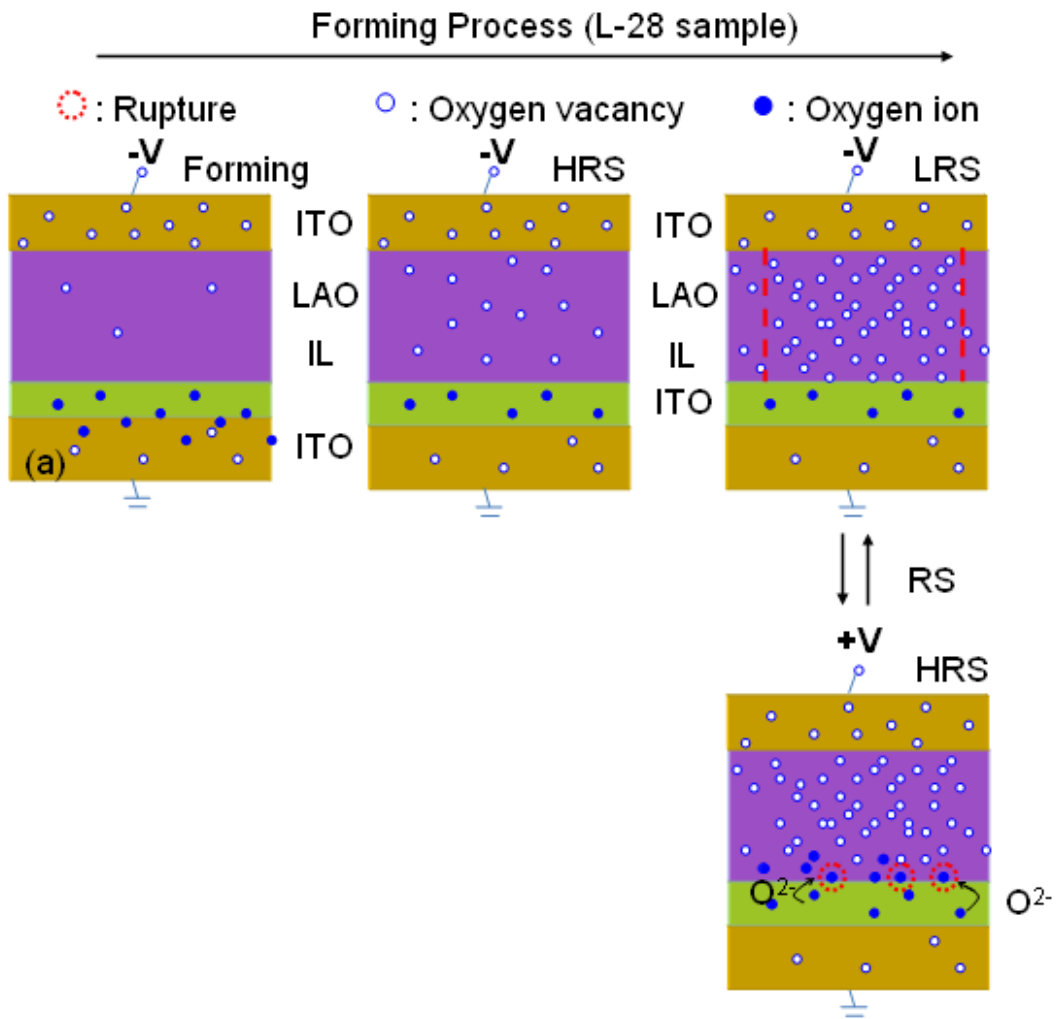
Fig. 5-28 Schematic diagrams for resistive switching mechanism in ITO/LAO/ITO structure on forming process (a) at low voltage bias (initial), (b) at middle voltage bias ($|-0.7|$ V $<$ V $<$ $|-8|$ V), (c) at large voltage bias (V $>$ $|-8$ V$|$). Under the positive bias, the oxygen ions can migrate back to reoxidize in the insulator film. (d) and (e) represent different HRS picture of the insulative matrix.

Fig. 5-29(a) The I-V curves operate at fixed Vreset = 2 V and varying Vset from -0.5 to -10 V of LAO-based memory grown at oxygen pressure of 7×10^{-3} torr.
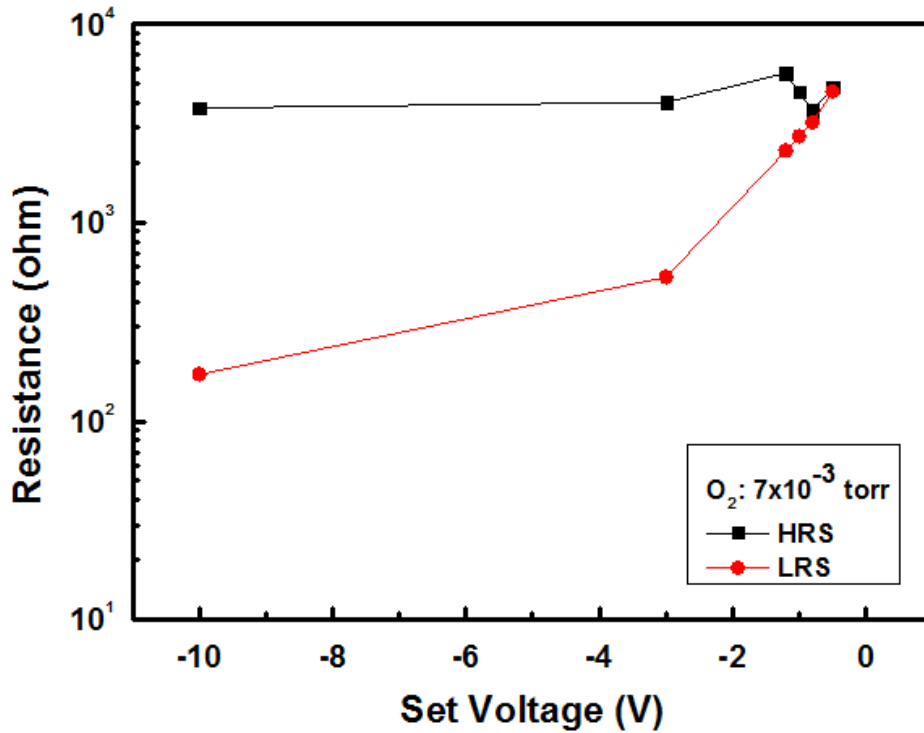
Fig. 5-29(b) Resistance values of HRS and LRS as a function of Vset of LAO-based memory grown at oxygen pressure of 7×10^{-3} torr.
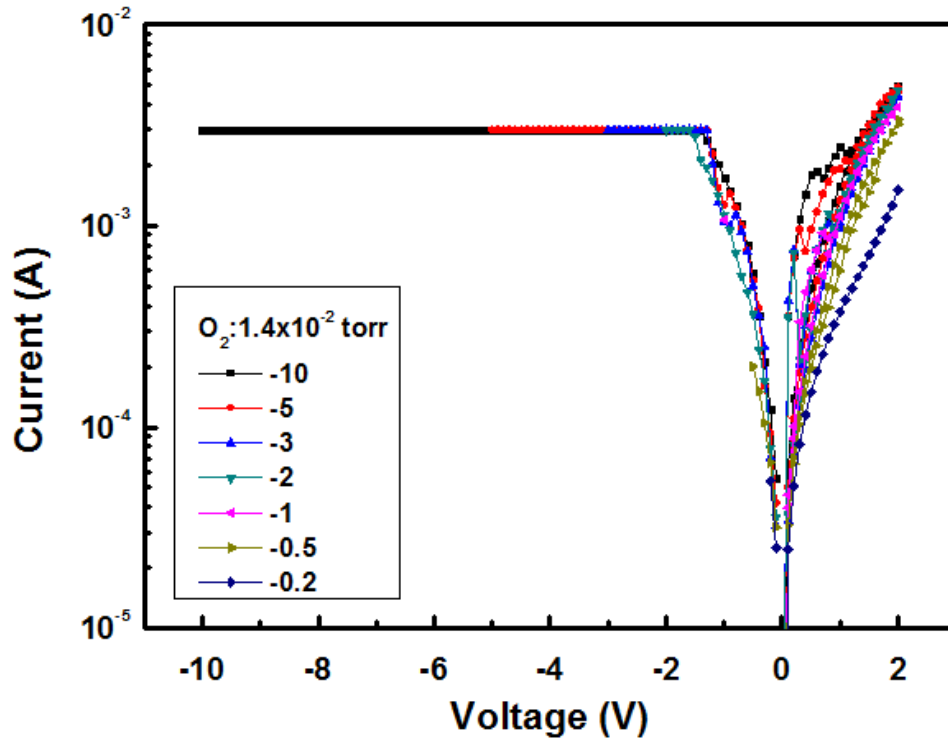
Fig. 5-30(a) The I-V curves operate at fixed Vreset = 2 V and varying Vset from -0.5 to -10 V of LAO-based memory grown at oxygen pressure of 1.4×10^{-2} torr.
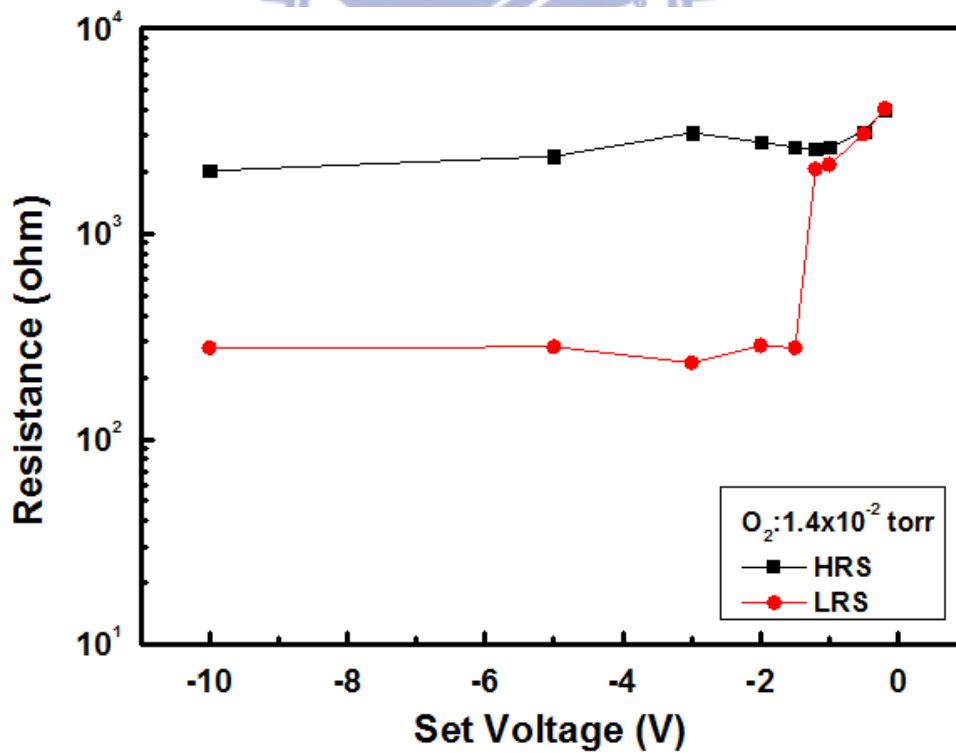
Fig. 5-30(b) Resistance values of HRS and LRS as a function of Vset of LAO-based memory grown at oxygen pressure of 1.4×10^{-2} torr.
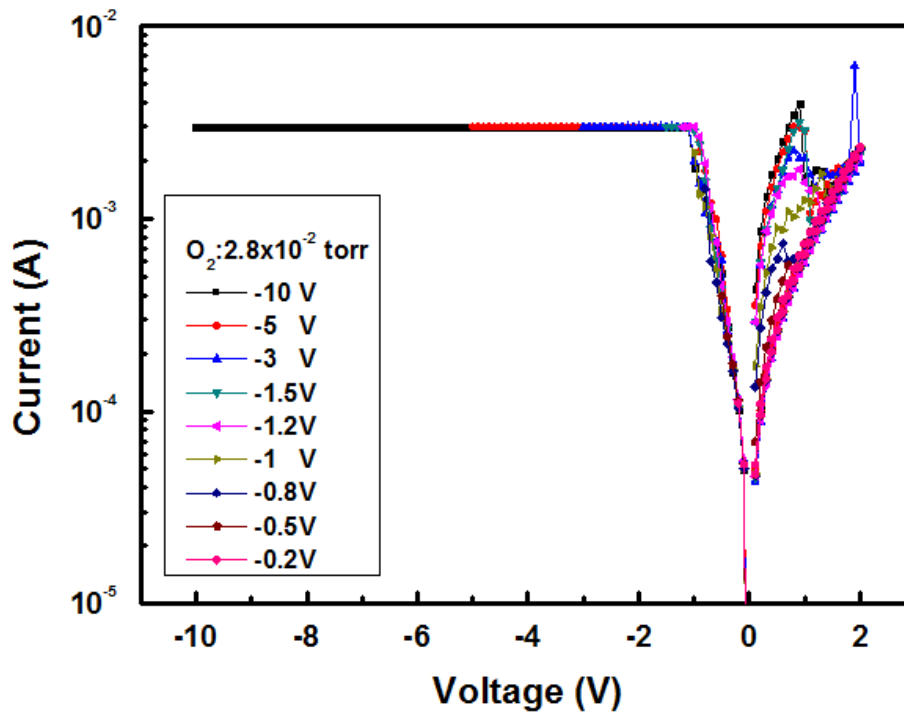
Fig. 5-31(a)　The I-V curves operate at fixed Vreset = 2 V and varying Vset from -0.5 to -10 V of LAO-based memory grown at oxygen pressure of 2.8×10^{-2} torr.
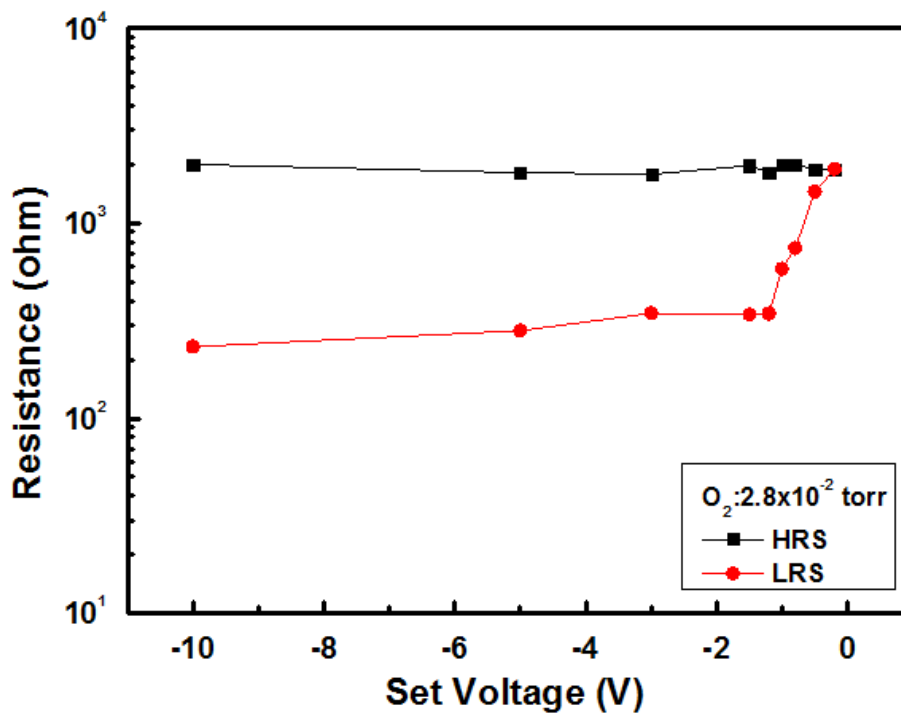
Fig. 5-31(b)　Resistance values of HRS and LRS as a function of Vset of LAO-based memory grown at oxygen pressure of 2.8×10^{-2} torr.
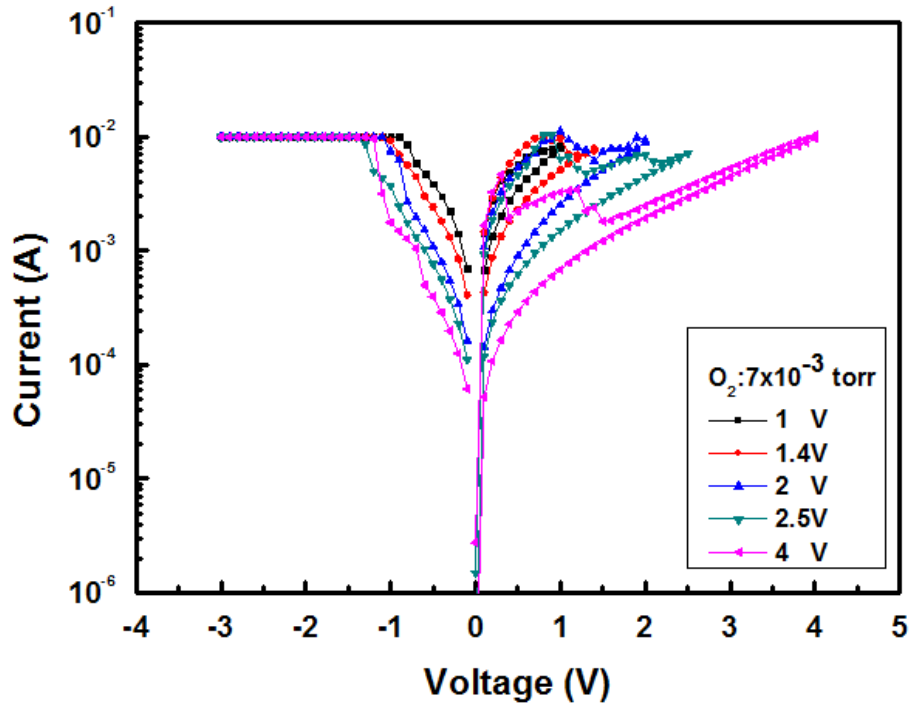
Fig. 5-32(a)　The I-V curves operate at fixed Vset = -3 V and varying Vreset from 1 to 4 V of LAO-based memory grown at oxygen pressure of 7×10^{-3} torr.
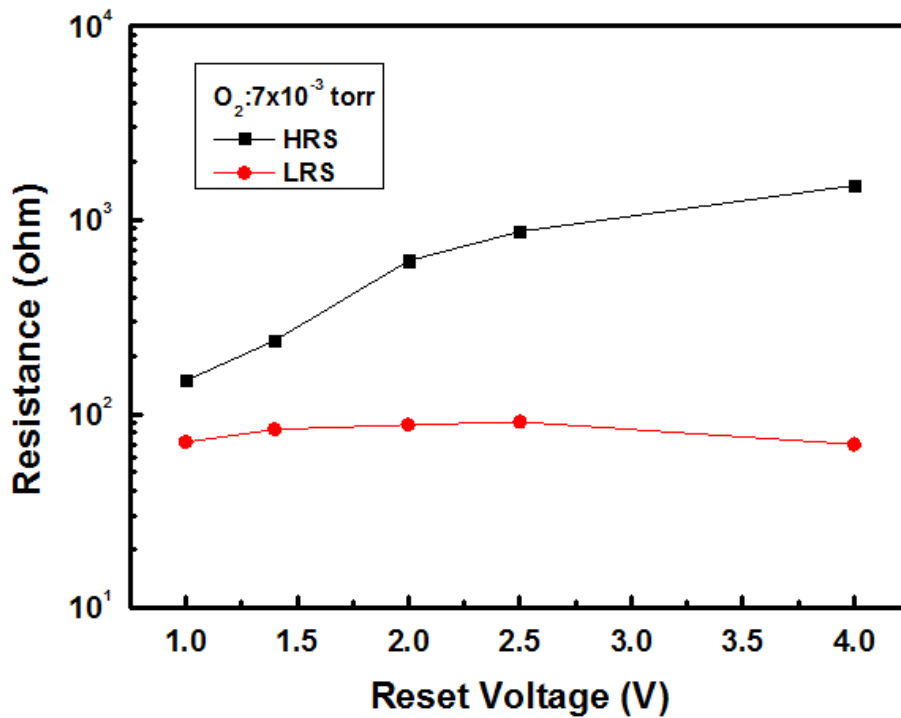
Fig. 5-32(b)　Resistance values of HRS and LRS as a function of Vreset of LAO-based memory grown at oxygen pressure of 7×10^{-3} torr.
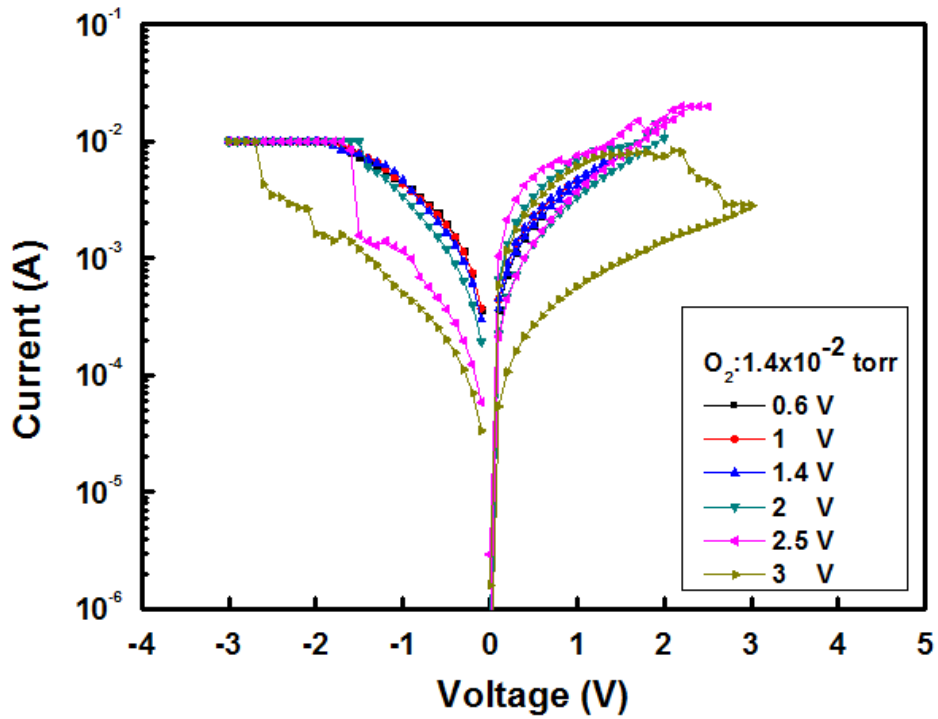
Fig. 5-33(a) The I-V curves operate at fixed Vset = -3 V and varying Vreset from 0.6 to 3 V of LAO-based memory grown at oxygen pressure of 1.4×10^{-2} torr.
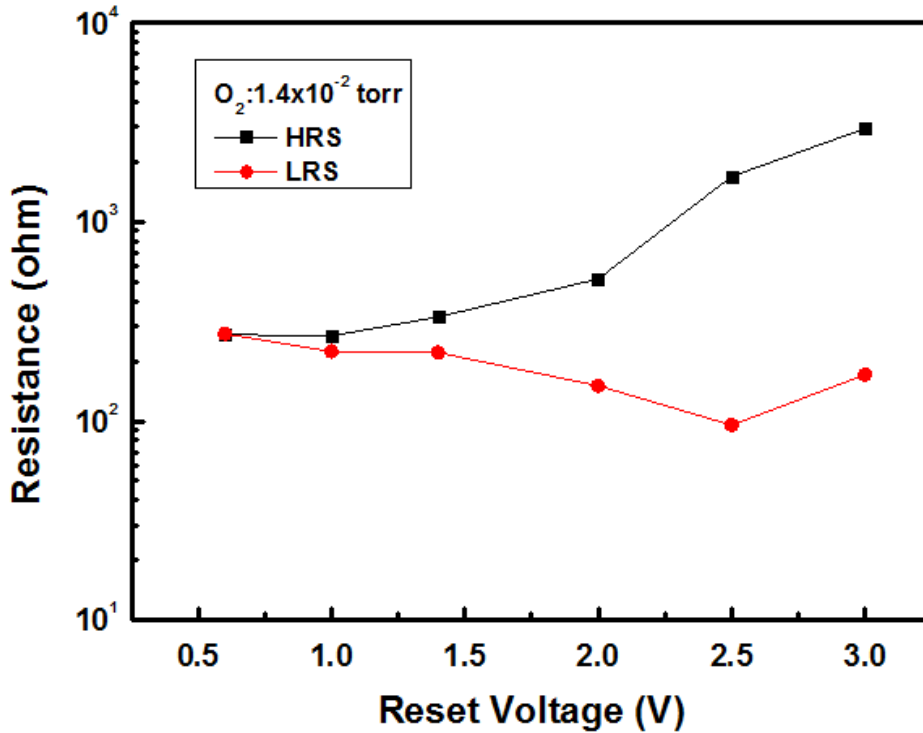
Fig. 5-33(b) Resistance values of HRS and LRS as a function of Vreset of LAO-based memory grown at oxygen pressure of 1.4×10^{-2} torr.
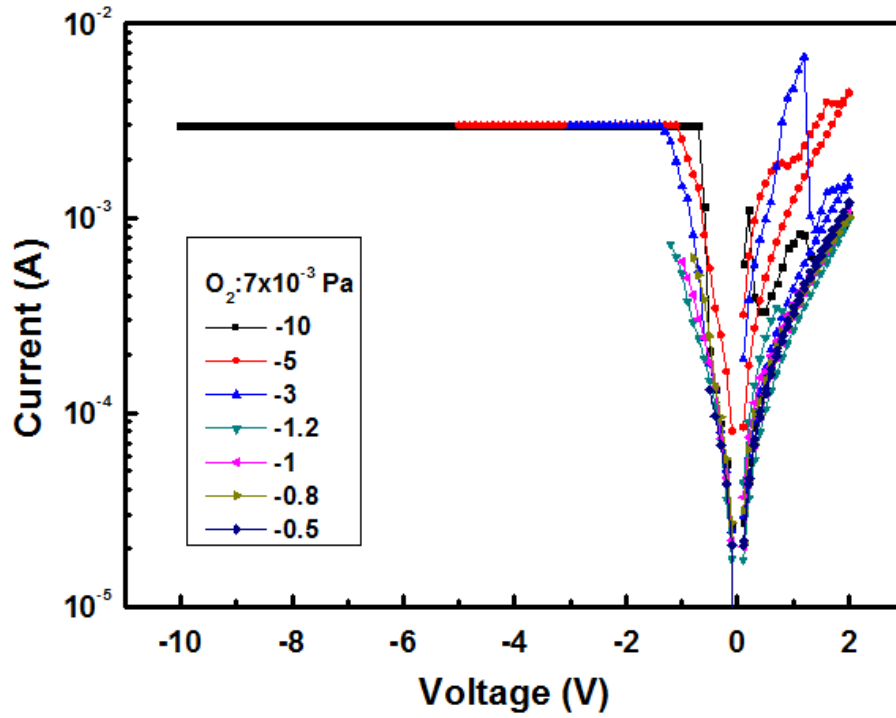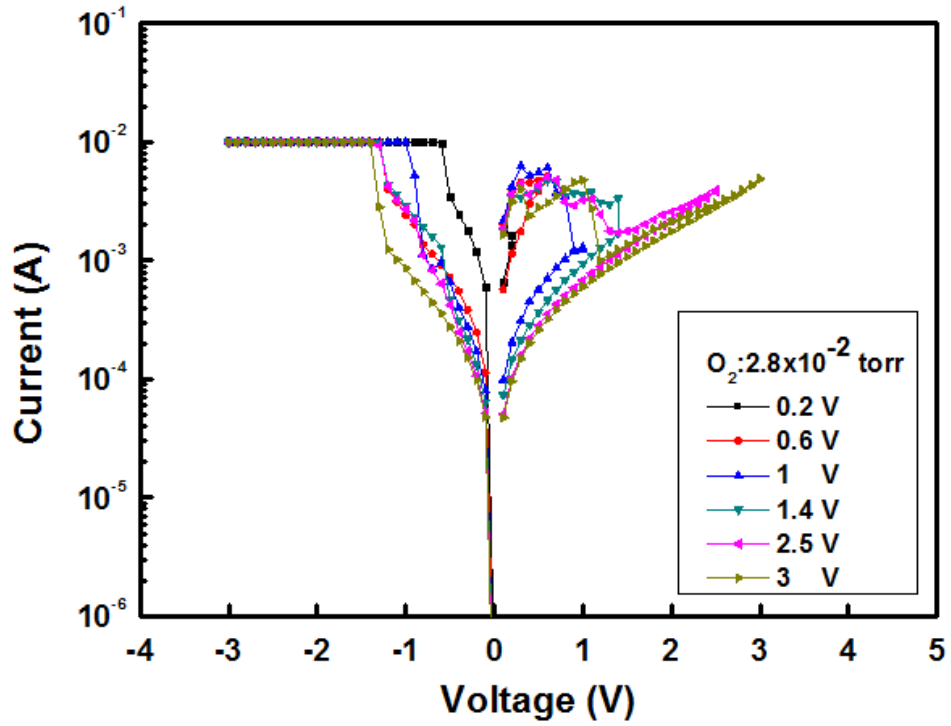
Fig. 5-34(a) The I-V curves operate at fixed Vset = -3 V and varying Vreset from 0.2 to 3 V of LAO-based memory grown at oxygen pressure of 2.8×10^{-2} torr.
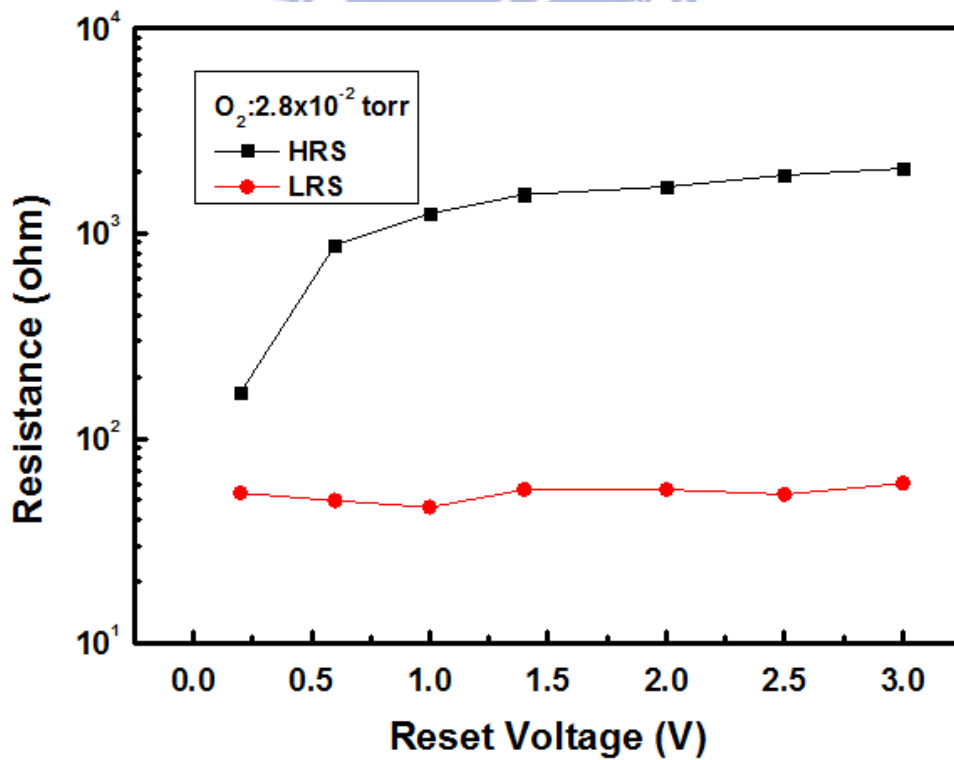
Fig. 5-34(b) Resistance values of HRS and LRS as a function of Vreset of LAO-based memory grown at oxygen pressure of 2.8×10^{-2} torr.
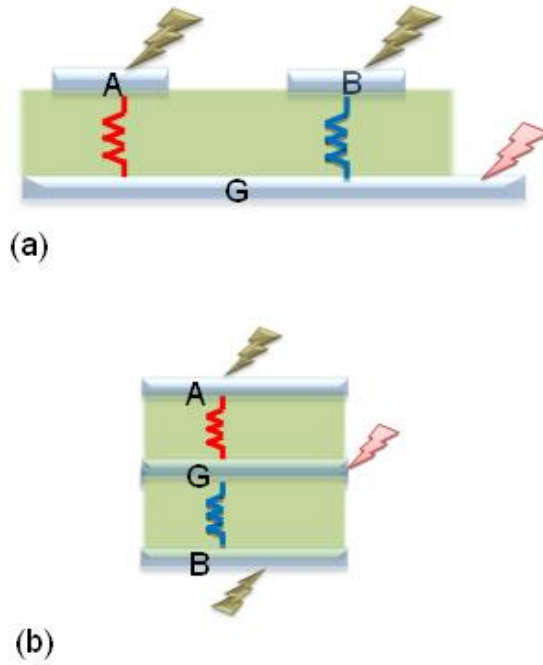
Fig. 5-35(a) Schematic diagrams for the measurement test. (b) Effective schematic diagrams for illustrating the measurement test.

	A-B	A-G	B-G	
1	1.62×10^9	6.09×10^8	2.37×10^8	
2			--	
3	3340	30	3190	HRS
4	56	30	58	LRS
5	1565	30	1210	HRS
6	117	60	98	LRS
7	4640	152	5970	HRS
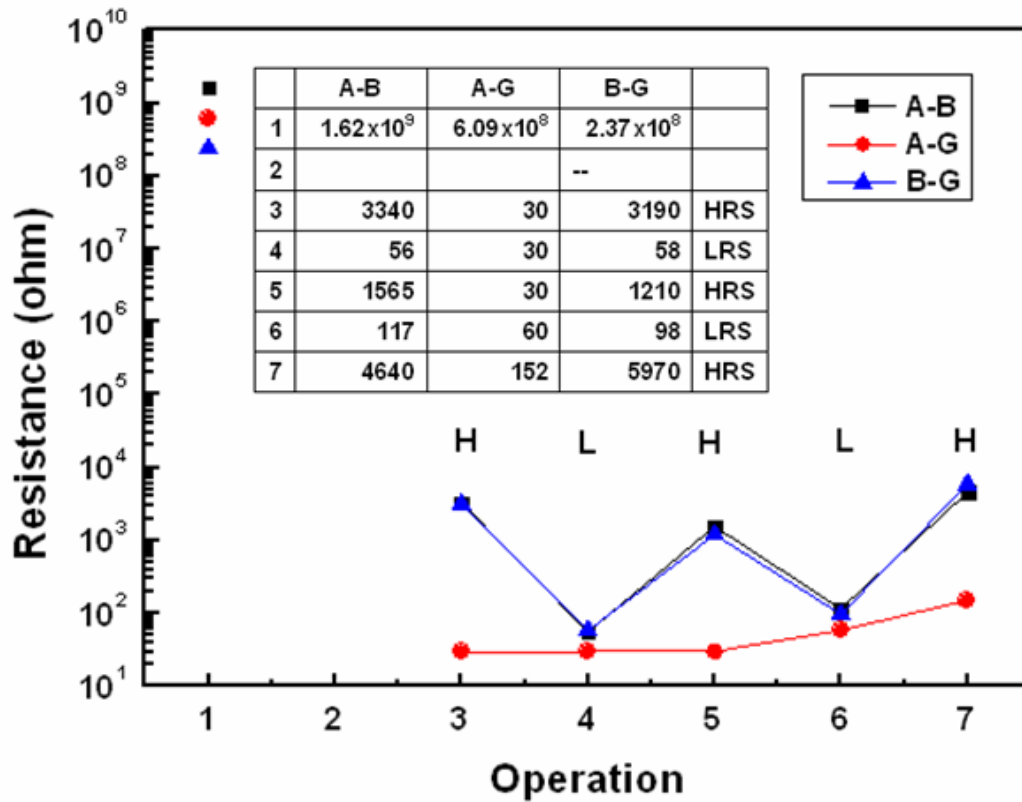
Fig. 5-36 Evolution on the resistance values of A-B, A-G, and B-G measuring test.
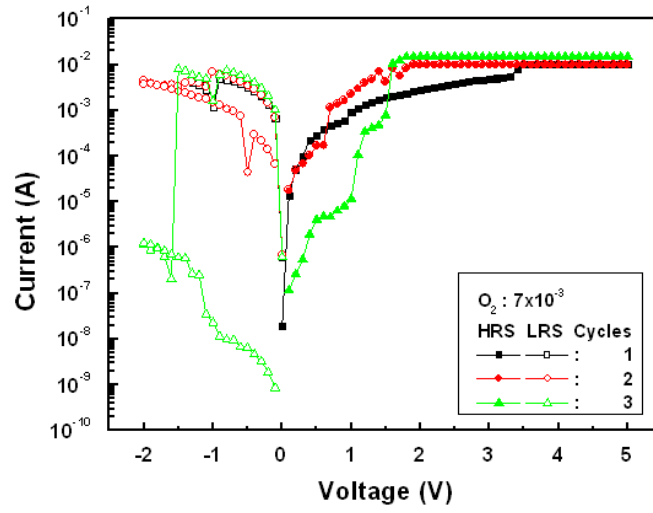
Fig. 5-37 (a) The I-V curves of L-7 sample.
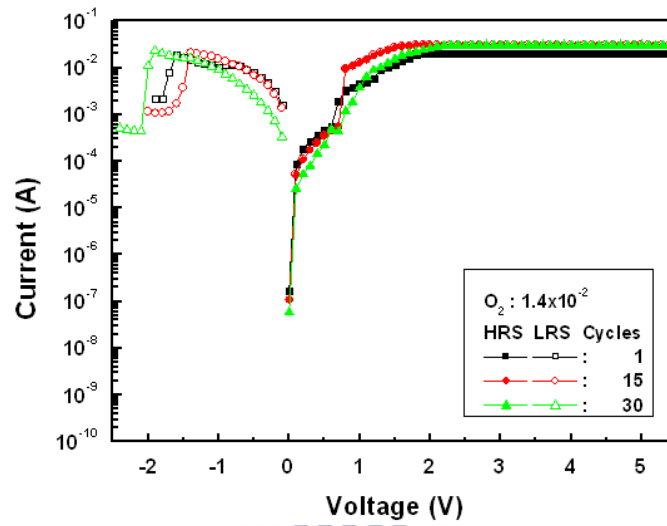
Fig. 5-37 (b) The I-V curves of L-14 sample.
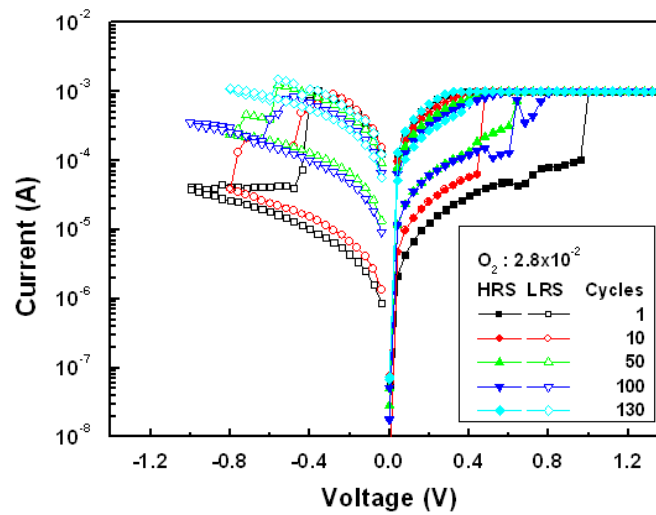
Fig. 5-37 (c) The I-V curves of L-28 sample.
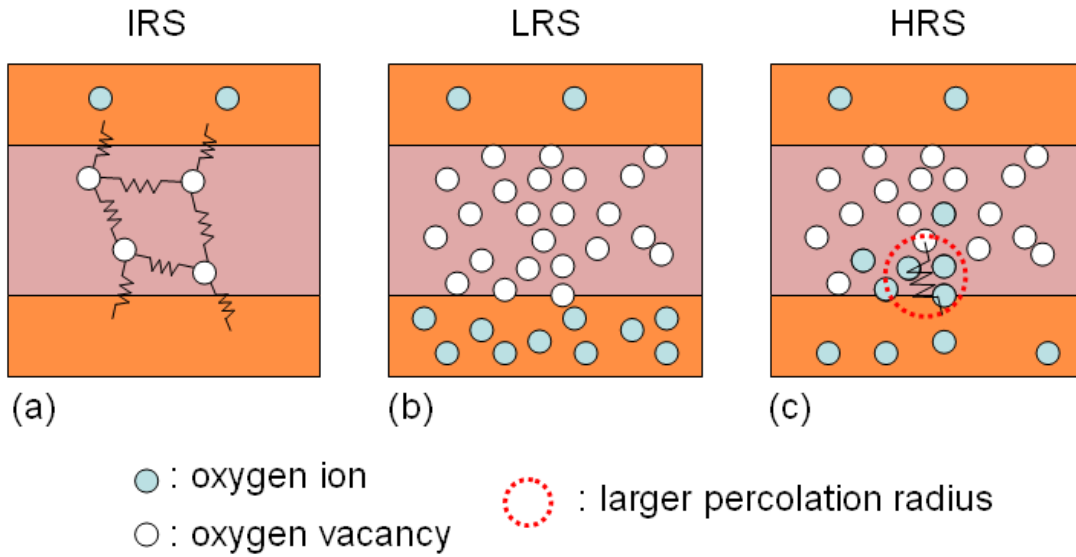
Fig. 5-38 Schematic diagram for the configuration of random resistor network model for (a) IRS, (b) LRS, and (c) HRS.
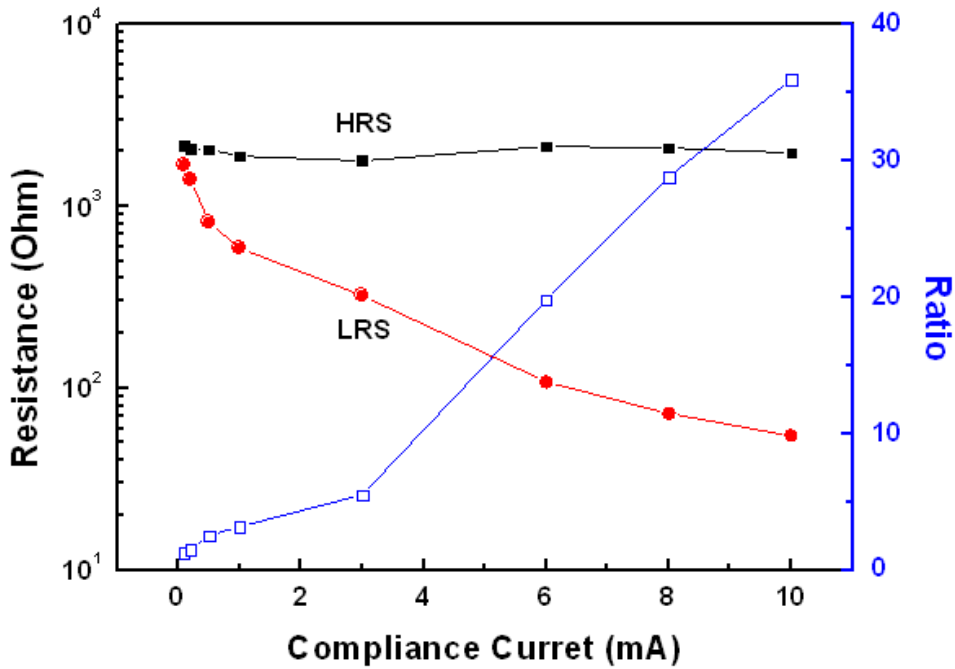
Fig. 5-39 The ON and OFF resistance values (left y-axis) and the ON/OFF ratios (right y-axis) as a function of compliance current.
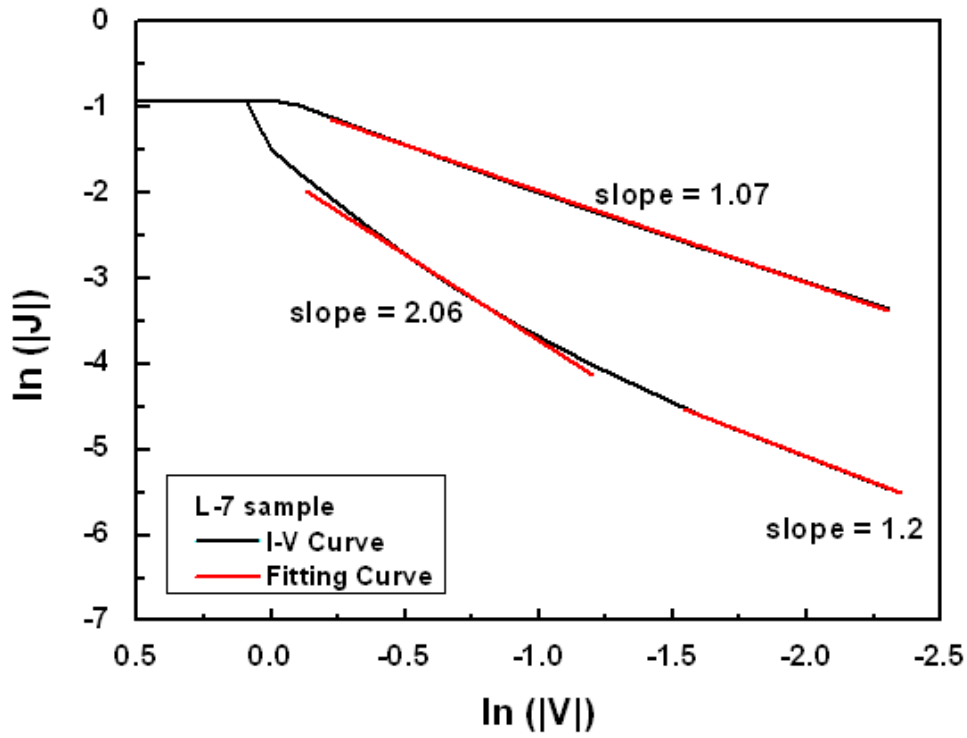
Fig. 5-40 (a) Electrical curves fitting on the negative side of the switching I-V curves L-7 samples.
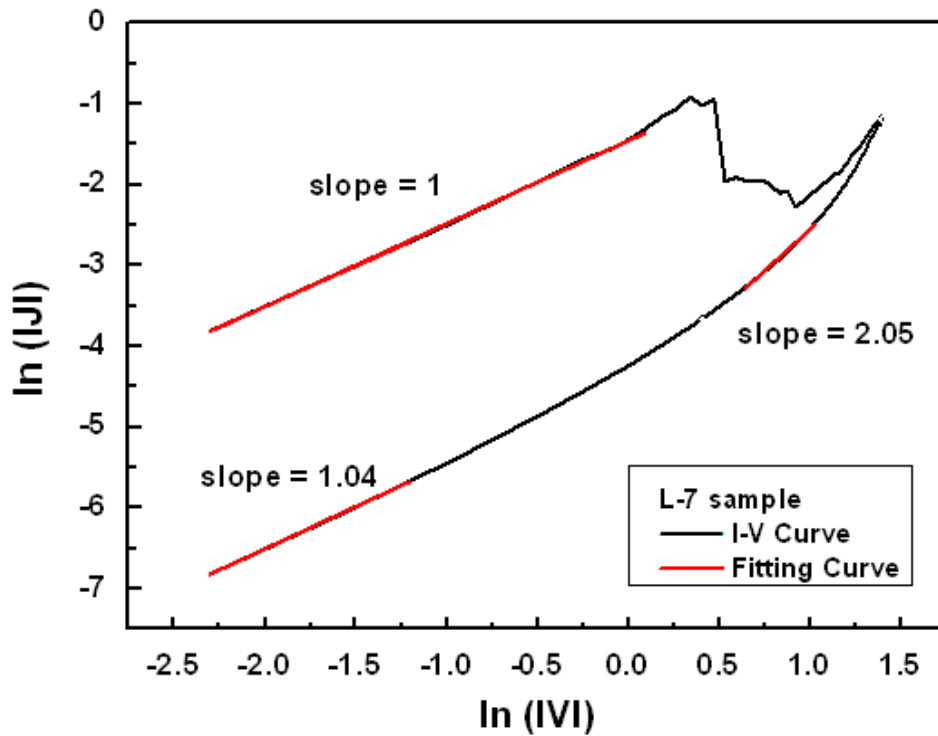
Fig. 5-40 (b) Electrical curves fitting on the positive side of the switching I-V curves L-7 samples.
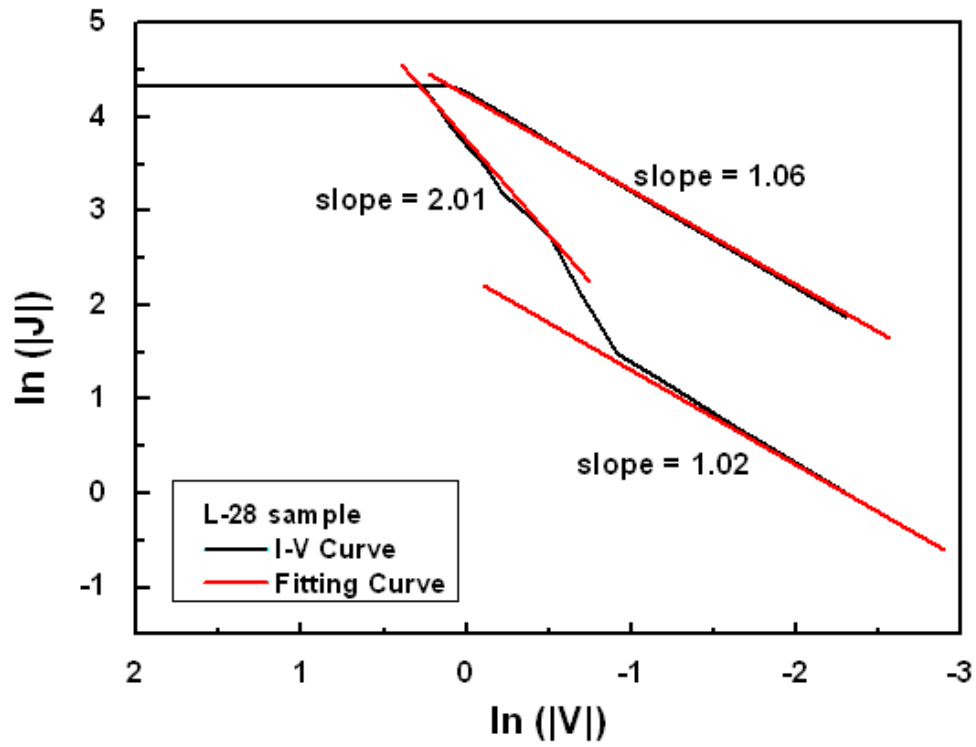
Fig. 5-41 (a) Electrical curves fitting on the negative side of the switching I-V curves L-28 samples.
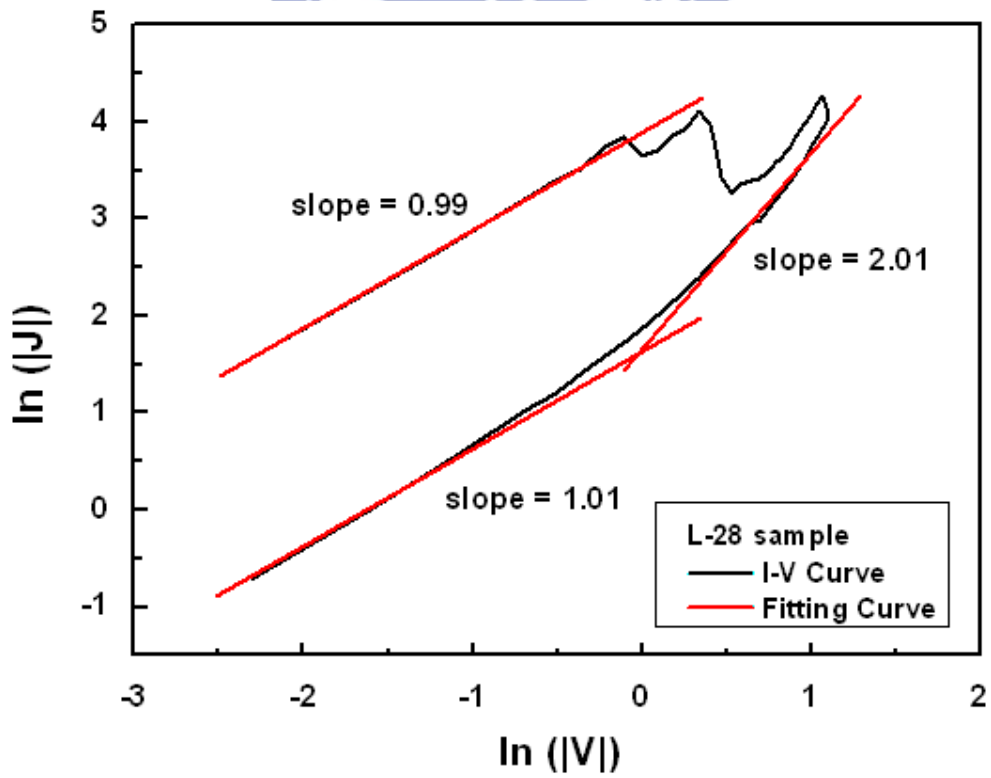
Fig. 5-41 (b) Electrical curves fitting on the negative side of the switching I-V curves L-28 samples.
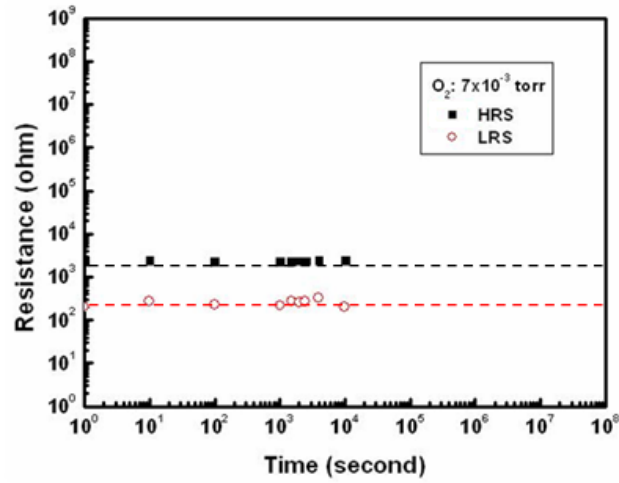
Fig. 5-42(a)   Data retention test of both HRS and LRS of L-7 over 10000 s at 0.1 V.
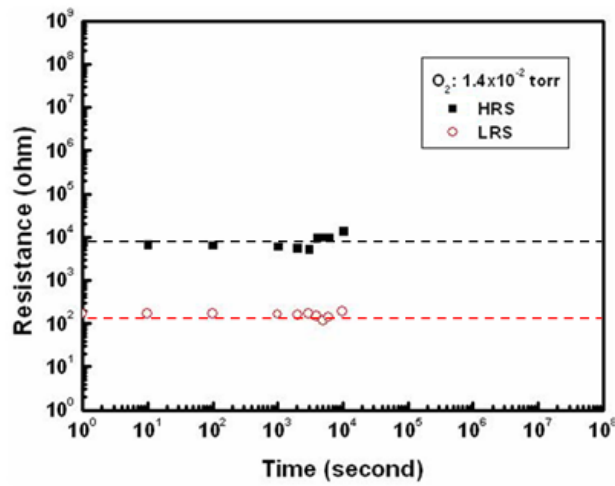
Fig. 5-42(b)   Data retention test of both HRS and LRS of L-14 over 10000 s at 0.1 V.
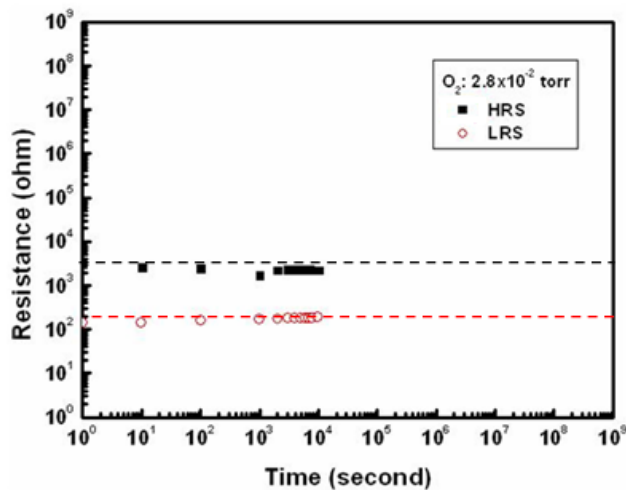
Fig. 5-42(c)   Data retention test of both HRS and LRS of L-28 over 10000 s at 0.1 V.
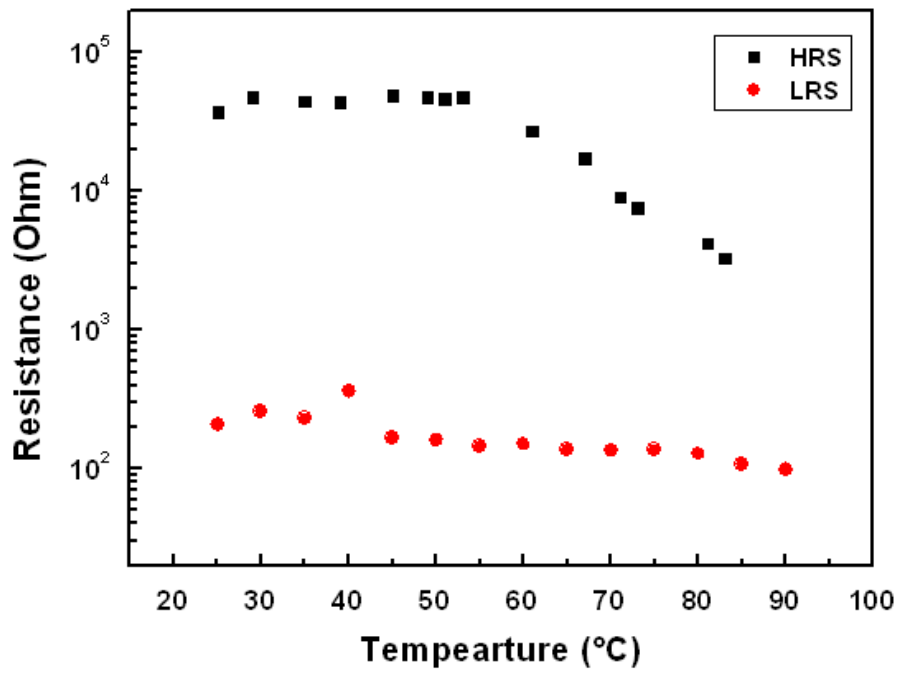
Fig. 5-43   Data retention test of both HRS and LRS of L-28 over 10000 s at 0.1 V.

Chapter 6　Conclusion

6.1 Conclusion

The RS memories based on HfO_x, Gd_2O_3, and $LaAlO_3$ thin film were fabricated, investigated, and discussed in this thesis. Some important factors were investigated including the intrinsic modulation (about MIM) and extrinsic modulation (post-treatment). The intrinsic modulated parameters included top electrode material, operation mode, operation polarity, electrode fabrication process, oxygen partial pressure condition, and deposition temperature. On the other hand, the extrinsic modulated parameters consisted of thermal treatment in N_2 and N_2/O_2, UV light exposure effect, among others. For the unipolar and bipolar RS characteristics, we then both propose the possible model to explain the switching mechanism. In addition, we can improve the electrical properties by modulating the above treatment.

A variety of factors of RS characteristics, including electrode material effect, electrode thickness effect, rapid thermal annealing effect in Ar or O_2 circumstance, electrode process effect, and UV light irradiation effect, were analyzed. A model based on the formation and rupture of the conducting filamentary paths through the pre-existing oxygen vacancies or grain boundaries may be the possible switching mechanism for our HfO_x thin film. Electrode is critical in determining the switching properties. Top portion of the HfO_x thin film is responsible for the RS under the applied bias, and can be well modulated by inserting a reactive metal Al, or by thermal annealing and/or recovery, electrode process, and UV light exposure. To sum up, as more oxygen ions are induced onto the HfO_x surface, the switching properties of the dispersion of operation voltage and high and low resistance values can be greatly improved. However, the conducting paths may be stemmed when the treatment condition is longer. When the crystallinity of the HfO_x surface was changed,

the switching behaviors became unstable and the switching parameters become dispersed. A well-chosen electrode material and fabrication process effectively improves the RS reliability.

The bipolar RS characteristics also greatly depend on the electrode materials. The Pd/HfO$_x$/TiN devices only exhibited the clockwise current loop, whereas the Pd/Al/HfO$_x$/TiN devices were able to perform both the clockwise and counterclockwise current loops. Such condition may be attributed to the interfacial layer formed at the Al/HfO$_x$ interface because the reactive metal Al will easily oxidize with the underlying HfO$_x$. The interfacial layer HfAlO composed of defects, such as oxygen vacancies or metallic defects, may be responsible for the migrated oxygen ions under applied bias. In addition, the effect of inserted thin Al layer can improve switching characteristics due to the increase in the crystallization temperature of the HfO$_x$ film. Given that the devices were free from thermal fluctuation factor, the structure of Pd/Al/HfO$_x$/TiN structure provided a better nonpolar RS characteristic and a reliable switching behavior, which widen the application of nonvolatile memory devices.

The Gd$_2$O$_3$ films for the RRAM application were successfully fabricated at RT by pulse laser deposition. The switching characteristics in the Ti/Gd$_2$O$_3$/Pt capacitor structure was investigated and discussed. Using XPS analysis data, we examined the distinction of the chemical composition between pristine and after forming samples, and confirmed that the metallic Gd defect inside the Gd$_2$O$_3$ films is necessary for the resistance switching behaviors. The RS behaviors of Ti/Gd$_2$O$_3$/Pt devices were observed and were found highly correlated with the anode electrode. Under positive bias operation, more than 100 switching characteristics could be detected with low voltage and resistance dispersion, whereas the switching properties became unstable and turned into a large fluctuation on the resistance and voltage values when the

devices were operated under negative bias. This phenomenon has already been explained in terms of the anode material. The current research demonstrates the switching properties of Gd_2O_3 film and its dependence on electrode material under a unipolar operation.

For the T-RRAM devices, highly transparent RRAM devices were successfully fabricated in this work based on the $ITO/Gd_2O_3/ITO$ sandwich structure on a glass substrate. The devices exhibited reliable and reproducible RS characteristics under bipolar operation for more than 2000 switching cycles, low operation voltage of approximately 1.6 V, and good data retention for more than 50000 seconds. Based on the results of the XPS analysis, the different composition ratio on the metallic (Gd^0) / oxidized (Gd^{3+}) were 65.5 % / 34.5 % and 49.3 % / 50.7 % for the 25 °C- and 300 °C-deposited samples, respectively. The large amounts of defects in the Gd_2O_3 film, including oxygen vacancies or metal atoms, among others, may considerably dominate the switching characteristics. The Gd_2O_3 particles gained higher kinetic energy to migrate on to the surface, and easily grew larger grains at 300 °C, resulting in the improvement in crystallinity of Gd_2O_3 film, more densification on film's structure, and lower leakage current. Therefore, a larger high to low resistance ratio was obtained.

The high-k dielectric LAO thin film deposited by pulsed laser deposition and grown at different oxygen partial pressure was investigated in this study. Based on the pulsed laser deposition growth mechanism, the effect of different oxygen partial pressures on surface roughness, the formation of the interfacial layer, the leakage current density, the breakdown voltage, and the RS characteristics of the LAO thin films were clearly investigated. The micro-structure and oxygen concentration difference inside the LAO thin films may be the main reason for the distinction of the RS characteristics. The conduction behavior of the electroforming procedure was

investigated using the electrical fitting curve. The conduction behavior changed from Ohmic conduction to Schottky emission in the middle voltage value, and to Frenkel emission in the vicinity of breakdown voltage. The residual electrons inside LAO contributed to the space-charge-limit conduction during the RS operation. Therefore, LAO films grown at higher oxygen partial pressure are beneficial for a more reliable RS performance because the formation of the interfacial layer and lower oxygen vacancy concentration exist in the LAO thin film. The interfacial layer can serve as a good oxygen reservoir residence and the involvement of more oxygen ions can ensure the switching reliability. The migration of the oxygen ions between the interfacial layer and the LAO films under applied bias may be the possible switching mechanism. The electroforming model was constructed to explain the reasons for the differing switching properties after the forming process. A blocking layer growth between LAO and ITO (BE) terminated the extended defects, leading to a uniform distribution on the oxygen vacancy concentration from top to bottom insulator film.

6.2 Future Work

In the present study, the appropriate treatment in O_2 and N_2 circumstance under specific temperature effectively improved the switching properties. Furthermore, a thin robust alumina formed at the interface of hafnium oxide enhanced the operation endurance and retention. Therefore, an insulator film composed of two different atomic distributions is needed for a stable switching operation. A conducting film was employed to control the amount of the injected electron, and another insulator film was used to control of the RS. Two stacked insulator films confined the conducting filamentary paths at some localized spot under applied bias, which improved the controllability on the filamentary path free from random fluctuation. For commercialized application, a pulse I-V test was conducted by applying the micro- or

nano-second square pulse to trigger the switch. Pulse I-V measurement decreased the measurement time to avoid the sample from being broken at long measurement time. Thus, when unipolar switching is operated, a material that can bear the high thermal budget is recommended for the insulator film. Note that the Hf has lower free energy of oxidation. Therefore, some higher free energy material oxide may be considered. The free energy of formation of oxidation of metals is important for selecting the metal electrode. This can be achieved using an alloy material, such as PtAl and PdTi, as top electrode. For bipolar HfO_x RRAM, the switching operation of SET and RESET under negative bias is needed for asymmetrical MIM structure. Chemical analysis is used to explore the oxygen concentration of HfO_x films. Pulse I-V measurement can provide not only an extra degree of freedom of measurement time, but also more precise reliability tests, endurance and data retention. Future research is necessary to determine with certainty the relationship between optimal condition of O_2 RTA, thickness, and oxygen content of HfO_x. The effect of thermal treatment on RRAM, which is constructed by the other metal top electrode, is also a great avenue for future research.

Research can also be focused on the different crystallinities of the insulator film. From the investigation on Gd_2O_3 and LAO thin film, we observed that different crystallines dominated the morphology, electrical characteristics, and RS properties of the thin films. For a suitable resistive operation, the optimal conditions of the thin film properties have to be well controlled. Forming process is needed before switch operation for all the memory cells. However, the main features of polycrystalline or amorphous semiconductors are quite different. For the crystalline thin film, defects such as metallic defects or oxygen vacancies inside the insulator thin film tended to migrate toward the grain boundaries first, and then tended to migrate along the grain boundaries, expanding toward the electrode under applied bias. However, for the

amorphous thin films, no preferential conducting path pre-existed inside the insulator film, which makes the injected electron mediate by random hopping or percolation phenomenon. The forming process for the two thin films with different crystallinity may induce alternative effect on each memory cells. Given that the forming process is necessary for most of the memory cells, a systematic study on how the forming process induces the defect sites inside the insulator thin film is beneficial for a universial understanding on RS.

We are hoping that future research will focus on these views to realize the commercial applications of RRAM, which we hope will ultimately result in better uniformity and reliability of its manufacture.

References

Chapter 1 - References:

[1]   W. W. Zhuang, W. Pan, B. D. Ulrich, J. J. Lee, L. Stecker, A. Burmaster, D. R. Evans, S. T. Hsu, M. Tajiri, A. Shimaoka, K. Inoue, T. Naka, N. Awaya, K. Sakiyama, Y. Wang, S. Q. Liu, N. J. Wu, and A. Ignatiev, "Novell colossal magnetoresistive thin film nonvolatile resistance random access memory (RRAM)," in *IEDM Tech. Dig.*, 2002, pp. 193-196.

[2]   A. K. Sharma, "*Semiconductor Memories: Technology, Testing and Reliability*," IEEE Press, New York, 1997.

[3]   D. Kahng, and S. M. Sze, "A floating gate and its application to memory devices,"*Bell Syst. Tech. J.*, 46, p. 1288, (1967).

[4]   J. Walker, S. Nallamothu, E. H. Chen, M. Mahajani, S. B. Herner, M. Clark, J. M. Cleeves, S. V. Dunton, V. L. Eckert, J. Gu, S. Hu, J. Knall, M. Konevecki, C. Petti, S. Radigan, U. Raghuram, J. Vienna, and M. A. Vvoda, "3D FT-SONOS memory cell for ultra-high density file storage application," in *Symp. On VLSI Tech. Dig.*, pp. 29-30, 2003.

[5]   T. Sugizaki, M. Kobayashi, M. Ishidao, H. Minakata, M. Yamaguchi, Y. Tamura, Y. Sugiyama, T. Nakanishi, and H. Tanaka, "Novel multi-bit SONOS type flash memory using a high-k charge trapping layer," in *Symp. on VLSI Tech. Dig.*, pp. 27-28, 2003.

[6]   Ramtron Application Note: FRAM Technology Backgrounder.

[7]   C. Y. Chang and S. M. Sze (Eds.), "*Nonvolatile Memory, in ULSI Devices*," John Wiley & Sons, New York, 2000.

[8]   C. A. Paz de Araujo et al., "Fatigue-free ferroelectric capacitors with platinum electrodes," *Nature*, vol. 374, pp. 627, 1995.

[9]   G. Binasch, P. Grunberg, F. Saurenbach, and W. Zinn, "Enhanced magnetoresistance in layered magnetic structures with antiferromagnetic interlayer exchange," *Phys. Rev. B*, vol. 39, pp. 4828-4830, 1989.

[10] J. S. Moodera, Lisa R. Kinder, Terrilyn M. Wong, and R. Meservey, "Large magnetoresistance at room temperature in ferromagnetic thin film tunnel junctions," *Phys. Rev. Lett.*, vol. 74, pp. 3273-3276, 1995.

[11] J. Solis, "Existence of electronic excitation enhanced crystallization in GeSb amorphous thin film upon ultrashort laser pulse irradiation," *Phys. Rev. Lett.*, vol. 76, no. 14, pp. 2519-2522, 1996.

[12] Standford R. Ovshinsky, "Reversible electrical switching phenomena in disordered structures," *Phys. Rev. Lett.*, vol. 21, pp. 1450-1453, 1968.

[13] S. Lai and T. Lowrey, "OUM-a 180 nm nonvolatile memory cell element

technology for stand alone and embedded applications," in *IEDM Tech. Dig.*, 2001. pp. 803-806.

[14] A. Redaelli, D. Ielmini, A. L. Lacaita, F. Pellizzer, A. Pirovano, and R. Bez, "Impact of crystallization statistics on data retention for phase change memories," in *IEDM Tech. Dig.*, 2005. pp. 742-745.

[15] T. W. Hickmott, "Potential distribution and negative resistance in thin oxide films," *J. Appl. Phys.*, vol. 35, pp. 2679-2689, 1964.

[16] J. G. Simmons, and R. R. Verderber, "New conduction and reversible memory phenomena in thin insulating films," *Proc. R. Soc.*, vol. A301, pp. 77-102, 1967.

[17] G. Dearnaley, "Electronic conduction through thin unsaturated oxide layers," *Phys. Lett. A*, vol. 25, pp. 760-761, 1967.

[18] D. C. Kim, S. Seo, S. E. Ahn, D. S. Suh, M. J. Lee, B. H. Park, I. K. Yoo, I. G. Baek, H. J. Kim, E. K. Yim, J. E. Lee, S. O. Park, H. S. Lim, U-ln Chung, J. T. Moon, and B. I. Ryu, "Electrical observations of filamentary conductions for the resistive memory switching in NiO films," *Appl. Phys. Lett.*, vol. 88, p. 202102, 2006.

[19] Y. Sato, K. Kinoshita, M. Aoki, and Y. Sugiyama, "Consideration of switching mechanism of binary metal oxide resistive junctions using a thermal reaction model," *Appl. Phys. Lett.*, vol. 90, p. 033503, 2007.

[20] A. Chen, S. Haddad, Y. C. Wu, T. N. Fang, S. Kaza, and Z. Lan, "Erasing characteristics of Cu_2O metal-insulator-metal resistive switching memory," *Appl. Phys. Lett.*, vol. 92, p. 013503, 2008.

[21] Y. He, J. Zhang, X. Guan, L. Zhao, Y. Wang, H. Qian, and Z. Yu, "Molecular dynamics study of the switching mechanism of Carbon-based resistive memory," *IEEE Trans. Electron Devices*, vol. 57, no.12, pp. 3434-3441, 2010.

[22] U. Russo, D. Ielmini, C. Cagli, and A. L. Lacaita, "Filament conduction and reset mechanism in NiO-based resistive-switching memory (RRAM) devices," *IEEE Trans. Electron Devices*, vol. 56, no.2, pp. 186-192, 2009.

[23] U. Russo, D. Ielmini, C. Cagli, and A. L. Lacaita, "Self-accelerated thermal dissolution model for reset programming in unipolar resistive-switching memory (RRAM) devices," *IEEE Trans. Electron Devices*, vol. 56, no.2, pp. 193-200, 2009.

[24] C. Cagli, F. Nardi, and D. Ielmini, "Modeling of set/reset operations in NiO-based resistive-switching memory devices," *IEEE Trans. Electron Devices*, vol. 56, no. 8, pp. 1712-1720, 2009.

[25] K. Kinoshita, T. Tamura, M. Aoki, Y. Sugiyama, and H. Tanaka, "Bias polarity dependent data retention of resistive random access memory consisting of binary transition metal oxide," *Appl. Phys. Lett.*, vol. 89, p. 103509, 2006.

[26] K. M. Kim, B. J. Choi, B. W. Koo, S. Choi, D. S. Jeong, and C. S. Hwang, "Resistive switching in Pt/Al$_2$O$_3$/TiO$_2$/Ru stacked structures," *Electrochem. Solid-State Lett.*, vol. 9, no. 12, pp. G343-G346, 2006.

[27] K. M. Kim, B. J. Choi, Y. C. Shin, S. Choi, and C. S. Hwang, "Anode-interface localized filamentary mechanism in resistive switching of TiO$_2$ thin films," *Appl. Phys. Lett.*, vol. 91, p. 012907, 2007.

[28] K. M. Kim, B. J. Choi, and C. S. Hwang, "Localized switching mechanism in resistive switching of atomic-layer-deposited TiO$_2$ thin films," *Appl. Phys. Lett.*, vol. 90, p. 242906, 2007.

[29] K. M. Kim, B. J. Choi, S. J. Song, G. H. Kim, and G. S. Hwang, "Filamentary resistive switching localized at cathode interface in NiO thin films," *J. Electrochem. Soc.,* vol. 156, no. 12, pp. G213-G216, 2008.

[30] H. Y. Lee, P. S. Chen, C. C. Wang, S. Maikap, P. J. Tzeng, C. H. Lin, L. S. Lee, and M. J. Tsai, "Low-power switching of nonvolatile resistive memory using hafnium oxide," *J. Jpn. Appl. Phys.*, vol. 46, no. 4B, pp. 2175-2179, 2007.

[31] C. Rohde, B. J. Choi, D. S. Jeong, S. Choi, J. S. Zhao, and C. S. Hwang, "Identification of a determining parameter for resistive switching of TiO$_2$ thin films," *Appl. Phys. Lett.*, vol. 86, p. 262907, 2005.

[32] J. B. Yun, S. Kim, S. Seo, M. J. Lee, D. C. Kim, S. E. Ahn, Y. Park, J. Kim, and H. Shin, "Random and localized resistive switching observation in Pt/NiO/Pt," *Phys. Stat. Sol. (RRL)*, vol. 1, no. 6, pp. 280-282, 2007.

[33] S. H. Chang, S. C. Chae, S. B. Lee, C. Liu, T. W. Noh, J. S. Lee, B. Kahng, J. H. Jang, M. Y. Kim, D. -W. Kim, and C. U. Jung, "Effects of heat dissipation on unipolar resistance switching in Pt/NiO/Pt capacitors," *Appl. Phys. Lett.*, vol. 92, p. 183507, 2008.

[34] G. S. Park, X. S. Li, D. C. Kim, R. J. Jung, M. J. Lee, and S. Seo, "Observation of electric-field induced Ni filament channels in polycrystalline NiO$_x$ film," *Appl. Phys. Lett.*, vol. 91, p. 222103, 2007.

[35] S. Seo, M. J. Lee, D. C. Kim, S. E. Ahn, B. H. Park, Y. S. Kim, I. K. Yoo, I. S. Byun, I. R. Hwang, S. H. Kim, J. S. Kim, J. S. Choi, J. H. Lee, S. H. Jeon, S. H. Hong, and B. H. Park, "Electrode dependence of resistance switching in polycrystalline NiO films," *Appl. Phys. Lett.*, vol. 87, p. 263507, 2005.

[36] S. Spiga, A. Lamperti, C. Wiemer, M. Perego, E. Cianci, G. Tallarida, H. L. Lu, M. Alia, F. G. Volpe, M. Fanciulli, "Resistance switching in amorphous and crystalline binary oxides grown by electron beam evaporation and atomic layer deposition," *Microelectronic Engineering*, vol. 85, pp. 2414-2419, 2008.

[37] C. B. Lee, B. S. Kang, A. Benayad, M. J. Lee, S. E. Ahn, K. H. Kim, G. Stefanovich, Y. Park, and I. K. Yoo, "Effects of metal electrodes on the resistive

memory switching property of NiO thin films," *Appl. Phys. Lett.*, vol. 93, p. 042115, 2008.

[38] D. C. Kim, M. J. Lee, S. E. Ahn, S. Seo, J. C. Park, I. K. Yoo, I. G. Baek, H. J. Kim, E. K. Yim, J. E. Lee, S. O. Park, H. S. Kim, U-ln Chung, J. T. Moon, and B. I. Ryu, "Improvement of resistive memory switching in NiO using IrO_2," *Appl. Phys. Lett.*, vol. 88, p. 232106, 2006.

[39] S. Go, K. Jeong, K. Lee, A. Kim, H. Ruh, C. S. Kim, and J. Lee, "Effects of Si interlayer on resistance switching of Pt/Si/TiO_2/Pt structures," *J. Vac. Sci. Technol. B*, vol. 27, no. 5, pp. 2175-2181, 2009.

[40] J. H. Choi, S. N. Das, and J. M. Myoung, "Controllable resistance switching behavior of NiO/SiO_2 double layers for nonvolatile memory application," *Appl. Phys. Lett.*, vol. 95, p. 062105, 2009.

[41] M. J. Lee, C. B. Lee, D. Lee, S. R. Lee, J. Hur, S. E. Ahn, M. Chang, Y. B. Kim, U. I. Chung, C. J. Kim, D. S. Kim, and H. Lee, "Improved resistive switching reliability in graded NiO multilayer for resistive nonvolatile memory devices," *IEEE Electron Device Lett.*, vol. 31, no. 7, pp. 725-727, 2010.

[42] J. Song, A. I. Inamdar, B. Jang, K. Jeon, Y. S. Kim, K. Jung, Y. Kim, H. Im, W. Jung, H. Kim, and J. P. Hong, "Effect of Ultra Al Layer Insertion on Resistive Switching performance in an Amorphous Aluminum Oxide Resistive Memory," *Appl. Phys. Exp.*, vol. 3, p. 091101, 2010.

[43] K. Tsunoda, K. Kinoshita, H. Noshiro, Y. Yamazaki, T. Iizuka, Y. Ito, A. akahashi, A. Okano, Y. Sato, T. Fukano, M. Aoki, and Y. Sugiyama, "Low power and high speed switching of Ti-doped NiO ReRAM under the unipolar voltage source of less than 3 V," in *IEDM Tech. Dig.*, 2007, pp. 767-770.

[44] K. Jung, J. Choi, Y. Kim, H. Im, S. Seo, R. Jung, D. C. Kim, J. S. Kim, B. H. Park, and J. P. Hong, "Resistance switching characteristics in Li-doped NiO," *J. Appl. Phys.*, vol. 103, p. 034504, 2008.

[45] L. F. Liu, J. F. Kang, N. Xu, X. Sun, C. Chen, B. Sun, Y. Wang, X. Y. Liu, X. Zhang, and R. Q. Han, "Gd doping improved resistive switching characteristics of TiO_2-based resistive memory deivces," *J. Jpn. Appl. Phys.*, vol. 47, no. 4, pp. 2701-2703, 2008.

[46] Q. Liu, S. Long, W. Guan, S. Zhang, M. Liu, and J. Chen, "Unipolar resistive switching of Au^+-implanted ZrO_2 films," J. Semicond., vol. 30, no. 4, p.042001, 2009.

[47] C. Y. Liu, X. J. Lin, H. Y. Wang, and C. H. Lai, "Improved resistive switching dispersion of NiO_x thin film by Cu-doping method," *J. Jpn. Appl. Phys.*, vol. 49, p. 056507, 2010.

[48] S. H. Phark, R. Jung, Y. J. Chang, T. W. Noh, and D. W. Kim, "Interfacial

reactions and resistive switching behaviors of metal/NiO/metal structures," *Appl. Phys. Lett.*, vol. 94, p. 022906, 2009.

[49] S. W. Chen, and J. M. Wu, "Unipolar resistive switching behavior of BiFeO$_3$ thin films prepared by chemical solution deposition," *Thin Solid Films*, vol. 519, pp. 499-504, 2010.

[50] D. Panda, A. Dhar, and S. K. Ray, "Nonvolatile and unipolar resistive switching characteristics of pulsed laser ablated NiO films," *J. Appl. Phys.,* vol. 108, p. 104513, 2010.

[51] Q. Mao, Z. Ji, and J. Xi, "Realization of forming-free ZnO-based resistive switching memory by controlling film thickness," *J. Phys. D*, vol. 43, p. 395104, 2010.

[52] J. S. Kwak, Y. H. Do, Y. C. Bae, H. Im, and J. P. Hong, "Reproducible unipolar resistive switching behaviors in the metal-deficient CoO$_x$ thin film," *Thin Solid Films*, vol. 518, pp. 6437-6440, 2010.

[53] F. Chen, B. Li, R. Jammy, R. A. Dufresne, and A. W. Strong, "Photo-enhanced negative differential resistance and photo-accelerated time-dependent dielectric breakdown in thin nitride-oxide dielectric film," *Appl. Phys. Lett.*, vol.78, no. 21 pp. 3241-3243, 2001.

[54] K. C. Liu, W. H. Tzeng, K. M. Chang, Y. C. Chan, and C. C. Kuo, "Effect of ultraviolet light exposure on a HfO$_x$ RRAM device," *Thin Solid Films*, vol. 518, pp. 7460-7463, 2010

[55] C. Y. Liu, and J. M. Hsu, "Effects of ultraviolet illumination on resistive switching properties of Cu$_x$O thin film," *J. Jpn. Appl. Phys.*, vol. 49, p. 084202, 2010.

[56] I. G. Baek, D. C. Kim, M. J. Lee, H. J. Kim, E. K. Yim, M. S. Lee, J. E. Lee, S. E. Ahn, S. Seo, J. H. Lee, J. C. Park, Y. K. Cha, S. O. Park, H. S. Kim, I. K. Yoo, U-In Chung, J. T. Moon, and B. I. Ryu, "Multi-layer cross-point binary oxide resistive memory (OxRRAM) for post-NAND storage application," in *IEDM Tech. Dig.*, 2005, pp. 750-753.

[57] C. B. Lee, B. S. Kang, M. J. Lee, S. E. Ahn, G. Stefanovich, W. X. Xianyu, K. H. Kim, J. H. Hur, H. X. Yin, Y. Park, I. K. Yoo, J. B. Park, and B. H. Park, "Electromigration effect of Ni electrodes on the resistive switching characteristics of NiO thin films," *Appl. Phys. Lett.*, vol. 91, p. 082104, 2007.

[58] R. Jung, M. J. Lee, S. Seo, D. C. Kim, G. S. Park, K. Kim, S. Ahn, Y. Park, I. K. Yoo, J. S. Kim, and B. H. Park, "Decrease in switching voltage fluctuation of Pt/NiO$_x$/Pt structure by process control," *Appl. Phys. Lett.*, vol. 91, p. 022112, 2007.

[59] S. Seo, M. J. Lee, D. H. Seo, S. K. Choi, D. S. Suh, Y. S. Joung, I. K. Yoo, I. S.

Byun, I. R. Hwang, S. H. Kim, and B. H. Park, "Conductivity switching characteristics and reset currents in NiO films," *Appl. Phys. Lett.*, vol. 86, p. 093509, 2005.

[60] Y. Sato, K. Tsunoda, K. Kinoshita, H. Noshiro, M. Aoki, and Y. Sugiyama, "Sub-100-µA reset current of nickel oxide resistive memory through control of filamentary conductance by current limit of MOSFET," *IEEE Trans. Electron Devices*, vol. 55, no. 5, pp. 1185-1191, 2008.

[61] T. N. Fang, S. Kaza, S. Haddad, A. Chen, Y. C. Wu, Z. Lan, S. Avanzino, D. Liao, C. Gopalan, S. Choi, S. Mahdavi, M. Buynoski, Y. Lin, C. Marrian, C. Bill, M. VanBuskirk, and M. Taguchi, "Erase mechanism for copper oxide resistive switching memory cells with Nickel electrode," *IEEE Trans. Electron Devices*, vol. 55, no. 5, pp. 789-792, 2006.

[62] L. Tang, P. Zhou, Y. R. Chen, L. Y. Chen, H. B. Lv, T. A. Tang, and Y. Y. Lin, "Temperature and electrode-size dependences of the resistive switching characteristics of Cu_xO thin films," *J. Korean Phys. Soc.*, vol. 53, pp. 2283-2286, 2008.

[63] A. Chen, S. Haddad, Y. C. Wu, T. N. Fang, S. Kaza, and Z. Lan, "Erasing characteristics of Cu_2O metal-insulator-metal resistive switching memory," *Appl. Phys. Lett.*, vol. 92, p. 013503, 2008.

[64] M. Yin, P. Zhou, H. B. Lv, J. Xu, Y. L. Song, X. F. Fu, T. A. Tang, B. A. Chen, and Y. Y. Lin, "Improvement of resistive switching in Cu_xO using new reset mode," *IEEE Electron Device Lett.*, vol. 29, no. 7, pp. 681-683, 2008.

[65] C. Schindler, G. Staikov, and R. Waser, "Electrode kinetics of $Cu-SiO_2$-based resistive switching cells: Overcoming the voltage-time dilemma of electrochemical metallization memories," *Appl. Phys. Lett.*, vol. 94, p. 072109, 2009.

[66] Y. Hirose, H. Hirose, "Polarity-dependent memory switching and behavior of Ag dendrite in Ag-photodoped amorphous As_2S_3 films," *J. Appl. Phys.*, vol. 47, p. 2767, 1976.

[67] M. Haemori, T. Nagata, and T. Chikyow, "Impact of Cu electrode on switching behavior in a $Cu/HfO_2/Pt$ structure and resultant Cu ion diffusion," *Appl. Phys. Exp.*, vol. 2, p. 061401, 2009.

[68] C. Chen, Y. C. Yang, F. Zeng, and F. Pan, "Bipolar resistive switching in Cu/AlN/Pt nonvolatile memory device," *Appl. Phys. Lett.*, vol. 97, p. 083502, 2010.

[69] F. Zhuge, W. Dai, C. L. He, A. Y. Wang, Y. W. Liu, M. Li, Y. H. Wu, P. Cui, and P. W. Li, "Nonvolatile resistive switching memory based on amorphous carbon," *Appl. Phys. Lett.*, vol. 96, p. 163505, 2010.

[70] T. Sakamoto, K. Lister, N. Banno, T. Hasegawa, K. Terabe, and M. Aono, "Electronic transport in Ta_2O_5 resistive switch," *Appl. Phys. Lett.*, vol. 91, p. 092110, 2007.

[71] S. Z. Rahaman, and S. Maikap, "Low power resistive switching memory using Cu metallic filament in $Ge_{0.2}Se_{0.8}$ solid-electrolyte," *Microelectronics Reliability*, vol. 50, pp. 643-646, 2010.

[72] S. Z. Rahaman, S. Maikap, H. C. Chiu, C. H. Lin, T. Y. Wu, Y. S. Chen, P. J. Tzeng, F. Chen, M. J. Kao, and M. J. Tsai, "Bipolar resistive switching memory using Cu metallic filament in $Ge_{0.4}Se_{0.6}$ solid electrolyte," *Electrochem. Solid-State Lett.*, vol. 13, no. 5, pp. H159-H162, 2010.

[73] K. Ono, K. Kurotsuchi, Y. Fujisaki, R. Takemura, M. Terao, and N. Takaura, "Resistive switching ion-plug memory for 32-nm technology node and beyond," *J. Jpn. Appl. Phys.,* vol. 48, p. 04C160, 2009.

[74] S. Puthen Thermadam, S. K. Bhagat, T. L. Alford, Y. Sakaguchi, M. N. Kozicki, and M. Mitkova, "Influence of Cu diffusion conditions on the switching of $Cu-SiO_2$-based resistive memory devices," *Thin Solid Films*, vol. 518, pp. 3293-3298, 2010.

[75] D. Lee, D. Seong, I. Jo, F. Xiang, R. Dong, S. Oh, and H. Hwang, "Resistance switching of copper doped MoO_x films for nonvolatile memory application," *Appl. Phys. Lett.*, vol. 90, p. 122104, 2007.

[76] C. Schindler, M. Weides, M. N. Kozicki, and R. Waser, "Low current resistive switching in $Cu-SiO_2$ cells," *Appl. Phys. Lett.*, vol. 92, p. 122910, 2008.

[77] M. Liu, Z. Abid, W. Wang, X. He, Q. Liu, and W. Guan, "Multilevel resistive switching with ionic and metallic filaments," *Appl. Phys. Lett.*, vol. 94, p. 233106, 2009.

[78] Y. C. Yang, F. Pan, F. Zeng, and M. Liu, "Switching mechanism transition induced by annealing treatment in nonvolatile Cu/ZnO/Cu/ZnO/Pt resistive memory: From carrier trapping/detrapping to electrochemical metallization," *J. Appl. Phys.,* vol. 106, p. 123705, 2009.

[79] W. Guan, M. Liu, S. Long, Q. Liu, and W. Wang, "On the resistive switching mechanisms of $Cu/ZrO_2:Cu/Pt$," *Appl. Phys. Lett.*, vol. 93, p. 223506, 2008.

[80] Y. Wang, Q. Liu, S. Long, W. Wang, Q. Wang, M. Zhang, S. Zhang, Y. Li, Q. Zuo, J. Yang, and M. Liu, "Investigation of resistive switching in Cu-doped HfO_2 thin film for multilevel non-volatile memory application," *Nanotechnology*, vol. 21, p. 045202, 2010.

[81] Q. Liu, S. Long, W. Wang, S. Tanachutiwat, Y. Li, Q. Wang, M. Zhang, Z. Huo, J. Chen, and M. Liu, "Low-power and highly uniform switching in ZrO_2-based ReRAM with a Cu nanocrystal insertion layer," *IEEE Electron Device Lett.*, vol.

31, no. 11, pp. 1299-1301, 2010.

[82] D. Varandani, B. Singh, B. R. Mehta, M. Singh, V. N. Singh, and D. Gupta, "Resistive switching mechanism in delafossite-transition metal oxide (CuInO$_2$-CuO) bilayer structure," *J. Appl. Phys.*, vol. 107, p. 103703, 2010.

[83] R. S. Potember, T. O. Poehler, D. O. Cowan, and A. N. Bloch, "Electrical switching and memory phenomena in Cu-TCNQ thin films," *Appl. Phys. Lett.*, vol. 34, p. 405, 1979.

[84] R. Muller, C. Krebs, L. Goux, D. J. Wouters, J. Genoe, P. Heremans, S. Spiga, and M. Fanciulli, "Bipolar resistive electrical switching of CuTCNQ memories incorporating a dedicated switching layer," *IEEE Electron Device Lett.*, vol. 30, no. 6, pp. 620-622, 2009.

[85] D. Deleruyelle, C. Muller, J. Amouroux, and R. Muller, "Electrical nanocharacterization of copper tetracyanoquinodimethane layers dedicated to resistive random access memories," *Appl. Phys. Lett.*, vol. 96, p. 263504, 2010.

[86] Ch. Muller, D. Deleruyelle, R. Muller, M. Thomas, A. Demolliens, Ch. Turquat, S. Spiga, "Resistance change in memory structures integrating CuTCNQ nanowires grown on dedicated HfO$_2$ switching layer," *Solid-State Electronics*, article in press, 2010.

[87] H. X. Guo, B. Yang, L. Chen, Y. D. Xia, K. B. Yin, Z. G. Liu, and J. Yin, "Resistive switching devices based on nanocrystalline solid electrolyte (AgI)$_{0.5}$(AgPO$_3$)$_{0.5}$," *Appl. Phys. Lett.*, vol. 91, p. 243513, 2007.

[88] X. F. Liang, Y. Chen, L. Shi, J. Lin, J. Yin, and Z. G. Liu, "Resistive switching and memory effects of AgI thin film," *J. Phys. D: Appl. Phys.*, vol. 40, pp. 4767-4770, 2007.

[89] U. Russo, D. Kamalanathan, D. Ielmini, A. L. Lacaita, M. N. Kozicki, "Study of multilevel programming in programmable metallization cell (PMC) memory," *IEEE Trans. Electron Devices*, vol. 56, no. 5, pp. 1040-1047, 2009.

[90] M. Morales-Masis, S. J. van der Molen, W. T. Fu, M. B. Hesselberth, and J. M. Van Ruitenbeek, "Conductance switching in Ag$_2$S devices fabricated by in situ sulfurization," *Nanotechnology*, vol. 20, p. 095710, 2009.

[91] X. B. Yan, J. Yin, H. X. Guo, Y. Su, B. Xu, H. T. Li, D. W. Yan, Y. D. Xia, and Z. G. Liu, "Bipolar resistive switching performance of the nonvolatile memory cells based on solid electrolyte films," *J. Appl. Phys.*, vol. 106, p. 054501, 2009.

[92] L. Chen, Z. Liu, Y. Xia, K. Yin, L. Gao, and J. Yin, "Electrical field induced precipitation reaction and percolation in Ag$_{30}$Ge$_{17}$Se$_{53}$ amorphous electrolyte films," *Appl. Phys. Lett.*, vol. 94, p. 162112, 2009.

[93] H. X. Guo, L. G. Gao, Y. D. Xia, K. Jiang, B. Xu, Z. G. Liu, and J. Yin, "The growth of metallic nanofilaments in resistive switching memory devices based

on solid electrolytes," *Appl. Phys. Lett.*, vol. 94, p. 153504, 2009.

[94] Y. C. Yang, F. Pan, Q. Liu, M. Liu, and F. Zeng, "Fully room-temperature-fabricated nonvolatile resistive memory for ultrafast and high-density memory application," *Nano Lett.*, vol. 9, no. 4, pp. 1636-1643, 2009.

[95] Y. Li, S. Long, M. Zhang, Q. Liu, L. Shao, S. Zhang, Y. Wang, Q. Zuo, S. Liu, and M. Liu, "Resistive switching properties of Au/ZrO₂/Ag structure for low-voltage nonvolatile memory applications," *IEEE Electron Device Lett.*, vol. 31, no. 2, pp. 117-119, 2010.

[96] X. B. Yan, K. Li, J. Yin, Y. D. Xia, H. X. Guo, L. Chen, and Z. G. Liu, "The resistive switching mechanism of Ag/SrTiO₃/Pt memory cells," *Electrochem. Solid-State Lett.*, vol. 13, no. 3, pp. H87-H89, 2010.

[97] W. Xu, X. Li, Y. Rui, X. Liu, Z. Wang, and L. Chen, "Improvement of resistive switching property in a noncrystalline and low-resistance La$_{0.7}$Ca$_{0.3}$MnO₃ thin film by using an Ag-Al alloy electrode," *J. Phys. D: Appl. Phys.*, vol. 41, p. 215409, 2008.

[98] X. Guo, C. Schindler, S. Menzel, and R. Waser, "Understanding the switching-off mechanism in Ag$^+$ migration based resistively switching model systems," *Appl. Phys. Lett.*, vol. 91, p. 133513, 2007.

[99] X. Liu, Matthew, T. Mayer, and D. Wang, "Negative differential resistance and resistive switching behaviors in Cu₂S nanowire devices," *Appl. Phys. Lett.*, vol. 96, p. 223103, 2010.

[100] Z. M. Liao, C. Hou, H. Z. Zhang, D. S. Wang, and D. P. Yu, "Evolution of resistive switching over bias duration of single Ag₂S nanowires," *Appl. Phys. Lett.*, vol. 96, p. 203109, 2010.

[101] C. Pi, Y. Ren, and W. K. Chim, "Investigation of bipolar resistive switching and the time-dependent SET process in silver sulfide/silver thin films and nanowire array structures," *Nanotechnology*, vol. 21, p. 085709, 2010.

[102] A. Schmehl, F. Lichtenberg, H. Bielefeldt, J. Mannhart, and D. G. Schlom, "Transport properties of LaTiO$_{3+x}$ films and heterostructures," *Appl. Phys. Lett.*, vol. 82, no. 8, pp. 3077-3079, 2003.

[103] A. Sawa, T. Fujii, M. Kawasaki, and Y. Tokura, "Hysteretic current-voltage characteristics and resistance switching at a rectifying Ti/Pr0.7Ca$_{0.3}$MnO₃ interface," *Appl. Phys. Lett.*, vol. 85, no. 18, pp. 4073-4075, 2004.

[104] M. C. Ni, S. M. Guo, H. F. Tian, Y. G. Zhao, and J. Q. Li, "Resistive switching effect in SrTiO$_{3-\delta}$/Nb-doped SrTiO₃ heterojunction," *Appl. Phys. Lett.*, vol. 91, p. 183502, 2007.

[105] D. J. Seong, M. Jo, D. Lee, and H. Hwang, "HPHA effect on reversible resistive

switching of Pt/Nb-doped $SrTiO_3$ Schottky junction o fnonvolatile memory," *Electrochem. Solid-State Lett.*, vol. 10, no. 6, pp. H168-H170, 2007.

[106] J. Ouyang, and Y. Yang, "Polymer:metal nanoparticle devices with electrode-sensitive bipolar resistive switchings and their application as nonvolatile memory devices," *Appl. Phys. Lett.*, vol. 96, p.063506, 2010.

[107] L. E. Yu, S. Kim, M. K. Ryu, S. Y. Choi, and Y. K. Choi, "Structure effects on resistive switching of $Al/TiO_x/Al$ devices for RRAM applications," *IEEE Electron Device Lett.*, vol. 29, no. 4, pp. 331-333, 2008.

[108] A. E. Rakhshani, "The role of space-charge-limited-current conduction in evaluation of the electrical properties of thin Cu_2O films," *J. Appl. Phys.*, vol. 69, no. 4, pp. 2365-2369, 1991.

[109] M. A. Lampert, and P. Mark, *Current Injection in Solid*. New York: Academic, 1970.

[110] W. Y. Yang, W. G. Kim, and S. W. Rhee, "Radio frequency sputter deposition of single phase cuprous oxide using Cu_2O as a target material and its resistive switching properties," *Thin Solid Films*, vol. 517, pp. 967-971, 2008.

[111] A. Chen, S. Haddad, and Y. C. Wu, "A temperature-accelerated method to evaluate data retention of resistive switching nonvolatile memory," *IEEE Electron Device Lett.*, vol. 29, no. 1, pp. 38-40, 2008.

[112] C. T. Tsai, T. C. Chang, P. T. Liu, Y. L. Cheng, and F. S. Huang, "Low temperature improvement on silicon oxide grown by electron-gun evaporation for resistance memory applications," *Appl. Phys. Lett.*, vol. 93, p. 052903, 2008.

[113] S. H. Hong, O. Kim, S. Choi, and M. Ree, "Bipolar resistive switching in a single layer memory device based on a conjugated copolymer," *Appl. Phys. Lett.*, vol. 91, p. 093517, 2007.

[114] D. Lee, H. Choi, H. Sim, D. Choi, H. Hwang, M. J. Lee, S. A. Seo, and I. K. Yoo, "Resistance switching of the nonstoichiometric Zirconium oxide for nonvolatile memory applications," *IEEE Electron Device Lett.*, vol. 26, no. 9, pp. 719-721, 2005.

[115] Q. Liu, W. Guan, S. Long, R. Jia, M. Liu, and J. Chen, "Resistive switching memory effect of ZrO_2 films with Zr^+ implanted," *Appl. Phys. Lett.*, vol. 92, p. 012117, 2008.

[116] Q. Liu, W. Guan, S. Long, M. Liu, S. Zhang, Q. Wang, and J. Chen, "Resistance switching of Au-implanted-ZrO_2 film for nonvolatile memory application," *J. Appl. Phys.*, vol. 104, p. 114514, 2008.

[117] W. Guan, S. Long, R. Jia, and M. Liu, "Nonvolatile resistive switching memory utilizing gold nanocrystals embedded in zirconium oxide," *Appl. Phys. Lett.*, vol. 91, p. 062111, 2007.

[118] H. Y. Jeong, J. Y. Kim, T. H. Yoon, and S. Y. Choi, "Bipolar resistive switching characteristics of poly(3,4-ethylene-dioxythiophene):Poly(styrenesulfonate) thin film," *Curr. Appl. Phys.*, vol. 10, pp. e46-e49, 2010.

[119] M. J. Rozenberg, I. H. Inoue, and M. J. Sanchez, "Nonvolatile memory with multilevel switching: a basic model," *Phys. Rev. Lett.*, vol. 92, no. 17, p. 178302, 2004.

[120] M. J. Rozenberg, I. H. Inoue, and M. J. Sanchez, "Strong electron correlation effects in nonvolatile electronic memory devices," *Appl. Phys. Lett.*, vol. 88, p. 033510, 2006.

[121] D. S. Kim, Y. H. Kim, C. E. Lee, and Y. T. Kim, "Colossal electroresistance mechanism in a $Au/Pr_{0.7}Ca_{0.3}MnO_3/Pt$ sandwich structure: Evidence for a Mott transition," *Phys. Rev. B.*, vol. 74, p. 174430, 2006.

[122] D. S. Kim, C. E. Lee, Y. H. Kim, and Y. T. Kim, "Effect of oxygen annealing on $Pr_{0.7}Ca_{0.3}MnO_3$ thin film for colossal electroresistance at room temperature," *J. Appl. Phys.*, vol. 100, p. 093901, 2006.

[123] M. Fujimoto, H. Koyama, Y. Nishi, and T. Suzuki, "Resistive switching properties of high crystallinity and low-resistance $Pr_{0.7}Ca_{0.3}MnO_3$ thin film with point-contacted Ag electrodes," *Appl. Phys. Lett.*, vol. 91, p. 223504, 2007.

[124] M. Fujimoto, H. Koyama, M. Konagai, Y. Hosoi, K. Ishihara, S. Ohnishi, and N. Awaya, "TiO_2 anatase nanolayer on TiN thin film exhibiting high-speed bipolar resistive switching," *Appl. Phys. Lett.*, vol. 89, p. 223509, 2006.

[125] N. Xu, L. F. Liu, X. Sun, C. Chen, Y. Wang, D. D. Han, X. Y. Liu, R. Q. Liu, J. F. Kang, and B. Yu, "Bipolar switching behavior in TiN/ZnO/Pt resistive nonvolatile memory with fast switching and long retention," *Semicond. Sci. Technol.*, vol. 23, p. 075019, 2008.

[126] B. Sun, Y. X. Liu, L. F. Liu, N. Xu, Y. Wang, X. Y. Liu, R. Q. Han, and J. F. Kang, "Highly uniform resistive switching characteristics of $TiN/ZrO_2/Pt$ memory devices," *J. Appl. Phys.*, vol. 105, p. 061630, 2009.

[127] B. Sun, L. Liu, N. Xu, B. Gao, Y. Wang, D. Han, X. Liu, R. Han, and J. Kang, "The effect of current compliance on the resistive switching behaviors in $TiN/ZrO_2/Pt$ memory device," *J. Jpn. Appl. Phys.*, vol. 48, p. 04C061, 2009.

[128] Y. H. Do, J. S. Kwak, Y. C. Bae, J. H. Lee, Y. Kim, H. Im, and J. P. Hong, "TiN electrode-induced bipolar resistive switching of TiO_2 thin films," *Curr. Appl. Phys.*, vol. 10, pp. e71-e74, 2010.

[129] M. C. Chen, T. C. Chang, C. T. Tsai, S. Y. Huang, S. C. Chen, C. W. Hu, S. M. Sze, and M. J. Tsai, "Influence of electrode material on the resistive memory switching property of indium gallium zinc oxide thin films," *Appl. Phys. Lett.*, vol. 96, p. 262110, 2010.

[130] J. S. Kwak, Y. H. Do, Y. C. Bae, H. S. Im, J. H. Yoo, M. G. Sung, Y. T. Hwang, and J. P. Hong, "Roles of interfacial TiO_xN_{1-x} layer and TiN electrode on bipolar resistive switching in $TiN/TiO_2/TiN$ frameworks," *Appl. Phys. Lett.*, vol. 96, p. 223502, 2010.

[131] C. Y. Lin, C. Y. Wu, C. Y. Wu, T. C. Lee, F. L. Yang, C. Hu, and T. Y. Tseng, "Effect of top electrode material on resistive switching properties of ZrO_2 film memory devices," *IEEE Electron Device Lett.*, vol. 28, no. 5, pp. 366-368, 2007.

[132] C. Y. Lin, C. Y. Wu, C. Y. Wu, T. Y. Tseng, and C. Hu, "Modified resistive switching behavior of ZrO_2 memory films based on the interface layer formed by using Ti top electrode," *J. Appl. Phys.*, vol. 102, p. 094101, 2007.

[133] C. Y. Lin, C. Y. Wu, C. Y. Wu, C. C. Lin, and T. Y. Tseng, "Memory effect of RF sputtered ZrO_2 thin films," *Thin Solid Films*, vol. 516, pp. 444-448, 2007.

[134] C. Y. Lin, C. Y. Wu, C. Y. Wu, C. Hu, and T. Y. Tseng, "Bistable resistive switching in Al_2O_3 memory thin films," *J. Electrochem. Soc.,* vol. 154, no. 9, pp. G189-G192, 2007.

[135] C. C. Lin, J. S. Yu, C. Y. Lin, C. H. Lin, and T. Y. Tseng, "Stable resistive switching behaviors of sputter deposited V-doped $SrZrO_3$ thin films," *Thin Solid Films*, vol. 516, pp. 402-406, 2007.

[136] M. H. Lin, M. C. Wu, C. H. Lin, and T. Y. Tseng, "Effects of Vanadium doping on resistive switching characteristics and mechanisms of $SrZrO_3$-based memory films," *IEEE Trans. Electron Devices*, vol. 57, no. 8, pp. 1801-1808, 2010.

[137] H. Zhang, B. Gao, B. Sun, G. Chen, L. Zeng, L. Liu, X. Liu, J. Lu, R. Han, J. Kang, and B. Yu, "Ionic doping effect in ZrO_2 resistive switching memory," *Appl. Phys. Lett.*, vol. 96, p. 123502, 2010.

[138] J. Choi, J. S. Kim, I. Hwang, S. Hong, I. S. Byun, S. W. Lee, S. O. Kang, and B. H. Park, "Different nonvolatile memory effects in epitaxial $Pt/PbZr_{0.3}Ti_{0.7}O_3/LSCO$," *Appl. Phys. Lett.*, vol. 96, p. 262113, 2010.

[139] H. Kim, C. Park, S. Lee, and D. W. Kim, "Inhomogeneous barrier and hysteretic transport properties of $Pt/SrTiO_3$ junctions," *J. Phys. D*, vol. 42, p. 055306, 2009.

[140] M. H. Lee, S. J. Song, K. M. Kim, G. H. Kim, J. Y. Seok, J. H. Yoon, and C. S. Hwang, "Scanning probe based observation of bipolar resistive switching NiO films," *Appl. Phys. Lett.*, vol. 97, p. 062909, 2010.

[141] D. S. Shang, J. R. Sun, L. Shi, and B. G. Shen, "Photoresponse of the Schottky junction $Au/SrTiO_3:Nb$ in different resistive states," *Appl. Phys. Lett.*, vol. 93, p. 102106, 2008.

[142] Z. L. Liao, Z. Z. Wang, Y. Meng, Z. Y. Liu, P. Gao, J. L. Gang, H. W. Zhao, X. J. Liang, X. D. Bai, and D. M. Chen, "Categorization of resistive switching of metal-$Pr_{0.7}Ca_{0.3}MnO_3$-metal devices," *Appl. Phys. Lett.*, vol. 94, p. 253503, 2009.

[143] S. L. Li, D. S. Shang, J. Li, J. L. Gang, and D. N. Zhong, "Resistive switching properties in oxygen-deficient $Pr_{0.7}Ca_{0.3}MnO_3$ junctions with active Al top electrodes," *J. Appl. Phys.*, vol. 105, p. 033710, 2009.

[144] S. L. Li, Z. L. Liao, J. Li, J. L. Gang, and D. N. Zheng, "Resistive switching properties and low resistance state relaxation in $Al/Pr_{0.7}Ca_{0.3}MnO_3/Pt$ junction," *J. Phys. D.*, vol. 42, p. 045411, 2009.

[145] K. Shono, H. Kawano, T. Yokota, and M. Gomi, "Origin of negative differential resistiance observed on bipolar resistance switching device with $Ti/Pr_{0.7}Ca_{0.3}MnO_3/Pt$ structure," *Appl. Phys. Exp.*, vol. 1, p. 055002, 2008.

[146] H. Kawano, K. Shono, T. Yokota, and M. Gomi, "Enhancement of switching capability on bipolar resistance switching device with $Ta/Pr_{0.7}Ca_{0.3}MnO_3/Pt$ structure," *Appl. Phys. Exp.*, vol. 1, p.101901, 2008.

[147] R. Yang, X. M. Li, W. D. Yu, X. D. Gao, D. S. Shang, X. J. Liu, X. Cao, Q. Wang, and L. D. Chen, "The polarity origin of the bipolar resistance switching behaviors in $metal/La_{0.7}Ca_{0.3}MnO_3/Pt$ junctions," *Appl. Phys. Lett.*, vol. 95, p. 072105, 2009.

[148] M. Hasan, R. Dong, H. Choi, J. Yoon, J. Park, D. Seong, and H. Hwang, "Dependence of the metal electrode and improved pulsed switching speed of $La_{0.7}Ca_{0.3}MnO_3$ as a resistance change memory device," *J. Electrochem. Soc.*, vol. 156, no. 4, pp. H239-H242, 2009.

[149] X. Liu, K. P. Biju, E. M. Bourim, S. Park, W. Lee, J. Shin, and H. Hwang, "Low programming voltage resistive switching in reactive metal/polycrystalline $Pr_{0.7}Ca_{0.3}MnO_3$ devices," *Solid-State Communications*, vol. 150, pp. 2231-2235, 2010.

[150] T. Harada, I. Ohkubo, K. Tsubouchi, H. Kumigashira, T. Ohnishi, M. Lippmaa, Y. Matsumoto, H. Koinuma, and M. Oshima, "Trap-controlled space-charge-limited current mechanism in resistance switching at $Al/Pr_{0.7}Ca_{0.3}MnO_3$ interface," *Appl. Phys. Lett.*, vol. 92, p. 222113, 2008.

[151] M. Jo. D. Seong, S. Kim, J. Lee, W. Lee, J. B. park, S. Park, S. Jung, J. Shin, D. Lee, and H. Hwang, "Novel cross-point resistive switching memory with self-formed Schottky barrier," in *Symp. on VLSI Tech. Dig.*, pp. 53-54, 2010.

[152] H. Y. Jeong, J. Y. Lee, S. Y. Choi, and J. W. Kim, "Microscopic origin of bipolar resistive switching of nanoscale titanium," *Appl. Phys. Lett.*, vol. 95, p. 162108, 2009.

[153] H. Y. Jeong, J. Y. Lee, M. K. Ryu, and S. Y. Choi, "Bipolar resistive switching in amorphous titanium oxide thin film," *Phys. Stat. Sol. RRL*, vol. 4, no. 1-2, pp. 28-30, 2010.

[154] D. J. Seong, M. Hassan, H. Choi, J. Lee, J. Yoon, J. B. Park, W. Lee, M. S. Oh,

and H. Hwang, "Resistive-switching characteristics of Al/Pr$_{0.7}$Ca$_{0.3}$MnO$_3$ for nonvolatile memory applications," *IEEE Electron Device Lett.*, vol. 30, no. 9, pp. 919-921, 2009.

[155] X. J. Liu, X. M. Li, Q. Wang, R. Yang, X. Cao, W. D. Yu, and L. D. Chen, "Interfacial resistive switching properties in Ti/La$_{0.7}$Ca$_{0.3}$MnO$_3$/Pt sandwich structures," *Phys. Stat. Sol. A*, vol. 207, no. 5, pp. 1204-1209, 2010.

[156] D. Y. Lee, S. Y. Wang, and T. Y. Tseng, "Ti-induced recovery phenomenon of resistive switching in ZrO$_2$ thin films," *J. Electrochem. Soc.,* vol. 157, no. 7, pp. G166-G167, 2010.

[157] S. Y. Wang, D. Y. Lee, T. Y. Huang, J. W. Wu, and T. Y. Tseng, "Controllable oxygen vacancies to enhance resistive switching performance in a ZrO$_2$-based RRAM with embedded Mo layer," *Nanotechnology*, vol. 21, p. 495201, 2010.

[158] Y. Wu, B. Lee, and H. S. Philip Wong, "Al$_2$O$_3$-based RRAM using atomic layer deposition (ALD) with 1-μA RESET current," *IEEE Electron Device Lett.*, vol. 31, no. 12, pp. 1449-1451, 2010.

[159] H. Lv, M. Wang, H. Wan, Y. Song, W. Luo, P. Zhou, T. Tang, Y. Lin, R. Huang, S. Song, J. G. Wu, H. M. Wu, and M. H. Chi, "Endurance enhancement of Cu-oxide based resistive switching memory with Al top electrode," *Appl. Phys. Lett.*, vol. 94, p. 213502, 2009.

[160] X. Sun, B. Sun, L. Liu, N. Xu, X. Liu, R. Han, J. Kang, G. Xiong, and T. P. Ma, "Resistive switching in CeO$_x$ films for nonvolatile memory application," *IEEE Electron Device Lett.*, vol. 30, no. 4, pp. 334-336, 2009.

[161] H. Y. Lee, Y. S. Chen, P. S. Chen, T. Y. Wu, F. Chen, C. C. Wang, P. J. Tzeng, M. J. Tsai, and C. Lien, "Low-power and nanosecond switching in robust Hafnium oxide resistive memory with a thin Ti cap," *IEEE Electron Device Lett.*, vol. 31, no. 1, pp. 44-46, 2010.

[162] Y. S. Chen, H. Y. Lee, P. S. Chen, T. Y. Wu, C. C. Wang, P. J. Tzeng, F. Chen, M. J. Tsai, and C. Lien, "An ultrathin forming-free HfO$_x$ resistance memory with excellent electrical performance," *IEEE Electron Device Lett.*, vol. 31, no. 12, pp. 1473-1475, 2010.

[163] P. S. Chen, H. Y. Lee, Y. S. Chen, P. Y. Gu, F. Chen, and M. J. Tsai, "Impact of engineered Ti layer on the memory performance of HfO$_x$-based resistive memory," *Electrochem. Solid-State Lett.*, vol. 13, no. 12, pp. H423-H425, 2010.

[164] L. Chen, Y. Xu, Q. Q. Sun, H. Liu, J. J. Gu, S. J. Ding, and D. W. Zhang, "Highly uniform bipolar resistive switching with Al$_2$O$_3$ buffer layer in robust NbAlO-based RRAM," *IEEE Electron Device Lett.*, vol. 31, no. 4, pp. 356-358, 2010.

[165] J. W. Park, M. K. Yang, and J. K. Lee, "Electrode dependence of bipolar

resistive switching in SrZrO$_3$:Cr perovskite film-based memory devices," *Electrochem. Solid-State Lett.*, vol. 11, no. 8, pp. H226-H229, 2008.

[166] Y. H. Do. J. S. Kwak, Y. C. Bae, K. Jung, H. Im, and J. P. Hong, "Hysteretic bipolar resistive switching characteristics in TiO$_2$/TiO$_{2-x}$ multilayer homojunctions," *Appl. Phys. Lett.*, vol. 95, p. 093507, 2009.

[167] J. Lee, E. M. Bourim, W. Lee, J. Park, M. Jo, S. Jung, J. Shin, and H. Hwang, "Effect of ZrO$_x$/HfO$_x$ bilayer structure on switching uniformity and reliability in nonvolatile memory applications," *Appl. Phys. Lett.*, vol. 97, p. 172105, 2010.

[168] X. J. Liu, X. M. Li, Q. Wang, W. D. Yu, R. Yang, X. Cao, X. D. Gao, and L. D. Chen, "Improved resistive switching properties in Ti/TiO$_x$/La$_{0.7}$Ca$_{0.3}$MnO$_3$/Pt stacked structures," *Solid-State Communications*, vol. 150, pp. 137-141, 2010.

[169] J. H. Hur, M. J. Lee, C. B. Lee, Y. B. Kim, and C. J. Kim, "Modeling for bipolar resistive memory switching in transition-metal oxides," *Phys. Rev. B*, vol. 82, p. 155321, 2010.

[170] M. H. Lin, M. C. Wu, C. Y. Huang, C. H. Lin, and T. Y. Tseng, "High-speed and localized resistive switching characteristics of double-layer SrZrO$_3$ memory devices," *J. Phys. D*, vol. 43, p. 295404, 2010.

[171] C. Y. Lin, M. H. Lin, M. C. Wu, C. H. Lin, T. Y. Tseng, "Improvement of resistive switching characteristics in SrZrO$_3$ thin films with embedded Cr layer," *IEEE Electron Device Lett.*, vol. 29, no. 10, pp. 1108-1111, 2008.

[172] S. Yu, B. Gao, H. Dai, B. Sun, L. Liu, X. Liu, R. Han, J. Kang, and B. Yu, "Improved uniformity of resistive switching behaviors in HfO$_2$ thin films with embedded Al Layers," *Electrochem. Solid-State Lett.*, vol. 13, no. 2, pp. H36-H38, 2010.

[173] Q. Zuo, S. Long, Q. Liu, S. Zhang, Q. Wang, Y. Li, Y. Wang, and M. Liu, "Self-rectifying effect in gold nanocrystal-embedded zirconium oxide resistive memory," *J. Appl. Phys.*, vol. 106, p. 073724, 2009.

[174] W. Y. Chang, K. J. Cheng, J. M. Tsai, H. J. Chen, F. Chen, M. J. Tsai, and T. B. Wu, "Improvement of resistive switching characteristics in TiO$_2$ thin films with embedded Pt nanocrystals," *Appl. Phys. Lett.*, vol. 95, p. 042104, 2009.

[175] M. H. Lin, M. C. Wu, C. H. Lin, and T. Y. Tseng, "Resistive switching characteristics and mechanism of Pt-embedded SrZrO$_3$ memory devices," *J. Appl. Phys.*, vol. 107, p. 124117, 2010.

[176] C. Y. Lin, D. Y. Lee, S. Y. Wang, C. C. Lin, T. Y. Tseng, "Effect of thermal treatment on resistive switching characteristics in Pt/Ti/Al$_2$O$_3$/Pt devices," *Surface & Coatings Tech.*, vol. 203, pp. 628-631, 2008.

[177] W. G. Kim, and S. W. Rhee, "Effect of post annealing on the resistive switching of TiO$_2$ thin film," *Microelectronic Engineering*, vol. 86, pp. 2153-2156, 2009.

[178] K. Yin, M. Li, Y. Liu, C. He, F. Zhuge, B. Chen, W. Lu, X. Pan, and R. W. Li, "Resistance switching in polycrystalline $BiFeO_3$ thin films," *Appl. Phys. Lett.*, vol. 97, p. 042101, 2010.

[179] B. Yang, H. X. Guo, K. B. Yin, Y. D. Xia, L. Chen, J. Yin, and Z. G. Liu, "The <001>-oriented growth of Cu_2S films and its switching properties," *J. Electroceram.*, vol. 22, pp. 87-90, 2009.

[180] X. J. Liu, X. M. Li, Q. Wang, R. Yang, X. Cao, W. D. Yu, and L. D. Chen, "Interfacial resistive switching properties in $Ti/La_{0.7}Ca_{0.3}MnO_3/Pt$ sandwich structures," *Phys. Status Solidi A*, vol. 207, no. 5, pp. 1204-1209, 2010.

[181] L. W. Feng, C. Y. Chang, Y. F. Chang, W. R. Chen, S. Y. Wang, P. W. Chiang, and T. C. Chang, "A study of resistive switching effects on a thin FeO_x transition layer produced at the oxide/iron interface of $TiN/SiO_2/Fe$-contented electrode structures," *Appl. Phys. Lett.*, vol. 96, p. 052111, 2010.

[182] K. P. Biju, X. Liu, E. M. Bourim, I. Kim, S. Jung, J. park, and H. Hwang, "Improved Resistive Switching Properties of Solution Processed TiO_2 Thin Films," *Electrochem. Solid-State Lett.*, vol. 13, no. 12, pp. H443-H446, 2010.

[183] J. Park, M. Jo, J. Lee, S. Jung, S. Kim, W. Lee, J. Shin, and H. Hwang, "Improved Switching Uniformity and Speed in Filament-Type RRAM Using Lightning Rod Effect," *IEEE Electron Device Lett.*, vol. 32, no. 1, pp. 63-65, 2011.

[184] B. Cho, S. Song, Y. Ji, and T. Lee, "Electrical characterization of organic resistive memory with interfacial oxide layers formed by O_2 plasma treatment," *Appl. Phys. Lett.*, vol. 97, p. 063305, 2010.

[185] G. H. Buh, I. Hwang, and B. H. Park, "Time-dependent electroforming in NiO resistive switching devices," *Appl. Phys. Lett.*, vol. 95, p. 142101, 2009.

[186] T. W. Hickmott, "Impurity conduction and negative resistance in thin oxide films," *J. Appl. Phys.*, vol. 35, pp. 2118-2122, 1964.

[187] G. Dearnaley, "Stored charge in oxide layer structures," *Int. J. Electron.*, vol. 29, pp. 299, 1970.

[188] P. D. Greene, E. L. Bush, and I. R. Rawlings, *Proc. Symp. Deposited Thin Film Dielectric Materials, Ed. F. Vratny, Electrochem. Soc.,* New York, pp. 167-185, 1968.

[189] K. Szot, W. Speier, G. Bihlmayer, and R. Waser, "Switching the electrical resistnace of individual dislocations in single-crystalline $SrTiO_3$," *Nature Mater.*, vol. 5, pp. 312, 2006.

[190] D. S. Jeong, H. Schroeder, U. Breuer, and R. Waser, "Characteristic electroforming behavior in $Pt/TiO_2/Pt$ resistive switching cells depending on atmosphere," *J. Appl. Phys.*, vol. 104, p. 123716, 2008.

[191] J. J. Yang, F. Miao, M. D. Pickett, D. A. A. Ohlberg, D. R. Stewart, C. N. Lau, and R. S. Williams, "The mechanism of electroforming of metal oxide memristive switches," *Nanotechnology*, vol. 20, p. 215201, 2009.

[192] D. S. Jeong, H. Schoroeder, and R. Waser, "Abnormal bipolar-like resistance change behavior induced by symmetric electroforming in Pt/TiO$_2$/Pt resistive switching cells," *Nanotechnology*, vol. 20, p. 375201, 2009.

[193] V. K. Yarmarkin, S. G. Shul'man, and V. V. Lemanov, "Resistive Switching in Au/TiO$_2$/Pt Thin Film Structures on Silicon,"

[194] T. Menke, R. Dittmann, P. Meuffels, K. Szot, and R. Waser, "Impact of the electroforming process on the device stability of epitaxial Fe-doped SrTiO$_3$ resistive switching cells," *J. Appl. Phys.,* vol. 106, p. 114507, 2009.

[195] X. B. Yan, Y. D. Xia, H. N. Xu, X. Gao, H. T. Li, R. Li, J. Yin, and Z. G. Liu, "Effects of the electroforming polarity on bipolar resistive switching characteristics of SrTiO$_{3-\delta}$ films," *Appl. Phys. Lett.*, vol. 97, p. 112101, 2010.

[196] C. Nauenheim, C. Kuegeler, A. Ruediger, and R. Waser, "Investigation of the electroforming process in resistively switching TiO$_2$ nanocrosspoint junctions," *Appl. Phys. Lett.*, vol. 96, p. 122902, 2010.

[197] A. Shih, W. Zhou, J. Qiu, H. J. Yang, S. Chen, Z. Mi, and I. Shih, "Highly stable resistive switching on monocrystalline ZnO," *Nanotechnology*, vol. 21, p. 125201, 2010

[198] J. P. Strachan, J. J. Yang, R. Munstermann, A. Scholl, G. Medeiros-Ribeiro, D. R. Stewart, and R. S. Williams, "Structural and chemical characterization of TiO$_2$ memristive devices by spatially-resolved NEXAFS," *Nanotechnology*, vol. 20, p. 485701, 2009.

[199] X. Gao, Y. Xia, B. Xu, J. Kong, H. Guo, K. Li, H. Li, H. Xu, K. Chen, J. Yin, and Z. Liu, "Unipolar resistive switching behaviors in amorphous lutetium oxide films," *J. Appl. Phys.*, vol. 108, p. 074506, 2010.

[200] L. M. Chen, T. Y. Lin, C. C. Chang, S. C. Chang, and T. S. Chin, "Electrode effect on resistive switching of Ti-added amorphous SiO$_x$ films," *Thin Solid Films*, vol. 518, pp. 7352-7355, 2010.

[201] K. Li, Y. Xia, B. Xu, X. Gao, H. Guo, Z. Liu, and J. Yin, "Conduction behavior change in amorphous LaLuO$_3$ dielectrics based on correlated barrier hopping theory," *Appl. Phys. Lett.*, vol. 96, p. 182904, 2010.

[202] M. Pyun, H. Choi, J. B. Park, D. Lee, M. Hasan, R. Dong, S. J. Jung, J. Lee, D. Seong, J. Yoon, and H. Hwang, "Electrical and reliability characteristics of copper-doped carbon (CuC) based resistive switching devices for nonvolatile memory applications," *Appl. Phys. Lett.*, vol. 93, p. 212907, 2008.

[203] T. Busani, and R. A. B. Devine, "Nonvolatile memory and antifuse behavior in

Pt/a-TiO$_2$/Ag structures," *J. Vac. Sci. Technol. B*, vol. 26, no. 5, pp. 1817-1820, 2008

[204] L. Chen, H. X. Guo, Y. D. Xia, J. Yin, and Z. G. Liu, "Resistive switching in the devices of Ag/amorphous Ag$_{30}$Ge$_{17}$Se$_{53}$ films/Pt," *Appl. Phys. A*, vol. 100, pp. 309-313, 2010.

[205] J. W. Seo, S. J. Baik, S. J. Kang, Y. H. Hong, J. H. Yang, L. Fang, and K. S. Lim, "Evidence of Al induced conducting filament formation in Al/amorphous silicon/Al resistive switching memory device," *Appl. Phys. Lett.*, vol. 96, p. 053504, 2010.

[206] X. Gao, Y. Xia, J. Ji, H. Xu, Y. Su, H. Li, C. Yang, H. Guo, J. Yin, and Z. Liu, "Effect of top electrode materials on bipolar resistive switching behavior of gallium oxide films," *Appl. Phys. Lett.*, vol. 97, p. 193501, 2010.

[207] H. Y. Jeong, J. Y. Lee, and S. Y. Choi, "Direct observation of microscopic change induced by oxygen vacancy drift in amorphous TiO$_2$ thin films," *Appl. Phys. Lett.*, vol. 97, p. 042109, 2010.

[208] S. Jung, J. Kong, S. Song, K. Lee, T. Lee, H. Hwang, and S. Jeon, "Resistive switching characteristics of solution-processed transparent TiO$_x$ for nonvolatile memory application," *J. Electrochem. Soc.*, vol. 157, no. 11, pp. H1042-1045, 2010.

[209] K. Oyoshi, S. Nigo, J. Inoue, O. Sakai, H. Kitazawa, and G. Kido, "Formation and disruption of current paths of anodic porous alumina films by conducting atomic force microscopy," *Appl. Surf. Sci.*, vol. 257, pp. 837-841, 2010.

[210] J. Lee, S. Nigo, Y. Nakano, S. Kato, H. Kitazawa, and G. Kido, "Structural analysis of anodic porous alumina used for resistive random access memory," *Sci. Technol. Adv. Mater.*, vol. 11, p. 025002, 2010.

[211] H. H. Huang, W. C. Shih, and C. H. Lai, "Nonpolar resistive switching in the Pt/MgO/Pt nonvolatile memory device," *Appl. Phys. Lett.*, vol. 96, p. 193505, 2010.

[212] S. Lee, H. Kim, D. J. Yun, S. W. Rhee, and K. Yong, "Resistive switching characteristics of ZnO thin film grown on stainless steel for flexible nonvolatile memory devices," *Appl. Phys. Lett.*, vol. 95, p. 262113, 2009.

[213] C. Y. Liu, and J. M. Hsu, "Dispersion improvement of unipolar resistive switching Ni/Cu$_x$O/Cu device by bipolar operation method," *Microelectronic Engineering*, article in press, 2010.

[214] C. Schindler, S. C. P. Thermadam, R. Waser, and M. N. Kozicki, "Bipoalr and unipolar resistive switching in Cu-doped SiO$_2$," *IEEE Trans. Electron Devices*, vol. 54, no.10, pp. 2762-2768, 2007.

[215] D. S. Jeong, H. chroeder, and R. Waser, "Coexistence of bipolar and unipolar

resistive switching behaviors in a Pt/TiO$_2$/Pt stack," *Electrochem. Solid-State Lett.*, vol. 10, no. 8, pp. G51-G53, 2007.

[216] S. Lee, H. Kim, J. Park, and K. Yong, "Coexistence of unipolar and bipolar resistive switching characteristics in ZnO thin films," *J. Appl. Phys.*, vol. 108, p. 076101, 2010.

[217] C. C. Lin, C. Y. Lin, M. H. Lin, C. H. Lin, and T. Y. Tseng, "Voltage-polarity-independent and high-speed resistive switching properties of V-doped SrZrO$_3$ thin films," *IEEE Trans. Electron Devices*, vol. 54, no.12, pp. 3146-3151, 2007.

[218] S. Y. Wang, D. Y. Lee, and T. Y. Tseng, "Effects of Ti top electrode thickness on the resistive switching behaviors of rf-sputtered ZrO$_2$ memory films," *Appl. Phys. Lett.*, vol. 95, p. 112904, 2009.

[219] W. G. Kim, and S. W. Rhee, "Effect of top electrode material on the resistive switching of TiO$_2$ thin film," *Microelectronic Engineering*, vol. 87, pp. 98-103, 2010.

[220] Y. H. Do, J. S. Kwak, Y. C. Bae, K. Jung, H. Im, and J. P. Hong, "Oxygen ion drifted bipolar resistive switching behaviors in TiO$_2$-Al electrode interfaces," *Thin Solid Films*, vol. 518, pp. 4408-4411, 2010.

[221] L. Zhang, R. Huang, M. Zhu, S. Qin, Y. Kuang, D. Gao, C. Shi, and Y. Wang, "Unipolar TaOx-based resistive change memory realized with electrode engineering," *IEEE Electron Device Lett.*, article in press, 2010.

[222] M. Meier, S. Gilles, R. Rosezin, C. Schindler, S. Trellenkamp, A. Rudiger, D. Mayer, C. Kugeler, and R. Waser, "Resistive switching Pt/spin-on glass/Ag nanocells for non-volatile memories fabricated with UV nanoimprint lithography," *Microelectronic Engineering*, vol. 86, pp. 1060-1062, 2009.

[223] R. Rosezin, M. Meier, S. Trellenkamp, C. Kugeler, and R. Waser, "Observation of unipolar resisting in silver doped methyl-silsesquioxane," *Microelectronic Engineering*, vol. 87, pp. 1531-1533, 2010.

[224] M. Meier, C. Schindler, S. Gilles, R. Rosezin, A. Rudiger, C. Kugeler, and R. Waser, "A nonvolatile memory with resistively switching Methyl-Silsesquioxane," *IEEE Electron Device Lett.*, vol. 30, no. 1, pp. 8-10, 2009.

[225] C. Kugeler, M. Meier, R. Rosezin, S. Gilles, and R. Waser, "High density 3D memory architecture based on the resistive switching effect," *Solid-State Electronics*, vol. 53, pp. 1287-1292, 2010.

[226] S. Song, B. Cho, T. W. Kim, Y. Ji, M. Jo, G. Wang, M. Choe, Y. H. Kahng, H. Hwang, and T. Lee, "Three-dimensional integration of organic resistive memory devices," *Adv. Mater.*, vol. 22, pp. 5048-5052, 2010.

[227] M. J. Lee, Y. Park, D. S. Suh, E. H. Lee, S. Seo, D. C. Kim, R. Jung, B. S. Kang, S. E. Ahn, C. B. Lee, D. H. Seo, Y. K. Cha, I. K. Yoo, J. S. Kim, and B. H. Park, "Two series oxide resistors applicable to high speed and high density nonvolatile memory," *Adv. Mater.*, vol. 19, pp. 3919-3923, 2007.

[228] Y. C. Shin, J. Song, K. M. Kim, B. J. Choi, S. Choi, H. J. Lee, G. H. Kim, T. Eom, and C. S. Hwang, "(In,Sn)$_2$O$_3$/TiO$_2$/Pt Schottky-type diode switch for the TiO$_2$ resistive switching memory array," *Appl. Phys. Lett.*, vol. 92, p. 162904, 2008.

[229] W. Y. Park, G. H. Kim, J. Y. Seok, K. M. Kim, S. J. Song, M. H. Lee, and C. S. Hwang, "A Pt/TiO$_2$/Ti Schottky-type selection diode for alleviating the sneak current in resistance switching memory arrays," *Nanotechnology*, vol. 21, p. 195201, 2010.

[230] M. J. Lee, S. I. Kim, C. B. Lee, H. Yin, S. E. Ahn, B. Kang, K. H. Kim, J. C. Park, C. J. Kim, I. Song, S. W. Kim, G. Stefanovich, J. H. Lee, S. J. Chung, Y. H. Kim, and Y. Park, "Low-temperature-grown transition metal oxide based storage materials and oxide transistors for high-density non-volatile memory," *Adv. Func. Mater.*, vol. 19, pp. 1587-1593, 2009.
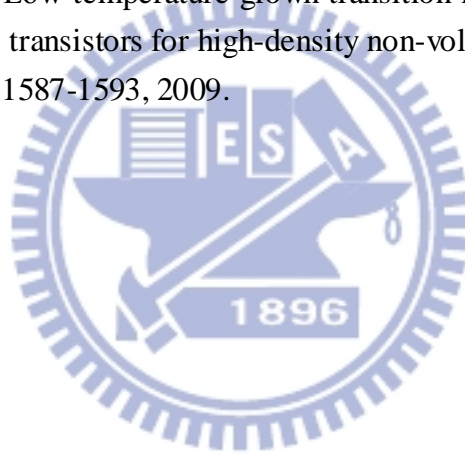
Chapter 3 - References:

[1]   I. G. Baek, M. S. Lee, S. Seo, M. J. Lee, D. H. Seo, D. S. Suh, J. C. Park, S. O. Park, H. S. Kim, I. K. Yoo, U. In. Chung, J. T. Moon, "Highly scalable non-volatile resistive memory using simple binary oxide driven by asymmetric unipolar voltage pulses," in *IEDM Tech. Dig*., 2004, pp. 587-590.

[2]   T. Fujii, M. Kawasaki, A. Sawa, H. Akoh, Y. Kawazoe, Y. Tokura, "Interface resistance switching at a few nanometer thick perovskite manganite active layers," *Appl. Phys. Lett.*, vol. 86, p. 012107, 2005.

[3]   S. Muraoka, K. Osano, Y. Kanzawa, S. Mitani, S. Fujii, K. Katayama, Y. Katoh, Z. Wei, T. Kikawa, K. Arita, Y. Kawashima, R. Zaua, K. Kawai, K. Shimakawa, A. Odagawa, and T. Takagi, "Fast switching and long retention Fe-O ReRAM and its switching mechanism," in *IEDM Tech. Dig*., 2007, pp. 779-782.

[4]   K. Aratani, K. Ohba, T. Mizuguchi, S. Yasuda, T. Shiimoto, T. Tsushima, T. Sone, K. Endo, A. Kouchiyama, S. Sasaki, A. Maesaka, N. Yamada, and H. Narisawa, "A novel resistance memory with high scalability and nanosecond switching, " in *IEDM Tech. Dig*., 2007, pp. 783-786.

[5]   H. Y. Lee, P. S. Chen, T. Y. Wu, Y. S. Chen, C. C. Wang, P. J. Tzeng, C. H. Lin, F. Chen, C. H. Lien, H. J. Tsai, "Low power and high speed bipolar switching with a thin reactive Ti buffer layer in robust HfO$_2$ based RRAM," in *IEDM Tech. Dig*., 2008, pp. 297-300.

[6]   K. Kinoshita, T. Tamura, M. Aoki, Y. Sugiyama, and H. Tanaka, "Bias polarity dependent data retention of resistive random access memory consisting of binary transition metal oxide," *Appl. Phys. Lett.*, vol. 89, p. 103509, 2006.

[7]   K. M. Kim, B. J. Choi, and C. S. Hwang, "Localized switching mechanism in resistive switching of atomic-layer-deposited TiO$_2$ thin films," *Appl. Phys. Lett.*, vol. 90, p. 242906, 2007.

[8]   K. M. Kim, B. J. Choi, Y. C. Shin, S. Choi, and C. S. Hwang, "Anode-interface localized filamentary mechanism in resistive switching of TiO thin films," *Appl. Phys. Lett.*, vol. 91, p. 012907, 2007.

[9]   D. C. Kim, S. Seo, S. E. Ahn, D. -S. Ahn, M. J. Lee, B. -H. Park, I. K. Yoo, I. G. Baek, H. -J. Kim, E. K. Yim, J. E. Lee, S. O. Park, H. S. Kim, U-In. Chung, J. T. Moon, and B. I. Ryu, "Electrical observations of filamentary conductions for the resistive memory switching in NiO films," *Appl. Phys. Lett.*, vol. 88, p. 202102, 2006.

[10] H. Y. Lee, P. S. Chen, T. Y. Wu, C. C. Wang, P. J. Tzeng, C. H. Lin, F. Chen, M. J. Tsai, and C. H. Lien, "Electrical evidence of unstable anodic interface in Ru/HfO/TiN unipolar resistive memory," *Appl. Phys. Lett.*, vol. 92, p. 142911,

2008.

[11] S. Seo, M. J. Lee, D. C. Kim, S. E. Ahn, B. H. Park, Y. S. Kim, I. K. Yoo, I. S. Byun, I. R. Hwang, S. H. Kim, J. S. Kim, J. S. Choi, J. H. Lee, S. H. Jeon, S. H. Hong, and B. H. Park, "Electrode dependence of resistance switching in polycrystalline NiO films," *Appl. Phys. Lett.*, vol. 87, p. 263507, 2005.

[12] W. G. Kim, and S. W. Rhee, "Effect of top electrode material on the resistive switching of TiO_2 thin film," *Microelectronic Engineering*, vol. 87, pp. 98-103, 2010.

[13] W. Y. Yang, and S. W. Rhee, "Effect of electrode material on the resistance switching of CuO film," *Appl. Phys. Lett.*, vol. 91, p. 23907, 2007.

[14] C. J. Kim, I. -W. Chen, "Effect of top electrode on resistance switching of (Pr, Ca)MnO_3 thin films," *Thin Solid Films*, vol. 515, pp. 2726-2729, 2006.

[15] C. B. Lee, B. S. Kang, A. Benayad, M. J. Lee, S. -E. Ahn, K. H. Kim, G. Stefanovich, Y. Park, and I. K. Yoo, "Effects of metal electrodes on the resistive memory switching property of NiO thin films," *Appl. Phys. Lett.*, vol. 93, p. 042115, 2008.

[16] H. -G. Lee, *Thermodynamics for Metals and Materials* (Imperial College, London, 1999), pp. 127-130.

[17] H. Y. Lee, P. S. Chen, C. C. Wang, S. Maikap, P. J. Tzeng, C. H. Lin, L. S. Lee, and M. J. Tsai, "Low power switching of nonvolatile resistive memory using hafnium oxide," *J. Jpn. Appl. Phys.*, vol. 46, pp. 2175-2179, 2007.

[18] Z. F. Hou, X. G. Gong, Q. Li, "Energetics and electronic structure of aluminum point defects in HfO_2: A first-principles study," *J. Appl. Phys.*, vol. 106, p. 014104, 2009.

[19] H. G. Lee, "*Chemical Thermodynamics for metals and materials*", Pohang University of Science & Technology Korea.

[20] D. J. Seong, M. Hassan, H. Choi, J. Lee, J. Yoon, J. B. Park, W. Lee, and H. Hwang, "Resistive-switching characteristics of Al/$Pr_{0.7}Ca_{0.3}MnO_3$ for nonvolatile memory applications," *IEEE Electron Device Lett.*, vol. 30, no. 9, pp. 919-921, 2009.

[21] H. Y. Yu, N. Wu, M. F. Li, C. Zhu, B. J. Cho, D. L. Kwong, and C. H. Tung, "Thermal stability of $(HfO_2)_x(Al_2O_3)_{1-x}$ on Si," *Appl. Phys. Lett.*, vol. 81, p. 3618, 2002.

[22] W. J. Zhu, T. Tamagawa, M. Gibson, T. Furukawa, and T. P. Ma, "Effect of Al inclusion in HfO_2 on the physical and electrical properties of the dielectrics," *IEEE Electron Device Lett.*, vol. 23, no. 11, pp. 649-651, 2002.

[23] M. Y. Ho, H. Gong, G. D. Wilk, B. W. Busch, M. L. Green, W. H. Lin, A. See, S. K. Lahiri, M. E. Loomans, P. I. Raisanen, and T. Gustafsson, "Suppressed

crystallization of Hf-based gate dielectrics by controlled addition of Al_2O_3 using atomic layer deposition," *Appl. Phys. Lett.*, vol. 81, p. 4218-4220, 2002.

[24] J. H. Hsu, H. W. Lai, H. N. Lin, C. C. Chuang, and J. H. Huang, "Fabrication of nickel oxide nanostructures by atomic force microscope nano-oxidation and wet etching," *J. Vac. Sci. Technol. B*, vol. 21, no. 6, pp. 2599-2601, 2003.

[25] K. C. Liu, W. H. Tzeng, K. M. Chang, Y. C. Chan, and C. C. Kuo, "Effect of ultraviolet light exposure on a HfO_x RRAM device," *Thin Solid Film*, vol. 518, pp. 7460-7463, 2010.

[26] K. M. Chang, W. H. Tzeng, K. C. Liu, Y. C. Chen, and C. C. Kuo, "Investigation on the abnormal resistive switching induced by ultraviolet light exposure based on HfO_x film," *Mic. Reliab.*, vol. 50, pp. 670-673, 2010.

[27] B. J. Choi, D. S. Jeong, S. K. Kim, S. Choi, J. H. Oh, C Rohde, H. J. Kim, C. S. Hwang, K. Szot, R. Waser, B. Reichenberg, S. Tiedke, "Resistive switching mechanism of TiO_2 thin films grown by atomic-layer deposition," *J. Appl. Phys.*, vol. 98, p. 033715, 2005.

[28] C. Rohde, B. J. Choi, D. S. Jeong, S. Choi, J. S. Zhao, and C. S. Hwang, "Identification of a determining parameter for resistive switching of TiO_2 thin films," *Appl. Phys. Lett.*, vol. 86, p. 262907, 2005.

[29] S. Seo, M. J. Lee, D. H. Seo, S. K. Choi, D. S. Suh, Y. S. Joung, I. K. Yoo, I. S. Byun, I. R. Hwang, S. H. Kim, and B. H. Park, "Conductivity switching characteristics and reset currents in NiO films," *Appl. Phys. Lett.*, vol. 86, p. 093509, 2005.

[30] S. C. Chae, J. S. Lee, S. Kim, S. B. Lee, S. H. Chang, C. Liu, B. Kahng, H. Shin, D. -W. Kim, C. U. Jung, S. Seo, M. -J. Lee, and T.W. Noh, "Random Circuit Breaker Network Model for Unipolar Resistance Switching," *Adv. Mater.*, vol. 20, pp. 1154-1159, 2008.

[31] K. M. Kim, B. J. Choi, B. W. Koo, S. Choi, D. S. Jeong, C. S. Hwang, "Resistive switching in $Pt/Al_2O_3/TiO_2/Ru$ stacked structures," *Electrochem. Solid-State Lett.*, vol. 9, pp. G343-G346, 2006.

[32] D. S. Jeong, H. Schroeder, U. Breuer, R. Waser, "Characteristic electroforming behavior in $Pt/TiO_2/Pt$ resistive switching cells depending on atmosphere," *J. Appl. Phys.*, vol. 104, p. 123716, 2008.

[33] H. Schroeder and D. S. Jeong, "Resistive switching in a $Pt/TiO_2/Pt$ thin film stack – a candidate for a non-volatile ReRAM," *Microelectronic Engineering*, vol. 84, pp. 1982-1985, 2007.

[34] L. Goux, J. G. Lisoni, M. Jurczak, D. J. Wouters, L. Courtade, Ch. Muller, "Coexistence of the bipolar and unipolar resistive-switching modes in NiO cells made by thermal oxidation of Ni layers," *J. Appl. Phys.*, vol. 107, p. 024512,

2010.

[35] A. Lamperti, S. Spiga, H.L. Lu, C. Wiemer, M. Perego, E. Cianci, M. Alia, M. Fanciulli, "Study of the interfaces in resistive switching NiO thin films deposited by both ALD and e-beam coupled with different electrodes (Si, Ni, Pt, W, TiN)," *Microelectronic Engineering*, vol. 85, p. 2425-2429, 2008.

[36] S. Seo, M. J. Lee, D. H. Seo, E. J. Jeoung, D. -S. Suh, Y. S. Joung, I. K. Yoo, I. R. Hwang, I. S. Byun, J. -S. Choi, and B. H. Park, "Reproducible resistance switching in polycrystalline NiO films," *Appl. Phys. Lett.*, vol. 85, p. 5655, 2004.

[37] W. G. Kim, and S. W. Rhee, "Effect of post annealing on the resistive switching of TiO_2 thin film," *Microelectronic Engineering*, vol. 86, pp. 2153-2156, 2009.

[38] C. Gabriel, and J. McVittie, "How plasma etching damages thin gate oxides," *Solid-State Technol.*, vol. 35, pp. 81-92, 1992.

[39] S. Fang, and J. McVittie, "A model and experiments for thin oxide damage from wafer charging in magnetron plasmas," *IEEE Electron Device Lett.*, vol. 13, no. 6, pp. 347-349, 1992.

[40] Ch. Walczyk, Ch. Wenger, R. Sohal, M. Lukosius, A. Fox, J. Dabrowski, D. Wolansky, B. Tillack, H. -J. Mussig, and T. Schroeder, "Pulse-induced low-power resistive switching in HfO_2 metal-insulator-metal diodes for nonvolatile memory applications," *J. Appl. Phys.*, vol. 105, p. 114103, 2009.

[41] M. A. Paesler, D. A. Anderson, E. C. Freeman, G. Moddel, and W. Paul, "New development in the study of amorphous Silicon hydrogen alloys: The story of O," *Phys. Rev. Lett.*, vol. 41, pp. 1492-1495, 1978.

[42] M. M. Al-Kaisi, and M. J. Thompson, "The temperature dependence of the characteristics of sputtered a-Si—H solar cells," *Solar Cells*, vol. 1, pp. 91-98, 1979.

[43] J. C. Bruyere, A. Deneuville, A. Mini, J. Fontenille, and R. Danielou, "Influence of hydrogen on optical properties of a-Si:H," *J. Appl. Phys.*, vol. 51, pp. 2199-2205, 1980.

[44] X. W. Zhou, and H. N. G. Wadley, "Hyperthermal vapor deposition of copper athermal and biased diffusion effects," *Surface Science*, vol. 431, pp. 42-57, 1999.

[45] P. K. Song, Y. Shigesato, M. Kamei, and I. Yasui, "Electrical and structural properties of Tin-doped Indium oxide films deposited by DC sputtering at room temperature," *Jpn. J. Appl. Phys.*, vol. 38, pp. 2921-2927, 1999.

[46] B. Chapman, *Glow Discharge Processes*. New York: Wiley-Inter-science, 1980.

[47] X. W. Zhou, and H. N. G. Wadley, "Hyperthermal vapor deposition of copper reflection and resputtering effects," *Surface Science*, vol. 431, pp. 58-73, 1999.

[48] D. W. Moon, Y. Ha, H. K. Kim, K. J. Kim, H. S. Kim, J. Y. Lee, and S. Kim,

"Low sputter damage of metal single crystalline surfaces investigated with medium energy ion scattering spectroscopy," *Appl. Surf. Sci.*, vol. 150, pp. 235-243, 1999.

[49] C. B. Lee, B. S. Kang, M. J. Lee, S. E. Ahn, G. Stefanovich, W. X. Xianyu, K. H. Kim, J. H. Hur, H. X. Yin, Y. Park, I. K. Yoo, J. -B. Park, and B. H. Park, "Electromigration effect of Ni electrodes on the resistive switching characteristics of NiO thin films," *Appl. Phys. Lett.*, vol. 91, p. 082104, 2007.

[50] C. Y. Lin, C. Y. Wu, T. C. Lee, F. L. Yang, C. Hu, and T. Y. Tseng, "Effect of top electrode material on resistive switching properties of ZrO_2 film memory devices," *IEEE Electron Dev. Lett.*, vol. 28, no. 5, pp. 366-368, 2007.

[51] B. Sun, Y. X. Liu, L. F. Liu, N. Xu, Y. Wang, X. Y. Liu, R. Q. Han, and J. F. Kang, "Highly uniform resistive switching characteristics of $TiN/ZrO_2/Pt$ memory devices," *J. Appl. Phys.*, vol. 105, p. 061630, 2009.

[52] C. Y. Lin, D. Y. Lee, S. Y. Wang, C. C. Lin, T. Y. Tseng, "Effect of thermal treatment on resistive switching characteristics in $Pt/Ti/Al_2O_3/Pt$ devices," *Surface & Coatings Tech.*, vol. 203, pp. 628-631, 2008.

[53] J. W. Seo, J. -W. Park, K. S. Lim, J. H. Yang, and S. J. Kang, "Transparent resistive random access memory and its characteristics for nonvolatile resistive switching," *Appl. Phys. Lett.*, vol. 93, p. 223505, 2008.

[54] C. W. Tang, and S. A. VanSlyke, "Organic electroluminescent diodes," *Appl. Phys. Lett.*, vol. 51, pp. 913-915, 1987.

[55] C. W. Tang, "Two-layer organic photovoltaic cell," *Appl. Phys. Lett.*, vol. 48, pp. 183-185, 1986.

[56] J. Olivier, B. Servet, M. Vergnolle, M. Mosca, and G. Garry, "Stability/instability of conductivity and work function changes of ITO thin films, UV-irradiated in air or vacuum: Measurements by the four-probe method and by Kelvin force microscopy," *Synthetic Metals*, vol. 122, p. 87-89, 2007.

[57] C. Xirouchaki, G. Kiriakidis, T. F. Pedersen, and H. Fritzsche, "Photoreduction and oxidation of as-deposited microcrystalline indium oxide," *J. Appl. Phys.*, vol. 79, pp. 9349-9352, 1996.

[58] F. Rainer, W. H. Lowdermilk, D. Milam, C. K. Carniglia, T. T. Hart, and T. L. Lichtenstein, "Materials for optical coatings in the ultraviolet," *Appl. Opt.*, vol. 24, pp. 496-500, 1985.

[59] P. Gu, X. Liu, and J. Tang, "Damage thresholds of $(ZrO_2-Y_2O_3)/SiO_2$ reflectors used for XeCl lasers," *Appl. Opt.*, vol. 32, pp. 1528-1530, 1993.

[60] E. Hacker, H. Lauth, and P. Weibbrodt, in: H. E. Bennet, A. H. Guenther, M. R. Kozlowski, B. E. Newnam, M. J. Soileau (Eds.), "*Laser-Induced Damage in Optical Materials*" 1995, Proc. SPIE, vol. 2714, pp. 316, 1996.

[61] S. Petzoldt, A. P. Elg, M. Reichling, J. Reif, and E. Matthias, "Surface laser damage thresholds determined by photoacoustic deflection," *Appl. Phys. Lett.*, vol. 53, pp. 2005-2007, 1988.

[62] M. Reichling, J. Siegel, E. Matthias, H. Lauth, and E. Hacker, "Photoacoustic studies of laser damage in oxide thin films," *Thin Solid Film*s, vol. 253, pp. 333-338, 1994.

[63] E. Welsch, K. Ettrich, H. Blaschke, P. Thomsen-Schmidt, D. Schafer, and N. Kaiser, "Investigation of the absorption induced damage in ultraviolet dielectric thin films," *Opt. Eng.*, vol. 36, pp. 504-512, 1997.

[64] K. G. Druiif, J. M. M. de Nijs, E. Van der Drift, E. H. A. Granneman, and P. Balk, "Recovery of vacuum ultraviolet irradiated metal-oxide-silicon systems," *J. Appl. Phys.*, vol. 78, p. 306-316, 1995.

[65] G. Legeay, X. Castel, R. Benzerga, and J. Pinel, "Excimer laser beam/ITO interaction: from laser processing to surface reaction," *Phys. Stat. Sol. (c)*, vol. 5, p. 3248-3254, 2008.

[66] L. F. Liu, J. F. Kang, N. Xu, X. Sun, C. Chen, B. Sun, Y. Wang, X. Y. Liu, X. Zhang, and R. Q. Han, "Gd doping improved resistive switching characteristics of TiO_2-based resistive memory deivces," *J. Jpn. Appl. Phys.,* vol. 47, no. 4, pp. 2701-2703, 2008.

[67] J. H. Choi, S. N. Das, and J. M. Myoung, "Controllable resistance switching behavior of NiO/SiO_2 double layers for nonvolatile memory application," *Appl. Phys. Lett.*, vol. 95, p. 062105, 2009.

[68] R. Jung, M. J. Lee, S. Seo, D. C. Kim, G. S. Park, K. Kim, S. Ahn, Y. Park, I. K. Yoo, J. S. Kim, and B. H. Park, "Decrease in switching voltage fluctuation of $Pt/NiO_x/Pt$ structure by process control," *Appl. Phys. Lett.*, vol. 91, p. 022112, 2007.

[69] D. C. Kim, M. J. Lee, S. E. Ahn, S. Seo, J. C. Park, I. K. Yoo, I. G. Baek, H. J. Kim, E. K. Yim, J. E. Lee, S. O. Park, H. S. Kim, U-ln Chung, J. T. Moon, and B. I. Ryu, "Improvement of resistive memory switching in NiO using IrO_2," *Appl. Phys. Lett.*, vol. 88, p. 232106, 2006.

[70] C. Liu, S. C. Chae, J. S. Lee, S. H. Chang, S. B. Lee, D. W. Kim, C. U. Jung, S. Seo, S. E. Ahn, B. Kahng, and T. W. Noh, "Abnormal resistance switching behaviours of NiO thin films: possible occurrence of both formation and rupturing of conducting channels," *J. Phys. D*, vol. 42, p. 015506, 2009.

[71] M. Fujimoto, H. Koyama, M. Konagai, Y. Hosoi, K. Ishihara, S. Ohnishi, and N. Awaya, "TiO_2 anatase nanolayer on TiN thin film exhibiting high-speed bipolar resistive switching," *Appl. Phys. Lett.*, vol. 89, p. 223509, 2006.

[72] N. Xu, L. F. Liu, X. Sun, C. Chen, Y. Wang, D. D. Han, X. Y. Liu, R. Q. Liu, J. F.

Kang, and B. Yu, "Bipolar switching behavior in TiN/ZnO/Pt resistive nonvolatile memory with fast switching and long retention," *Semicond. Sci. Technol.*, vol. 23, p. 075019, 2008.

[73] C. Yoshida, K. Tsunoda, H. Noshiro, and Y. Sugiyama, "High speed resistive switching in Pt/TiO$_2$/TiN film for nonvolatile memory application," *Appl. Phys. Lett.*, vol. 91, p. 223510, 2007.

[74] Z. L. Liao, Z. Z. Wang, Y. Meng, Z. Y. Liu, P. Gao, J. L. Gang, H. W. Zhao, X. J. Liang, X. D. Bai, and D. M. Chen, "Categorization of resistive switching of metal-Pr$_{0.7}$Ca$_{0.3}$MnO$_3$-metal devices," *Appl. Phys. Lett.*, vol. 94, p. 253503, 2009.

[75] M. Hasan, R. Dong, H. J. Choi, D. S. Lee, D. J. Seong, M. B. Pyun, and H. Hwang, "Uniform resistive switching with a thin reactive metal interface layer in metal-La$_{0.7}$Ca$_{0.3}$MnO$_3$-metal heterostructures," *Appl. Phys. Lett.*, vol. 92, p. 202102, 2008.

[76] C. Y. Lin, C. Y. Wu, C. Y. Wu, and T. Y. Tseng, "Modified resistive switching behavior of ZrO$_2$ memory films based on the interface layer formed by using Ti top electrode," *J. Appl. Phys.*, vol. 102, p. 094101, 2007.
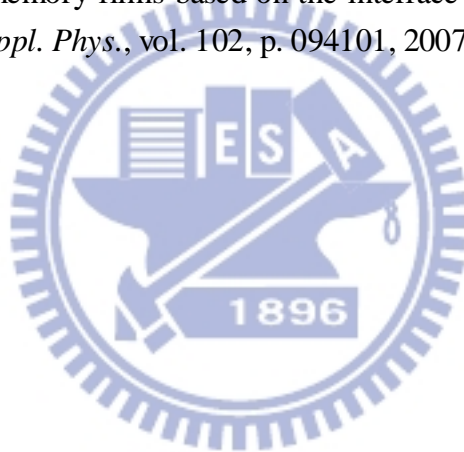
Chapter 4 - References:

[1] S. Q. Liu, N. J. Wu, A. Ignatiev, "Electric-pulse-induced reversible resistance change effect in magnetoresistive films," *Appl. Phys. Lett.*, vol. 76, pp. 2749-2751, 2005.

[2] D. Lee, H. Choi, H. Sim, D. Choi, H. Hwang, M. J. Lee, S. A. Seo, and I. K. Yoo, "Resistance switching of the nonstoichiometric Zirconium oxide for nonvolatile memory applications," *IEEE Electron Device Lett.*, vol. 26, no. 9, pp. 719-721, 2005.

[3] J. W. Park, M. K. Yang, K. Jung, and J. K. Lee, "Effects of switching parameters on resistive switching behaviors of polycrystalline $SrZrO_3$:Cr-based metal-oxide-metal structure," *IEEE Trans. Electron Devices*, vol. 55, no. 7, pp.1782-1786, 2008.

[4] A. Sawa, T. Fujii, M. Kawasaki, and Y. Tokura, "Hysteretic current-voltage characteristics and resistance switching at a rectifying $Ti/Pr_{0.7}Ca_{0.3}MnO_3$ interface," *Appl. Phys. Lett.*, vol. 85, pp. 4073-4075, 2004.

[5] C. B. Lee, B. S. Kang, A. Benayad, M. J. Lee, S. E. Ahn, K. H. Kim, G. Stefanovich, Y. Park, and I. K. Yoo, "Effects of metal electrodes on the resistive memory switching property of NiO thin films," *Appl. Phys. Lett.*, vol. 93, p. 042115, 2008.

[6] C. Lin, D. Lee, S. Wang, C. Lin, and T. Tseng, "Reproducible resistive switching behavior in sputtered CeO_2 polycrystalline films," *Surface & Coatings Tech.*, vol. 203, pp. 480-483, 2008.

[7] X. Sun, B. Sun, L. Liu, N. Xu, X. Liu, R. Han, J. Kang, G. Xiong, and T. P. Ma, "Resistive switching in CeO_x films for nonvolatile memory application," *IEEE Electron Device Lett.*, vol. 30, no. 4, pp. 334-336, 2009.

[8] X. Cao, X. Li, X. Gao, W. Yu, X. Liu, Y. Zhang, L. Chen, and X. Cheng, "Forming-free colossal resistive switching effect in rare-earth-oxide Gd_2O_3 films for memristor applications," *J. Appl. Phys.*, vol. 106, p. 073723, 2009.

[9] S. Seo, M. J. Lee, D. H. Seo, E. J. Jeoung, D. S. Suh, Y. S. Joung, I. K. Yoo, I. R. Hwang, S. H. Kim, I. S. Byun, J. S. Kim, J. S. Choi, and B. H. Park, "Reproducible resistance switching in polycrystalline NiO films," *Appl. Phys. Lett.*, vol. 85, p. 5655-5657, 2004.

[10] H. Y. Lee, P. S. Chen, T. Y. Wu, C. C. Wang, P. J. Tzeng, C. H. Lin, F. Chen, M. J. Tsai, and C. H. Lien, "Electrical evidence of unstable anodic interface in Ru/HfO/TiN unipolar resistive memory," *Appl. Phys. Lett.*, vol. 92, p. 142911, 2008.

[11] C. Y. Lin, C. Y. Wu, C. Y. Wu, and T. Y. Tseng, "Modified resistive switching

behavior of ZrO_2 memory films based on the interface layer formed by using Ti top electrode," *J. Appl. Phys.*, vol. 102, p. 094101, 2007.

[12] C. Y. Lin, C. Y. Wu, C. Y. Wu, T. Y. Tseng, and C. Hu, "Modified resistive switching behavior of ZrO_2 memory films based on the interface layer formed by using Ti top electrode," *J. Appl. Phys.*, vol. 102, p. 094101, 2007.

[13] D. C. Kim, S. Seo, S. E. Ahn, D. S. Suh, M. J. Lee, B. H. Park, I. K. Yoo, I. G. Baek, H. J. Kim, E. K. Yim, J. E. Lee, S. O. Park, H. S. Lim, U-ln Chung, J. T. Moon, and B. I. Ryu, "Electrical observations of filamentary conductions for the resistive memory switching in NiO films," *Appl. Phys. Lett.*, vol. 88, p. 202102, 2006.

[14] K. S. Chang, L. Z. Hsieh, S. K. Huang, C. Y. Lee, and Y. S. Chiu, "Characteristics of high dielectric cubic Gd_2O_3 thin films deposited on cubic $LaAlO_3$ by pulsed laser deposition," *J. Crys. Grow.*, vol. 310, p. 1961-1965, 2008.

[15] Q. Mao, Z. Ji, and J. Xi, "Realization of forming-free ZnO-based resistive switching memory by controlling film thickness," *J. Phys. D*, vol. 43, p. 395104, 2010.

[16] C. Y. Lin, D. Y. Lee, S. Y. Wang, C. C. Lin, T. Y. Tseng, "Effect of thermal treatment on resistive switching characteristics in $Pt/Ti/Al_2O_3/Pt$ devices," *Surface & Coatings Tech.*, vol. 203, pp. 628-631, 2008.

[17] H. Zhang, B. Gao, B. Sun, G. Chen, L. Zeng, L. Liu, X. Liu, J. Lu, R. Han, J. Kang, and B. Yu, "Ionic doping effect in ZrO_2 resistive switching memory," *Appl. Phys. Lett.*, vol. 96, p. 123502, 2010.

[18] D. S. Kim, C. E. Lee, Y. H. Kim, and Y. T. Kim, "Effect of oxygen annealing on $Pr_{0.7}Ca_{0.3}MnO_3$ thin film for colossal electroresistance at room temperature," *J. Appl. Phys.*, vol. 100, p. 093901, 2006.

[19] S. R. Lee, K. Char, D. C. Kim, R. Jung, S. Seo, X. S. Li, G. -S. Park, and I. K. Yoo, "Resistive memory switching in epitaxially grown NiO," *Appl. Phys. Lett.*, vol. 91, p. 202115, 2007.

[20] G. S. Park, X. S. Li, D. C. Kim, R. J. Jung, M. J. Lee, and S. Seo, "Observation of electric-field induced Ni filament channels in polycrystalline NiO_x film," *Appl. Phys. Lett.*, vol. 91, p. 222103, 2007.

[21] J. A. Gupta, D. Landheer, G. I. Sproule, J. P. McCaffrey, M. J. Graham, K. C. Yang, Z. H. Lu, and W. N. Lennard, "Interfacial layer formation in Gd_2O_3 films deposited directly on Si (001)," *Appl. Surf. Sci.*, vol. 173, p. 318-326, 2001.

[22] K. S. Yook, J. Y. Lee, S. H. Kim, and J. Jang, "Transparent organic bistable memory device with pure organic active material and Al/indium tin oxide electrode," *Appl. Phys. Lett.*, vol. 92, p. 223305, 2008.

Chapter 5 - References:

[1]   K. K. Uprety, L. E. Ocola, and O. Auciello, "Growth and characterization of transparent Pb(Zi,Ti)O$_3$ capacitor on glass substrate," *J. Appl. Phys.*, vol. 102, p. 084107, 2007.

[2]   A. Kudo, H. Yanagi, K. Ueda, H. Hosono, H. Kawazoe, and Y. Yano, "Fabrication of transparent p-n heterojunction thin film diodes based entirely on oxide semiconductors," *Appl. Phys. Lett.*, vol. 75, pp. 2851-2853, 1999.

[3]   B. Y. Oh, M. C. Jeong, T. H. Moon, W. Lee, J. M. Myoung, J. Y. Hwang, and D. S. Seo, "Transparent conductive Al-doped ZnO films for liquid crystal displays," *J. Appl. Phys.*, vol. 99, p. 124505, 2006.

[4]   P. Gorrn, M. Sander, J. Meyer, M. Kroger, E. Becker, H. -H. Johanne, W. Kowalsky, T. Riedl, "Towards see-through displays: fully transparent thin-film transistors driving transparent organic light-emitting diodes," *Adv. Mater.*, vol. 18, p. 738-741, 2006.

[5]   A. Du Pasquier, H. E. Unalan, A. Kanwal, S. Miller, and M. Chhowalla, "Conducting and transparent single-wall carbon nanotube electrodes for polymer-fullerene solar cells," *Appl. Phys. Lett.*, vol. 87, p. 203511, 2005.

[6]   B. J. Luff, J. S. Wilkinson, and G. Perrone, "Indium tin oxide overlayered waveguides for sensor applications," *Appl. Opt.*, vol. 36, pp. 7066-7072, 1997.

[7]   J. W. Seo, J. -W. Park, K. S. Lim, J. H. Yang, and S. J. Kang, "Transparent resistive random access memory and its characteristics for nonvolatile resistive switching," *Appl. Phys. Lett.*, vol. 93, p. 223505, 2008.

[8]   L. Shi, D. Shang, J. Sun, and B. Shen, "Bipolar resistance switching in fully transparent ZnO:Mg-based devices," *Appl. Phys. Ex.*, vol. 2, p. 101602, 2009.

[9]   S. Seo, M. J. Lee, D. H. Seo, E. J. Jeoung, D. -S. Suh, Y. S. Joung, I. K. Yoo, I. R. Hwang, I. S. Byun, J. -S. Choi, and B. H. Park, "Reproducible resistance switching in polycrystalline NiO films," *Appl. Phys. Lett.*, vol. 85, pp. 5655-5657, 2004.

[10] B. J. Choi, D. S. Jeong, S. K. Kim, S. Choi, J. H. Oh, C. Rohde, H. J. Kim, C. S. Hwang, K. Szot, R. Waser, B. Reichenberg, and S. Tiedke, "Resistive switching mechanism of TiO$_2$ thin films grown by atomic-layer deposition," *J. Appl. Phys.*, vol. 98, p. 033715, 2005.

[11] D. Lee, H. Choi, H. Sim, D. Choi, H. Hwang, M. J. Lee, S. A. Seo, and I. K. Yoo, "Resistance switching of the nonstoichiometric Zirconium oxide for nonvolatile memory applications," *IEEE Electron Device Lett.*, vol. 26, no. 9, pp. 719-721, 2005.

[12] J. W. Park, M. K. Yang, K. Jung, and J. K. Lee, "Effects of switching parameters

on resistive switching behaviors of polycrystalline $SrZrO_3$:Cr-based metal-oxide-metal structures," *IEEE Trans. Electron Devices*, vol. 55, no. 7, pp. 1782-1786, 2008.

[13] R. Dong, Q. Wang, L. D. Chen, D. S. Shang, T. L. Chen, X. M. Li, and W. Q. Zhang, "Retention behavior of the electric-pulse-induced reversible resistance change effect in $Ag-La_{0.7}Ca_{0.3}MnO_3$-Pt sandwiches," *Appl. Phys. Lett.*, vol. 86, p. 172107, 2005.

[14] B. -E. Park, H. Ishiwara, "Electrical properties of $LaAlO_3$/Si and $Sr_{0.8}Bi_{2.2}Ta_2O_9/LaAlO_3$/Si structures," *Appl. Phys. Lett.*, vol. 79, pp. 806-808, 2001.

[15] L. F. Edge, D. G. Schlom, S. A. Chambers, E. Cicerrella, J. L. Freeouf, B. Hollander, J. Schubert, "Measurement of the band offsets between amorphous $LaAlO_3$ and silicon," *Appl. Phys. Lett.*, vol. 84, pp. 726-728, 2004.

[16] M. Suzuki, T. Yamaguchi, N. Fukushima, M. Koyama, "$LaAlO_3$ gate dielectric with ultrathin equivalent oxide thickness and ultralow leakage current directly deposited on Si substrate," *J. Appl. Phys.*, vol. 103, p. 034118, 2008.

[17] Y. Y. Mi, Z. Yu, S. J. Wang, P. C. Lim, Y. L. Foo, A. C. H. Huan, C. K. Ong, "Epitaxial $LaAlO_3$ thin film on silicon: Structure and electronic properties," *Appl. Phys. Lett.*, vol. 90, p. 181925, 2007.

[18] K. L. Ovanesyan, A. G. Petrosyan, G. O. Shirinyan, C. Pedrini, L. Zhang, "Single crystal growth and characterization of $LaLuO_3$," *Opt. Mater.*, vol. 10, p. 291-295, 1998.

[19] P. E. Dyer, A. Issa, P. H. Key, "Dynamics of excimer laser ablation of superconductors in an oxygen environment," *Appl. Phys. Lett.*, vol. 57, p. 186, 1990.

[20] Y. Nishikawa, K. Tanaka, Y. Yoshida, "Morphology of particles generated from thin film by excimer laser ablation," *Nippon Kinzoku Gakkaishi*, vol. 55, p. 581-587, 1991.

[21] W. Xiang, H. Lu, L. Yan, H. Guo, L. Liu, Y. Zhou, G. Yang, J. Jiang, H. Cheng, and Z. Chen, "Characteristics of $LaAlO_3$/Si(100) deposited under various oxygen pressures," *J. Appl. Phys.*, vol. 93, p. 533, 2003.

[22] K. Xiong, J. Robertson, S. J. Clark, "Defects states in the high-dielectric-constant gate oxide $LaAlO_3$," *Appl. Phys. Lett.*, vol. 89, p. 022907, 2006.

[23] S. Choopun, R. D. Vispute, W. Noch, A. Balsamo, R. P. Sharma, T. Venkatesan, A. Iliadis, D. C. Look, "Oxygen pressure-tuned epitaxy and optoelectronic properties of laser-deposited ZnO films on sapphire," *Appl. Phys. Lett.*, vol. 75, p. 3947, 1999.

[24] X. B. Lu, H. B. Lu, J. Y. Dai, Z. H. Chen, M. He, G. Z. Yang, H. L. W. Chan, C. L. Choy, "Oxygen pressure dependence of physical and electrical properties of LaAlO$_3$ gate dielectric," *Microelectronic Engineering*, vol. 77, p. 399-404, 2005.

[25] B. S. Lim, A. Rahtu, P. de Rouffignac, and R. G. Gordon, "Atomic layer deposition of lanthanum aluminum oxide nano-laminates for electrical applications," *Appl. Phys. Lett.*, vol. 84, p. 3957-3959, 2004.

[26] J. W. Seo, J. Fompeyrine, A. Guiller, G. Norpa, C. Marchiori, H. Siegwart, and J. P. Locquet, "Interface formation and defect structures in epitaxial La$_2$Zr$_2$O$_7$ thin films on (111) Si," *Appl. Phys. Lett.*, vol. 83, p. 5211-5213, 2003.

[27] R. Jha, B. Lee, B. Chen, S. Novak, P. Majhi, and V. Misra, "Dependence of PMOS metal work functions on surface condictions of high-K gate dielectrics," in *IEDM Tech. Dig*., 2005, pp. 43-46.

[28] D. S. Jeong, H. Schroeder, U. Breuer, and R. Waser, "Characteristic electroforming behavior in Pt/TiO$_2$/Pt resistive switching cells depending on atmosphere," *J. Appl. Phys.*, vol. 104, p. 123716, 2008.

[29] J. W. Park, J. W. Park, K. Jung, M. K. Yang, and J. K. Lee, "Influence of oxygen content on electrical properties of NiO films grown by rf reactive sputtering for resistive random-access memory applications," *J. Vac. Sci. Technol. B*, vol. 24, no. 5, pp. 2205-2208, 2009.

[30] W. Y. Chang, Y. T. Ho, T. C. Hsu, F. Chen, M. J. Tsai, and T. B. Wu, "Influence of crystalline constituent on resistive switching properties of TiO$_2$ memory films," *Electrochem. Solid-State Lett.*, vol. 12, no. 4, pp. H135-H137, 2009.

[31] D. S. Jeong, H. Schoroeder, and R. Waser, "Abnormal bipolar-like resistance change behavior induced by symmetric electroforming in Pt/TiO$_2$/Pt resistive switching cells," *Nanotechnology*, vol. 20, p. 375201, 2009.

[32] T. Menke, R. Dittmann, P. Meuffels, K. Szot, and R. Waser, "Impact of the electroforming process on the device stability of epitaxial Fe-doped SrTiO$_3$ resistive switching cells," *J. Appl. Phys.,* vol. 106, p. 114507, 2009.

[33] C. Tang, B. Tuttle, and R. Ramprasad, "Diffusion of O vacancies near Si:HfO$_2$ interfaces: An ab initio investigation," *Phys. Rev. B.*, vol. 76, p. 073306, 2007.

[34] K. McKenna and A. Shluger, "The interaction of oxygen vacancies with grain boundaries in monoclinic HfO$_2$," *Appl. Phys. Lett.*, vol. 95, p. 222111, 2009.

[35] W. F. Wu, and B. S. Chiou, "Effect of oxygen concentration in the sputtering ambient on the microstructure, electrical and optical properties of radio-frequency magnetron-sputtered indium tin oxide films," *Semicond. Sci. Technol.*, vol. 11, pp. 196-202, 1996.

[36] A. Miller, and E. Abrahams, "Impurity conduction at low concentration," *Phys. Rev., vol.*, 120, pp. 745-750, 1960.

[37] S. W. Kenkel, and J. P. Straley, "Percolation theory of nonlinear circuit elements," *Phys. Rev. B.*, vol. 29, p. 6299, 1982.

[38] J. P. Straley, and S. W. Kenkel, "Percolation theory for nonlinear conductors," *Phys. Rev. B.*, vol. 29, p. 6299, 1984.

[39] B. I. Shklovskii, and A. L. Efros, "Impurity band and conductivity of compensated semiconductors," *Sov. Phys. JETP.*, vol. 33, p. 468, 1971.

自　　　傳

姓名：曾文賢

性別：男

出生日期：民國七十一年四月二日

出生地：高雄縣

住址：宜蘭縣羅東鎮羅莊里站東路176-1號3樓

學歷：義守大學電機工程學系
　　　（民國八十九年九月～民國九十三年六月）
　　　國立交通大學電子工程學系暨電子研究所固態組碩士班
　　　（民國九十三年七月～民國九十五年六月）
　　　國立交通大學電子工程學系暨電子研究所固態組博士班
　　　（民國九十五年七月～民國一百年五月）

博士論文：
　　　電阻式記憶體之特性研究及電性探討
The Investigation on Electrical Characteristics and Switching Properties
of Resistive Random Acce